Limited contribution of interchromosomal gene conversion to NF1 gene mutation

Luijten, M.; Fahsold, R.; Mischung, C.; Westerveld, A.; Nürnberg, P.; Hulsebos, T.J.M.

DOI
10.1136/jmg.38.7.481

Publication date
2001

Published in
Journal of Medical Genetics

Limited contribution of interchromosomal gene conversion to NF1 gene mutation

M Luijten, R Fahsold, C Mischung, A Westerveld, P Nürnberg and T J M Hulsebos

J. Med. Genet. 2001;38;481-485
doi:10.1136/jmg.38.7.481

Letters to the Editor

Pseudoxanthoma elasticum: evidence for the existence of a pseudogene highly homologous to the *ABCC6* gene

Dominique P Germain

J Med Genet 2001;**38**:457–460

Clinical Genetics Unit, Department of Genetics, Hôpital Européen Georges Pompidou, 20 rue Leblanc, 75015 Paris, France
D P Germain

Correspondence to: Dr Germain, dominique.germain@hop.egp.ap-hop-paris.fr

EDITOR—Pseudoxanthoma elasticum (PXE, MIM 264800) is an inherited disorder of connective tissue in which the elastic fibres of the skin, eyes, and cardiovascular system slowly become calcified, causing a spectrum of disease involving these three organ systems, with highly variable phenotypic expression.[1,2] Mutations in the *ABCC6* gene (previously known as *MRP6*), encoding a 1503 amino acid membrane transporter, have recently been identified by our group and others[3–7] as the genetic defect responsible for PXE. We subsequently designed a strategy for a complete mutational analysis of the *ABCC6* gene, in order to provide accurate molecular and prenatal diagnosis of PXE. During this mutational screening, we have found evidence for the existence of at least one pseudogene highly homologous to the 5' end of *ABCC6*. Sequence variants in this *ABCC6*-like pseudogene could be mistaken for mutations in the *ABCC6* gene and consequently lead to erroneous genotyping results in pedigrees affected with pseudoxanthoma elasticum.

Material and methods

Seven unrelated patients presenting with PXE were evaluated for mutational analysis of the *ABCC6* gene. For each proband, diagnosis of PXE was consistent with previously reported consensus criteria,[8] which include a positive von Kossa stain of a skin biopsy, indicating calcification of elastic fibres, in combination with specific cutaneous and ocular manifestations (angioid streaks).

Whole blood samples were obtained after participants had provided written consent using a form that was approved by the Institutional Review Board of our academic institution. High molecular weight DNA was isolated from peripheral blood leucocytes, using a standard salting out procedure. Primers for amplification of the *ABCC6* gene were designed from the published sequence of human chromosome 16 bacterial artificial chromosome (BAC) clone A-962B4 (GenBank accession number U91318). PCR amplifications of *ABCC6* exon 2 and exon 9 were done in 20 µl volumes with 100 nmol/l of each of the respective PCR primers (table 1), 100 ng of genomic DNA, 100 µmol/l of each dNTP, 1.0 U Ampli*taq* Gold DNA polymerase (PE Biosystems), 10 mmol/l pH 8.3 Tris-HCl, 50 mmol/l KCl, and 1.5 mmol/l $MgCl_2$. The thermal cycling profile used was 95°C for 10 minutes, followed by 35 cycles at 95°C for 30 seconds, 58°C for 30 seconds, and 72°C for one minute, followed by one cycle at 72°C for 10 minutes and a soak at 6°C.

RNA was isolated from lymphoblastoid cell lines or skin fibroblasts using Rneasy™ (Qiagen) and was reverse transcribed using random hexamers and Superscript-RT (Gibco BRL). Following reverse transcription, RT-PCR amplifications encompassing exon 2 in the published *ABCC6* cDNA sequence[9] (GenBank accession number AF076622) were done in 20 µl volumes with 4 µl of RT reaction. An aliquot of the amplified product was analysed by ethidium bromide visualisation on a 1.5% agarose gel. A 1/50 dilution was submitted to a nested PCR, using internal specific primers (table 1) and 2.0 U Ampli*taq* Gold DNA polymerase (PE Biosystems), under the following conditions: 95°C for 10 minutes, followed by 20 cycles at 95°C for 30 seconds, annealing temperature gradient ranging from 48°C to 70°C for 30 seconds, and 72°C for one minute 30 seconds, followed by one cycle at 72°C for 10 minutes, and a soak at 10°C, on a Robocycler gradient 96 (Stratagene).

All PCR and RT-PCR fragments were purified using QIAquick Spin PCR Purification Kit (Qiagen) according to the manufacturer's protocol, and 4 µl of the purified PCR products were sequenced using the Big Dye Terminator Ampli*Taq* FS Cycle Sequencing Kit on an automated ABI 310 DNA sequencer (PE Biosystems). DNA sequences were handled with Navigator 2.0 software.

Table 1 Primers for amplification of the ABCC6 gene and cDNA

Primer	*Sequence*	*Product size (bp)*
Genomic		
ABCC6 exon 2 forward	5'-TCT GCG TCC TGG AGT TGT TA-3'	800
ABCC6 exon 2 forward	5'-ATG GGA GTG TAT GCG TAT GT-3'	
ABCC6 exon 9 forward	5'-GGA CAG TGG GGG AAA TAA CG-3'	676
ABCC6 exon 9 reverse	5'-TAG CTG GGC GTG GTG ACA CG-3'	
cDNA (nested PCR)		
ABCC6 exon 2 forward	5'-GAG CCT GAA CCT GCC GCC AC-3'	334
ABCC6 exon 2 reverse	5'-GAA TCA GGA ACA CTG CGA AG-3'	

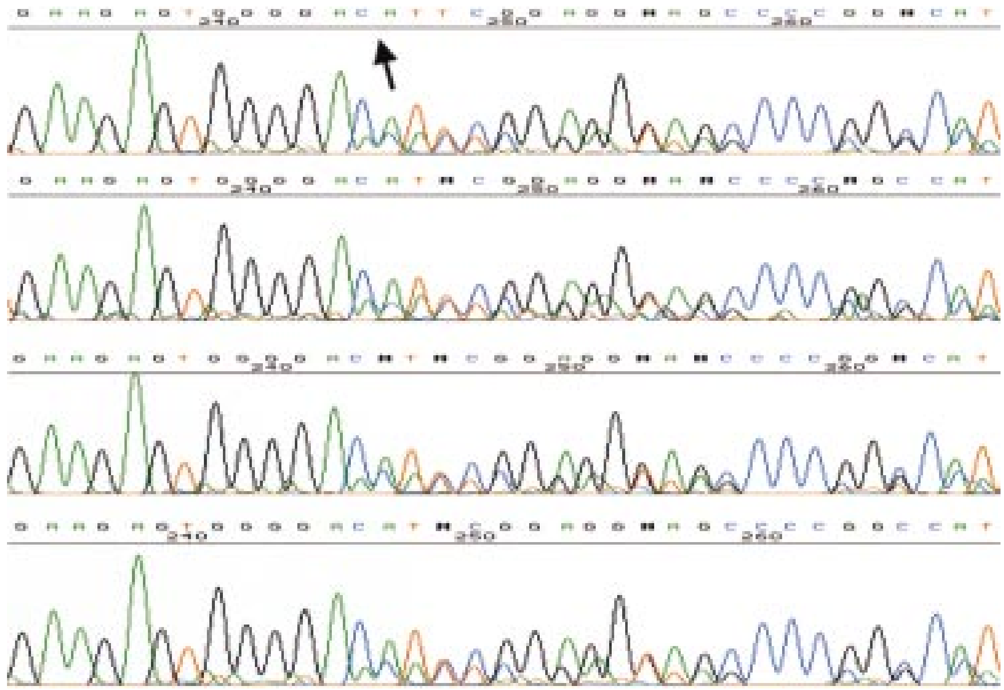

Figure 1 Detection of a frameshift mutation (c196insT) in what was initially thought to be exon 2 of the ABCC6 gene. Genomic PCR products were sequenced using an antisense primer. Chromatograms show the insertion of an adenine (A) on the antisense strand (arrow), corresponding to a thymine (T) insertion on the sense strand. This single nucleotide insertion is responsible for a frameshift with consequent premature appearance of a stop codon. Heterozygosity for this frameshift mutation is shown here in two PXE patients (lanes 1 and 2) and two controls (lanes 3 and 4), but was also found in all 58 tested controls without exception. Sequencing of the other strand yielded the same result (not shown).

Results

During our mutational screening of the *ABCC6* gene, we disclosed sequence changes which, although predicted to be truncating mutations, were unexpectedly detected not only in PXE patients but also in all tested controls. We first identified a single nucleotide insertion (c196insT) in the heterozygous state in a sporadic 14 year old female PXE patient. This mutation causes a shift in the reading frame, predicting a premature stop at codon 100 of the ABCC6 protein. Since we found this single nucleotide insertion in six other PXE patients, we initially interpreted this sequence change as a mutational hotspot. However, sequencing of the sporadic case's parents' DNA showed that, although unrelated to each other and phenotypically normal, they were both heterozygous for this frameshift mutation. These results were puzzling; if autosomal dominant inheritance with a de novo mutation[2] had occurred, neither of the unaffected parents should be a carrier, and, conversely, if autosomal recessive transmission had occurred, the proband should be a compound heterozygote on the basis of our results, and, consequently, only one of the parents would be expected to be a carrier of the c196insT mutation. These odd results prompted us to investigate 58 controls, all of whom showed a heterozygous profile for the frameshift mutation in what was thought to be exon 2 of the *ABCC6* gene (fig 1).

Similarly, a heterozygous C to T transition was found at cDNA position 1132 in exon 9 of the *ABCC6* gene. This nucleotide substitution alters the codon (CAG) for glutamine to a stop codon (TAG), predicting termination of translation at position 378 of the ABCC6 protein (Q378X). This nonsense mutation was detected in the heterozygous state in all seven PXE patients and in one healthy volunteer. Mutation Q378X predicted the loss of a *Pst*I

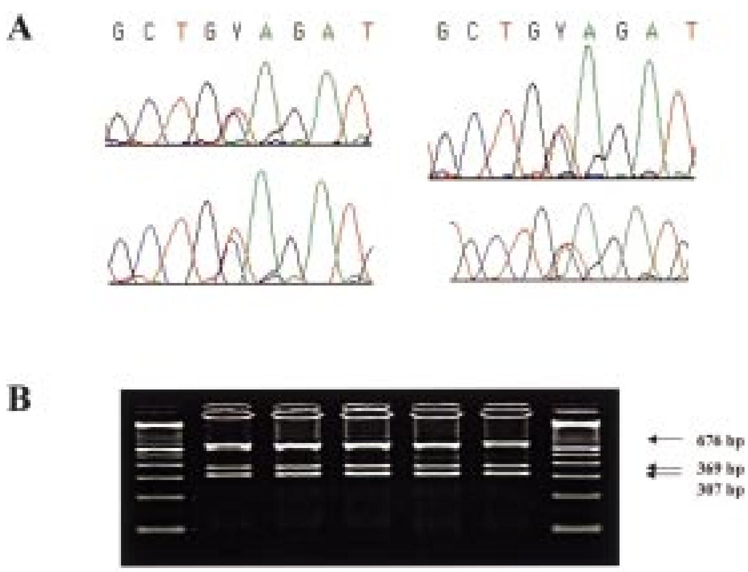

Figure 2 Detection of a nonsense mutation (Q378X) in what was initially thought to be exon 9 of the ABCC6 gene. (A) Upper panel: identification of a heterozygous nonsense mutation in four patients affected with PXE by direct automated sequencing of exon 9 of the ABCC6 gene. The heterozygous C to T transition alters the codon (CAG) for glutamine to a stop codon (TAG) at position 378 of the ABCC6 protein. The position of the mutation is shown by the letter Y (Y=C and T). (B) Lower panel: mutation c1132C>T (Q378X) predicted the loss of a PstI restriction site. Restriction digests using PstI were performed on PCR amplified exon 9 of the ABCC6 gene. Five healthy volunteers, who although unaffected with PXE display heterozygozity for the Q378X nonsense mutation, are shown. The study of 75 additional white controls yielded the same result. This indicates that rather than being amplified from two genomic copies, the PCR products were being amplified from four genomic copies.

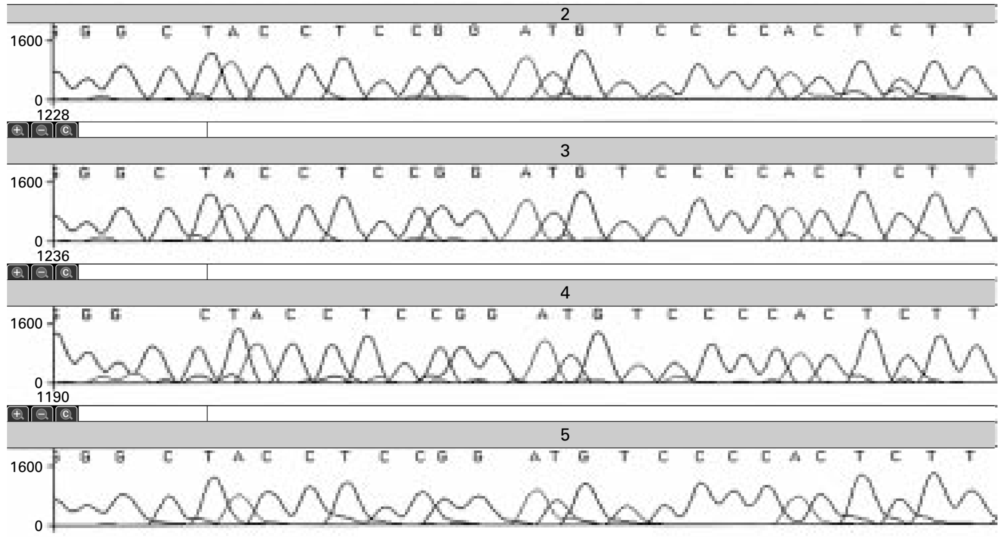

Figure 3 RT-PCR chromatograms of the region corresponding to exon 2 in the ABCC6 cDNA in the four subjects shown in lanes 1-4 in fig 1. ABCC6 mRNA was reverse transcribed and amplified through a nested PCR procedure. Direct automated sequencing of the region corresponding to the mutation detected in exon 2 at the genomic level does not show a thymine insertion in the mRNA and consequently no frameshift is seen. The same nucleotides as in fig 1 are shown, but sequencing was performed with a sense primer. These data indicate that the pseudogene is not expressed.

restriction site. To test for the presence or absence of this nucleotide change, we used *Pst*I to digest PCR amplified genomic DNA of 79 additional controls and found all of them to be heterozygotes for the Q378X nonsense mutation (fig 2).

Discussion

Both results are interesting although surprising, since they identify two mutations, one nonsense and the other one inducing a frameshift, expected to cause truncation of the protein and thereby compromise its function. However, these mutations have been shown to be non-pathogenic since they are consistently found in healthy subjects. Among possible explanations for these results, we initially thought of the existence of mutational hotspots, but this hypothesis was ruled out through the discovery of the same mutations in controls. A technical artefact of direct automated sequencing was also considered, but was eliminated through the use of other experimental techniques, including restriction digest experiments. We then checked for possible homologies within the ATP binding cassette (ABC) superfamily.[10] ABC genes are divided into seven distinct subfamilies (*ABC1*, *MDR/TAP*, *MRP*, *ALD*, *OABP*, *GCN20*, and *White*). However, if homologies do exist within the MRP subfamily (subfamily C) to which *ABCC6* belongs, they are not important enough to explain our results, according to our database searches.

Finally, one likely explanation is the existence of a pseudogene with high homology with the 5' end of the *ABCC6* gene, the PCR products being amplified from four rather than two genomic copies. Since we have used intronic primers to amplify *ABCC6* genomic sequences, an *ABCC6*-like pseudogene with introns is expected, as has been, for instance, reported for the gene encoding acid β-glucosidase.[11] Indeed, as is found in Gaucher disease, the existence of a highly homologous *ABCC6* pseudogene hampers the accuracy of molecular diagnosis of PXE, since sequence variants in the pseudogene might be mistaken for pathogenic mutations in the active *ABCC6* gene.

Pseudogenes are thought to arise from tandem gene duplication events caused by chromosome misalignment and unequal crossing over during meiosis. This mechanism would explain the high homology observed in both exonic and intronic sequences of the *ABCC6* gene and pseudogene.

The pseudogene could be located on a different chromosome or could be close to *ABCC6* on chromosome 16. In favour of the later hypothesis is the fact that the short arm of chromosome 16 has been shown to be a site where complex rearrangements have taken place.[12] Further evidence also comes from preliminary FISH experiments which detected double signals at 16p13.1, when fragments of BAC containing the *ABCC6* gene were used as probes.[13]

In order to determine whether the pseudogene is expressed or not, RNA was isolated from skin fibroblasts and lymphoblastoid cell lines and RT-PCR experiments amplifying exon 2 in *ABCC6* cDNA were performed. We found *ABCC6* mRNA to be expressed at low level in cultured skin fibroblasts and lymphoblastoid cell lines from both PXE patients and controls, in agreement with previous data indicating that *ABCC6* is mainly expressed in liver and kidney.[9,14] This prompted us to develop a nested PCR strategy, which proved efficient for the molecular analysis of *ABCC6* mRNA. No frameshift was shown when nested RT-PCR fragments, encompassing the region corresponding to *ABCC6* exon 2, were sequenced (fig 3). This indicates that the pseudogene that we describe belongs to the unprocessed category.

In conclusion, we have found nonsense and frameshift sequence variations in the *ABCC6* gene, both of which appear to be non-pathogenic, thereby indicating the existence of at least one highly homologous pseudogene, which greatly complicates genotyping in families affected by pseudoxanthoma elasticum. Further studies are needed to map and fully characterise the sequence of the pseudogene(s). However, our results already emphasise the importance of not confusing variants in the pseudogene with pathogenic mutations in the *ABCC6* gene, especially in genetic counselling or prenatal diagnosis.

- Pseudoxanthoma elasticum (PXE) is an inherited systemic disorder of connective tissue with highly variable phenotypic expression.
- Mutations in the *ABCC6* gene were recently identified as the genetic defect responsible for PXE.
- We have characterised two truncating mutations (c196insT and Q378X) in the *ABCC6* gene, always found in the heterozygous state, not only in PXE patients but also in all controls.
- This indicates the existence of a highly homologous pseudogene.
- Sequence variants in the pseudogene should not be confused with mutations in the *ABCC6* gene, especially in genetic counselling or prenatal diagnosis.

The author thanks the patients and their families for their help during this project and gratefully acknowledges F Letourneur, J Perdu, and I Roncelin for excellent technical assistance and Dr D Recan for providing lymphoblastoid cell lines.

1 McKusick VA. Pseudoxanthoma elasticum. In: McKusick VA, ed *Heritable disorders of connective tissue*. 4th ed. New York: Mosby, 1972.
2 Pope FM. Historical evidence for the genetic heterogeneity of pseudoxanthoma elasticum. *Br J Dermatol* 1975;**92**:493-509.
3 Bergen AA, Plomp AS, Schuurman EJ, Terry S, Breuning M, Dauwerse H, Swart J, Kool M, van Soest S, Baas F, ten Brink JB, de Jong PT. Mutations in ABCC6 cause pseudoxanthoma elasticum. *Nat Genet* 2000;**25**:228-31.
4 Germain DP, Perdu J, Remones V, Jeunemaitre X. Homozygosity for the R1268Q mutation in *MRP6*, the pseudoxanthoma elasticum gene, is not disease-causing. *Biochem Biophys Res Commun* 2000;**274**:297-301.
5 Le Saux O, Urban Z, Tschuch C, Csiszar K, Bacchelli B, Quaglino D, Pasquali-Ronchetti I, Pope FM, Richards AJ, Terry S, Bercovitch L, de Paepe A, Boyd CD. Mutations in a gene encoding an ABC transporter cause pseudoxanthoma elasticum. *Nat Genet* 2000;**25**:223-7.
6 Ringpfeil F, Lebwohl MG, Christiano AM, Uitto J. Pseudoxanthoma elasticum: mutations in the MRP6 gene encoding a transmembrane ATP-binding cassette (ABC) transporter. *Proc Natl Acad Sci USA* 2000;**97**:6001-6.
7 Struk B, Cai L, Zach S, Ji W, Chung J, Lumsden A, Stumm M, Huber M, Schaen L, Kim CA, Goldsmith LA, Viljoen D, Figuera LE, Fuchs W, Munier F, Ramesar R, Hohl D, Richards R, Neldner KH, Lindpaintner K. Mutations of the gene encoding the transmembrane transporter ABC-C6 cause pseudoxanthoma elasticum. *J Mol Med* 2000;**78**:282-6.
8 Lebwohl M, Neldner K, Pope FM, de Paepe A, Christiano AM, Boyd CD, Uitto J, McKusick VA. Classification of pseudoxanthoma elasticum: report of a consensus conference. *J Am Acad Dermatol* 1994;**30**:103-7.
9 Kool M, van der Linden M, de Hass M, Baas F, Borst P. Expression of human MRP6, a homologue of the multidrug resistance protein gene MRP1, in tissues and cancer cells. *Cancer Res* 1999;**59**:175-82.
10 Borst P, Evers R, Kool M, Wijnholds T. The multidrug resistant protein family. *Biochim Biophys Acta* 1999;**1461**: 347-57.
11 Horowitz M, Wilder S, Horowitz Z, Reiner O, Gelbart T, Beutler E. The human glucocerebrosidase gene and pseudogene: structure and evolution. *Genomics* 1989;**4**:87-96.
12 Loftus BJ, Kim UJ, Sneddon VP, Kalush F, Brandon R, Fuhrmann J, Mason T, Crosby ML, Barnstead M, Cronin L, Deslattes Mays A, Cao Y, Xu RX, Kang HL, Mitchell S, Eichler EE, Harris PC, Venter JC, Adams MD. Genome duplications and other features in 12 Mb of DNA sequence from human chromosome 16p and 16q. *Genomics* 1999;**60**: 295-308.
13 Cai L, Struk B, Adams MD, Ji W, Haaf T, Kang HL, Dho SH, Xu X, Ringpfeil F, Nancarrow J, Zach S, Schaen L, Stumm M, Niu T, Chung J, Lunze K, Verrecchia B, Goldsmith LA, Viljoen D, Figuera LE, Fuchs W, Lebwohl M, Uitto J, Richards R, Hohl D, Ramesar R. A 500-kb region on chromosome 16p13.1 contains the pseudoxanthoma elasticum locus: high-resolution mapping and genomic structure. *J Mol Med* 2000;**78**:36-46.
14 Belinsky MG, Kruh GD. MOAT-E (ARA) is a full length MRP/cMOAT subfamily transporter expressed in kidney and liver. *Br J Cancer* 1999;**80**:1342-9.

Hereditary and somatic DNA mismatch repair gene mutations in sporadic endometrial carcinoma

Robert B Chadwick, Robert E Pyatt, Theodore H Niemann, Samuel K Richards, Cheryl K Johnson, Michael W Stevens, Julie E Meek, Heather Hampel, Thomas W Prior, Albert de la Chapelle

J Med Genet 2001;**38**:461–466

Division of Human Cancer Genetics, The Ohio State University, Department of Molecular Virology, Immunology, and Medical Genetics, and the Comprehensive Cancer Center, The Ohio State University, 420 West 12th Avenue, Columbus, Ohio 43210, USA
R B Chadwick
S K Richards
C K Johnson
M W Stevens
J E Meek
H Hampel
A de la Chapelle

Department of Pathology, The Ohio State University Medical Center, 121 Hamilton Hall, 1645 Neil Avenue, Columbus, Ohio 43210, USA
R E Pyatt
T H Niemann
T W Prior

Correspondence to: Dr de la Chapelle, delachapelle-1@medctr.osu.edu

EDITOR—Endometrial cancer (EC) is the second most common malignancy in the hereditary non-polyposis colorectal cancer (HNPCC) syndrome.[1] In a recent large study, cumulative cancer incidences by the age of 70 in HNPCC mutation carriers were: colorectal 82%, endometrial 60%, gastric 13%, and ovarian 12%.[2] Interestingly, in female mutation carriers the incidence of endometrial cancer (60%) exceeded that of colorectal cancer (CRC) (54%), as had been suggested earlier.[2 3]

Predisposition to HNPCC is the result of germline mutations in the mismatch repair genes.[4] Detectable mutations in the two major genes, *MLH1* and *MSH2*, account for some 3% of all colorectal cancers.[5] One might therefore assume that a similar proportion of all endometrial cancer patients would have such mutations; however, in a number of studies addressing this question, extremely few germline mutations have been found. Summarising the studies by Katabuchi *et al*,[6] Kobayashi *et al*,[7] Lim *et al*,[8] Gurin *et al*,[9] and Kowalski *et al*,[10] only one germline mutation (in *MLH1*) was found in a total of 352 EC patients (0.3%). In these studies, mutations were sought in all patients whose tumours were microsatellite instability (MSI) positive.

Recent reports have suggested that *MSH6* might account for many endometrial cancers and that families with these mutations show atypical features of HNPCC with endometrial and ovarian cancers outnumbering colorectal cancers.[11 12] Additionally, MSI, a hallmark of HNPCC, was low in most tumours associated with *MSH6* mutations or was preferentially shown by mononucleotide repeats rather than dinucleotide repeats.[12–14] Previous studies have reported that 9-25% of sporadic endometrial cancers display microsatellite instability .[7 9 15–18] In the majority of cases, this instability arises through hypermethylation of the *MLH1* promoter region.[9 19–21] This epigenetic change results in reduced (or no) expression of the *MLH1* transcript.[22]

This study was undertaken to revisit the issue of microsatellite instability and mismatch repair gene mutations in sporadic endometrial cancer. By initially studying tumour tissue, both germline and somatic mutations were evaluated in the *MSH2*, *MLH1*, and *MSH6* genes in a retrospective series of microsatellite stable and microsatellite unstable endometrial cancers.

Material and methods

All patients diagnosed with endometrial adenocarcinoma between October 1996 and February 1998 at the Ohio State University Hospital were considered retrospectively. Among these 85 patients, archival tissue was available from 74.

After appropriate investigational review board (IRB) approval, these 74 charts were reviewed and the tissue blocks recovered. Histological sections were made, stained with haematoxylin and eosin, and the histological diagnosis critically re-evaluated. Sections 50 µm thick were cut from regions of the tumour containing as high a proportion of tumour cells as possible (typically >50%). To obtain non-malignant tissue, sections were obtained either from tissue emanating from other organs, primarily lymph nodes, that were histologically cancer free, or alternatively sections were made from parts of the endometrial tissue that had no cancer cells. All materials were unlinked from their identifiers before being subjected to DNA extraction and genetic analyses.

Tissue sections were deparaffinised with two xylene washes. Rehydration was accomplished through 20 minute incubations in decreasing concentrations of alcohol (100%, 80%, 50%) at room temperature followed by an overnight incubation in double distilled water at 4°C. DNA was extracted by lysis of the tissue for 18 hours at 55°C with 1 mg/ml proteinase K in 400 µl of buffer (10 mmol/l Tris, 400 mmol/l NaCl, 2 mmol/l EDTA, and 0.7% sodium dodecyl sulphate, pH 8.2). Degraded proteins were precipitated with 2.5 volumes of saturated NaCl after centrifugation. DNA was precipitated with 2.5 volumes of 100% ethanol at –20°C, washed in 70% cold ethanol, then dissolved in 50 µl of TE buffer (10 mmol/l Tris and 1 mmol/l EDTA, pH 8.0).

Microsatellite sequences were amplified using the Bethesda panel.[13] Owing to limited availability of normal tissue, tumour DNA was used for MSI determination without its corresponding normal DNA pair. Amplifications were done in 15 µl PCR reaction volumes using 1 µl of each 8 µmol/l primer (the 5' primer is fluorescently labelled), 10 ng of genomic DNA, and 8 µl of Qiagen's HotStar*Taq* Master Mix. The thermal cycling profile was one cycle at 95°C for 12 minutes, followed by 45 cycles at 95°C for 10 seconds, 55°C for 15 seconds, and 72°C for 30 seconds, followed by one cycle at 72°C for 30 minutes, followed by a soak at 4°C. Respective PCR reactions for each marker were pooled together and loaded on to the PE3700 automated sequencer. Allele sizing and calling was done using Genotyper software (Applied Biosystems). For polymorphic markers D2S123, D5S346, and D17S250 samples were scored as MSI positive if more than two alleles were present. Since normal DNA was not available for comparison from all samples, it is possible that instances of MSI where the normal sample was homozygous and the tumour sample had only two alleles were missed. However, this limitation does not apply to the two mononucleotide repeat markers, suggesting that this did not lead to any serious underestimate of MSI, as these markers are more sensitive to MSI than the dinucleotide repeats.[23 24] For homozygous markers BAT25 and BAT26, samples were scored as MSI positive if the pattern deviated from the normal homozygous pattern. The BAT markers are polymorphic in African Americans.[25 26] However, the ethnicity of the subjects in this study was known and all three African American subjects (Nos 31, 65, and 70) were screened for mutations in the mismatch repair genes. Out of the 74 tumours tested, 17 (or 23%) were found to be MSI positive, 14 MSI high and 3 MSI low (table 1).

Table 1 Summary of results in those 42 patients in whom mutational analyses were carried out

Patient No	Age at diagnosis	Family history and site	MSI markers positive	MSI classification	MSH2	MLH1	MSH6
2	39	Father prostate, paternal grandmother CSU, patient had second primary colon cancer, Hodgkin's lymphoma	0/5	N	No	No	No
3	74	No	4/5	H	No	Germline GAG(Glu) to GGG(Gly) at codon 578	No
5	73	Yes, CSU	0/5	N	No	No	No
7	40	Mother ovarian	0/5	N	No	No	No
9	67	Mother breast	4/5	H	No	No	No
10	77	Mother GI & sister pancreatic	0/5	N	No	No	No
13	50	Brother testicular	0/5	N	No	Somatic GAA(Glu) to AAA(Lys) at codon 668	Somatic GAT(Asp) to TAT(Tyr) at codon 575 Somatic GAA(Glu) to TAA(stop) at codon 1359
14	66	Mother & father CSU	0/5	N	No	No	No
15	51	Maternal aunt, mother, sister lymphoma	4/5	H	No	No	No
16	38	Aunt breast	0/5	N	No	No	No
17	58	Father lung, mother breast, maternal grandmother gallbladder	0/5	N	No	No	No
19	79	Sister breast, daughter colon	1/5	L	No	No	No
21	45	Sister melanoma, grandmother breast	0/5	N	No	No	No
23	65	Mother endometrial	0/5	N	No	No	No
26	64	Father, sister, brother colon Sister breast, grandson brain	0/5	N	No	No	No
30	57	Maternal grandmother rectal	0/5	N	No	No	No
31	78	Half sister breast	2/5	H	Somatic A deletion in (A)7 repeat of exon 4	No	No
34	78	Aunt & sister breast	0/5	N	No	No	No
37	76	Family history of stomach cancer	0/5	N	No	Somatic GAG(Glu) to AAG(Lys) at codon 515	No
38	54	Father CSU	0/5	N	No	No	No
41	52	Mother leukaemia and colon	0/5	N	No	No	no
42	50	No	1/5	L	No	No	No
45	85	Mother pancreatic	0/5	N	No	No	No
48	57	Mother colon, father lung	4/5	H	No	No	No
50	67	Maternal aunt bone	3/5	H	No	No	Somatic C deletion in (C)8 repeat of exon 5
51	74	No	2/5	H	No	No	No
52	49	Family history of breast, bladder and colon Also family history of haematological malignancies	3/5	H	Germline GGC(Gly) to GAC(Asp) at codon 322 Somatic A deletion in (A)7 repeat of exon 4	Somatic GAT (Asp) to AAT(Asn) at codon 203	No
55	78	Brother bladder	0/5	N	No	No	No
56	77	Mother & sister pancreatic, maternal uncle CSU	3/5	H	No	No	No
57	68	Mother and two sisters colon	3/5	H	No	No	Somatic C insertion in (C)8 repeat of exon 5
60	52	Mother breast & colon, two sisters breast	0/5	N	No	No	No
61	56	Mother breast, ovarian, colon, sister colon, grandmother endometrial	0/5	N	No	No	No
64	85	Patient had second primary colon cancer	0/5	N	No	No	No
65	60	Father, two aunts & uncle leukaemia, sister breast, uncle stomach	3/5	H	No	No	No
66	56	Mother colon, uncle prostate	0/5	N	No	No	No
67	77	Sister CSU	0/5	N	No	No	No
68	49	Maternal grandmother & aunt gastric, maternal aunt breast, father lung cancer	5/5	H	No	No	No
70	57	Mother breast	1/5	L	No	No	No
78	59	Mother gastric	5/5	H	No	No	No
79	80	Sister colon, sister ovarian	0/5	N	No	No	No
83	57	Niece breast	0/5	N	No	No	No
84	72	Sister breast	2/5	H	No	No	No

CSU=cancer site unspecified, H=high, L=low, N=negative.

Table 2 Primers used to amplify all exons of the MSH6 gene. In order to facilitate subsequent direct sequencing, 5' primers were tailed with M13 forward (TGTAAAACGACGGCCAGT) and M13 reverse (CAGGAAACAGCTATGACC) sequences

MSH6	*Primer sequences*
Exon 1	Fw: TGTAAAACGACGGCCAGTTCCGTCCGACAGAACGGTTG
	Rv: CAGGAAACAGCTATGACCCCCCAAATGCTCCAGACTCG
Exon 2	Fw: TGTAAAACGACGGCCAGTGCCAGAAGACTTGGAATTGTTTATTTG
	Rv: CAGGAAACAGCTATGACCACACAAACACACACACATGGCAGTAG
Exon 3	Fw: TGTAAAACGACGGCCAGTCGTGAGCCTCTGCACCCGGCCC
	Rv: CAGGAAACAGCTATGACCCCCCATCACCCTAACATAAA
Exon 4A	Fw: TGTAAAACGACGGCCAGTGTCTTACATTATGGTTTTCC
	Rv: CAGGAAACAGCTATGACCCCACATCAGAGCCACCAATG
Exon 4B	Fw: TGTAAAACGACGGCCAGTCGAAGGGTCATATCAGATTC
	Rv: CAGGAAACAGCTATGACCATACCAAACAGTAGGGCGAC
Exon 4C	Fw: TGTAAAACGACGGCCAGTCGTTAGTGGAGGTGGTGATG
	Rv: CAGGAAACAGCTATGACCATGAATACCAGCCCCAGTTC
Exon 4D	Fw: TGTAAAACGACGGCCAGTCTGTACCACATGGATGCTCT
	Rv: CAGGAAACAGCTATGACCCTTCCTCTTTTTCTTTGAGG
Exon 4E	Fw: TGTAAAACGACGGCCAGTAAAGTAGCACGAGTGGAACAGACTGAG
	Rv: CAGGAAACAGCTATGACCAACATCACCCCAATGCCATCAC
Exon 4F	Fw: TGTAAAACGACGGCCAGTCTGTTCTCTTCAGGAAGGTC
	Rv: CAGGAAACAGCTATGACCAGCCATTGCTTTAGGAGCCG
Exon 4G	Fw: TGTAAAACGACGGCCAGTACTTGCCATACTCCTTTTGG
	Rv: CAGGAAACAGCTATGACCCCTGCTTTGGGAGTAATAAG
Exon 4H	Fw: TGTAAAACGACGGCCAGTGAAAAGGCTCGAAAGACTGG
	Rv: CAGGAAACAGCTATGACCCCAAAGGGCTACTAAGATAAAAGCGAG
Exon 5	Fw: TGTAAAACGACGGCCAGTGGGGAGATCGTTGGACTGTAATTG
	Rv: CAGGAAACAGCTATGACCTTGCTTCCTATTAAGTCACTGGCTG
Exon 6	Fw: TGTAAAACGACGGCCAGTGTTTATGAAACTGTTACTACC
	Rv: CAGGAAACAGCTATGACCGCAAATATCTTTTATCACAT
Exon 7	Fw: TGTAAAACGACGGCCAGTGCCAATAATTGCATAGTCTCTTAATG
	Rv: CAGGAAACAGCTATGACCGCCACAATGGTGAGTGCGTG
Exon 8	Fw: TGTAAAACGACGGCCAGTCCTTTTTTGTTTTAATTCCT
	Rv: CAGGAAACAGCTATGACCCAACAGAAGTGCCCTCTCAA
Exon 9	Fw: TGTAAAACGACGGCCAGTGATTATTCTCAAAATGTTGCTGTGCG
	Rv: CAGGAAACAGCTATGACCTTCACTAGCCAGGCAAACTTCCC
Exon 10	Fw: TGTAAAACGACGGCCAGTATTTTAAGGGAAGTTTGCC
	Rv: CAGGAAACAGCTATGACCGTTTATTAGATCATAATGTT

All exons of the *MSH2*, *MLH1*, and *MSH6* genes were screened by direct sequencing of genomic PCR products. In order to facilitate direct sequencing of PCR products for mutational analysis, all 5' and 3' PCR primers were tailed with M13 forward (TGTAAAACGACGGCCAGT) and M13 reverse (CAGGAAACAGCTATGACC) sequences (table 2 and supplemental data).[27] PCR reactions were done in 25 µl volumes with 100 nmol/l of each of the respective PCR primers, 25 ng of genomic DNA, 100 µmol/l of each dNTP, 1.0 U Ampli*Taq* Gold DNA polymerase (Perkin-Elmer), 10 mmol/l pH 8.3 Tris-HCl, 50 mmol/l KCl, and 2 mmol/l $MgCl_2$. PCR fragments were purified using the Exonuclease I/Shrimp Alkaline Phosphatase PCR Product Presequencing Kit (USB). After purification according to the manufacturer's protocol, 2 µl of the PCR products were sequenced using the BigDye Terminator Ampli*Taq* FS Cycle Sequencing Kit (Applied Biosystems). Determination of somatic or hereditary mutation status for all mutations was done by comparing tumour chromatograms to normal DNA chromatograms amplified from archival lymph node tissue DNA from the respective patients.

Results

Out of the 17 MSI positive endometrial tumours and an additional 25 that were MSI negative, only two germline changes were found (table 1 and supplemental data). These were a GAG(Glu) to GGG(Gly) mutation at codon 578 of the *MLH1* gene in patient 3 and a GGC(Gly) to GAC(Asp) at codon 322 of the *MSH2* gene in patient 52. The *MLH1* mutation has been reported to be pathogenic previously and the tumour from this person was MSI high.[28] Additionally, a functional assay indicates that this mutation is pathogenic.[29] Also, MLH1 immunohistochemistry showed virtually no expression of MLH1 in this patient's tumour (supplemental data). The patient is a 74 year old white female with a history of hypertension, diabetes mellitus type II since the age of 54, and chronic renal failure. It was noted that her family history was positive for diabetes mellitus and hypertension, but there was no mention of a family history of cancer on chart review.

The GGC(Gly) to GAC(Asp) at codon 322 mutation of *MSH2* found in patient 52 is listed in the ICG-HNPCC database (http://www.nfdht.nl/) as both a pathogenic mutation and a polymorphism.[30–32] In the first paper describing this change it was considered a clinically insignificant polymorphism because it was found in one out of 30 unrelated controls.[30] Moreover, in another study the same change was reported not to segregate with the cancer predisposition.[33] To investigate its incidence further, we tested 50 grandparents from the families collected by the Centre d'Etude du Polymorphisme Humain and found it in one person. The glycine is conserved among human, mouse, rat, and yeast. MSH2 immunohistochemistry of this tumour showed reduced expression of MSH2 suggesting that this amino acid change may potentially contribute to pathogenicity (supplemental data). Notably, this tumour was MSI high and had an additional somatic truncating mutation in exon 4 of *MSH2* (fig 1). The MSH2 antibody is specific for the carboxy terminus of *MSH2* and thus less protein would be expected to be detected in a tumour with a truncating mutation in the amino terminus. Additionally, the tumour had a somatic mutation of GAT(Asp) to AAT(Asn) at codon 203 of *MLH1*. Immunohistochemistry using anti-human MLH1 antibody also showed reduced expression of MLH1 protein (supplemental data). The patient is a 49 year old white woman with a history of ulcerative colitis since the age of 20. The family history is significant for her mother with breast cancer alive at the age of 71, her father with bladder cancer who died at the age of 79, and her paternal grandfather who died from colon cancer in his late 60s. Thus, in summary, the evidence regarding the MSH2 germline amino acid substitution is inconclusive in that it may be either an innocuous polymorphism or a low penetrant pathogenic mutation. For these reasons we do not count it as a pathogenic germline mutation in this study. No pathogenic germline mutations were found in the *MSH6* gene in the 42 endometrial cancers studied.

Somatic truncating frameshift mutations were found in the coding repeat of seven adenosines in exon 4 of *MSH2* (fig 1). These 1 bp deletions lead to a predicted truncation at amino acid 245 of the MSH2 protein and both tumours were MSI high. This region of *MSH2* has not been reported previously to be hypermutable. Mutations in this repeat were confined to MSI positive cancers, indicating

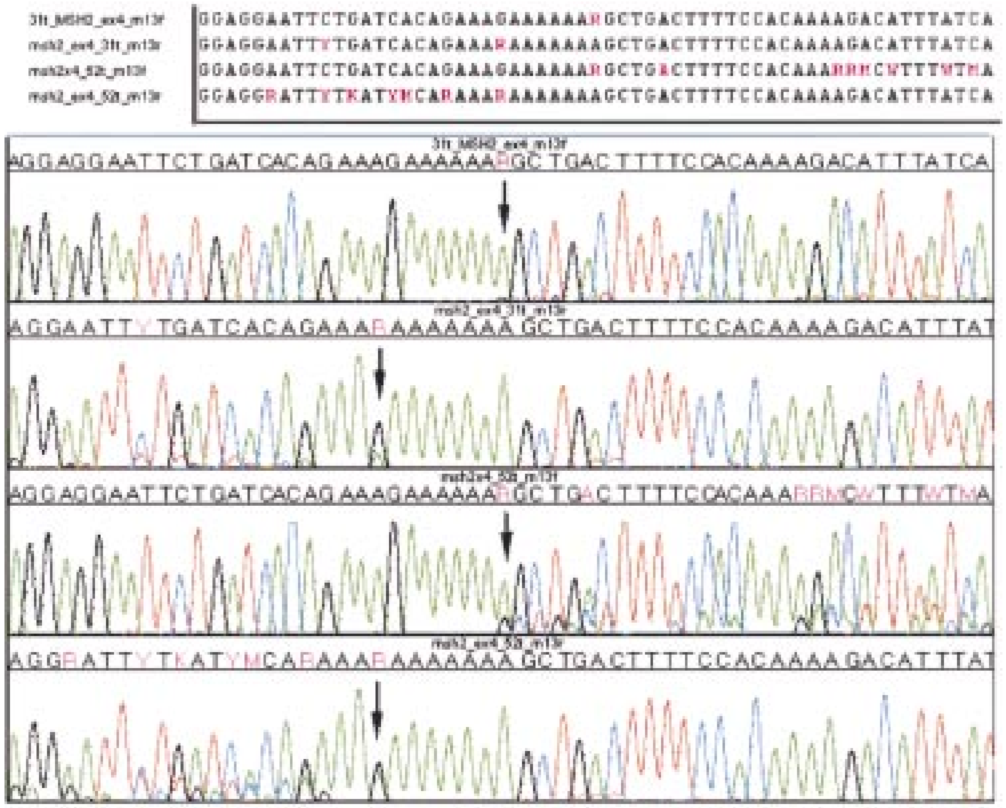

Figure 1 *Somatic truncating frameshift mutations in exon 4 of MSH2. MSI positive endometrial tumours 31 and 35 have 1 bp deletions in the coding (A)$_7$ repeat. This creates a termination codon at amino acid 245 of MSH2. Panels 1 and 3 are forward direction sequences of samples 31 and 52. Panels 2 and 4 are reverse direction sequences of these samples that have been reverse complemented. Owing to contaminating normal DNA, the frameshift is more evident in the reverse direction sequenced, particularly in sample 31 (panel 2).*

that *MSH2* is also a target in the microsatellite instability model of carcinogenesis similar to the *TGFBRII, BAX, IGF2R, MSH3, MSH6, TCF4, MBD4*, and *RIZ* genes.[34–41] We are unable to evaluate the clinical and pathogenic significance of mutations that arise in mismatch repair genes in tumours that are already mismatch repair deficient. A case in point is tumour 52 that showed immunohistochemical deficiency of both MLH1 and MSH2 protein, no MLH1 germline mutation, but two genetic changes in *MSH2*. Owing to the absence of high quality tissue in this retrospective study we were unable to determine the methylation status of the *MLH1* promoter and whether or not the two changes in *MSH2* affected different alleles. Such studies need to be done in order to determine if somatic mismatch repair gene mutations in mismatch repair deficient cells confer additional functional properties. In this context it is important to note that coding mononucleotide tracts that are vulnerable to frameshifts exist not only in MSH6, but also in MSH2 as shown here.[13] Somatic mutation of the mismatch repair genes (not including *MLH1* promoter methylation) occurred at a rate of 5-10% in endometrial cancers, 2/42, 3/42, and 4/42 for *MSH2*, *MLH1*, and *MSH6* respectively (table 1).

Discussion

In an unselected consecutive retrospective series of 74 endometrial cancers, microsatellite instability was found in 17 (23%). These 17 patients plus 25 other patients whose tumours were MSI negative were studied for *MSH2*, *MLH1*, and *MSH6* somatic and germline mutations. Germline mutation in *MLH1* was found in one endometrial cancer patient. Thus, hereditary mutations in these genes contribute to sporadic endometrial cancer at a rate of at least 1.4% (1/74). If the germline missense change in *MSH2* is causally related to the cancer in one patient then the contribution of hereditary mutations would be 2/74. This incidence is higher than in several previous studies.[6–10]

In all, the previous authors studied 352 EC tumours for microsatellite instability and found 78 that were MSI positive (22%). These 78 patients were studied by various methods for germline mutations in *MLH1* and *MSH2* and only one was found, corresponding to a frequency of 1/352 or 0.3%. Because of small numbers and varying methodologies, it is not possible to assess which of the two estimates (this study of 1.4% and that by previous authors of 0.3%) is most likely to be correct. Intuitively, the high incidence of EC in HNPCC families would seem to suggest that germline mutation must occur with appreciable frequency in "sporadic" EC. The large study of Wijnen *et al*[12] disclosed as many as 10 different truncating germline mutations of *MSH6* among HNPCC or HNPCC-like families. These families had been ascertained clinically as being positive for the original or modified Amsterdam criteria. The families in which *MSH6* was mutated characteristically had many patients with EC. It therefore seems that in addition to *MLH1* and *MSH2*, one would expect *MSH6* to be mutated in some "sporadic" EC patients. As can be seen in table 1, "sporadic" EC patients nevertheless often have some degree of a family history of cancer. This study is the first one that specifically searched for mutations in *MSH6* in sporadic EC; the absence of mutations is somewhat surprising in view of the findings of Wijnen *et al*.[12] It remains to be seen whether a larger series of patients might disclose mutations in *MSH6*. If not, one may need to consider whether truncating mutations of *MSH6* are somehow enriched in the Dutch population and rare elsewhere.

- To revisit the previously stated minimal role of hereditary nonpolyposis colorectal cancer (HNPCC) in "sporadic" endometrial cancer (EC), 74 unselected ECs were studied for microsatellite instability (MSI); 17/74 (23%) were MSI(+).
- Mutational analyses were performed for *MSH2*, *MLH1*, and *MSH6* in these 17 patients and an additional 25 MSI negative patients, most with a family history of cancer.
- One definite germline mutation was found in *MLH1*. A missense change in *MSH2* needs further study. Thus, the proportion of hereditary mutations was at least 1/74 (1.4%), but *MSH6* did not contribute.
- Frameshifts in a previously unreported hypermutable region of seven coding adenosines in exon 4 of *MSH2* were discovered in two MSI positive tumours.
- In conclusion, hereditable mismatch repair deficiency accounts for a small but definite proportion of sporadic EC.

We thank Dr Päivi Peltomäki for critical reading of this manuscript and Dr Wendy Frankel, Dr Gerard Nuovo, and Tina McKeegan for assistance with immunohistochemistry. This work was supported by NIH grants CA16058 and CA67941 and European Commission Grant BMH4CT960772.

1 Watson P, Lynch HT. Extracolonic cancer in hereditary nonpolyposis colorectal cancer. *Cancer* 1983;**71**:677-85.
2 Aarnio M, Sankila R, Pukkala E, Salovaara R, Aaltonen LA, de la Chapelle A, Peltomäki P, Mecklin JP, Järvinen HJ. Cancer risk in mutation carriers of DNA-mismatch-repair genes. *Int J Cancer* 1999;**81**:214-18.
3 Dunlop MG, Farrington SM, Carothers AD, Wyllie AH, Sharp L, Burn J, Liu B, Kinzler KW, Vogelstein B. Cancer risk associated with germline DNA mismatch repair gene mutations. *Hum Mol Genet* 1997;**6**:105-10.
4 Lynch HT, de la Chapelle A. Genetic susceptibility to nonpolyposis colorectal cancer. *J Med Genet* 1999;**36**:801-18.
5 Salovaara R, Loukola A, Kristo P, Kääriäinen H, Ahtola H, Eskelinen M, Härkönen N, Julkunen R, Kangas E, Ojala S, Tulikoura J, Valkamo E, Järvinen H, Mecklin JP, Aaltonen LA, de la Chapelle A. Population-based molecular detection of hereditary nonpolyposis colorectal cancer. *J Clin Oncol* 2000;**18**:2193-200.
6 Katabuchi H, van Rees B, Lambers AR, Ronnett BM, Blazes MS, Leach FS, Cho KR, Hedrick L. Mutations in DNA mismatch repair genes are not responsible for microsatellite instability in most sporadic endometrial carcinomas. *Cancer Res* 1995;**55**:5556-60.
7 Kobayashi K, Matsushima M, Koi S, Saito H, Sagae S, Kudo R, Nakamura Y. Mutational analysis of mismatch repair genes, hMLH1 and hMSH2, in sporadic endometrial carcinomas with microsatellite instability. *Jpn J Cancer Res* 1996;**87**:141-5.
8 Lim PC, Tester D, Cliby W, Ziesmer SC, Roche PC, Hartmann L, Thibodeau SN, Podratz KC, Jenkins RB. Absence of mutations in DNA mismatch repair genes in sporadic endometrial tumors with microsatellite instability. *Clin Cancer Res* 1996;**11**:1907-11.
9 Gurin CC, Federici MG, Kang L, Boyd J. Causes and consequences of microsatellite instability in endometrial carcinoma. *Cancer Res* 1999;**59**:462-6.
10 Kowalski LD, Mutch DG, Herzog TJ, Rader JS, Goodfellow PJ. Mutational analysis of MLH1 and MSH2 in 25 prospectively-acquired RER+ endometrial cancers. *Genes Chrom Cancer* 1997;**18**:219-27.
11 Hofstra RMW, Wu Y, Berends MJW, Mensink RGJ, Sijmons RH, van der Zee AGJ, Hollema H, Kleibeuker JH, Buys CHCM. *Am J Hum Genet* 1998;**63**:A21.
12 Wijnen J, de Leeuw W, Vasen H, van der Klift H, Moller P, Stormorken A, Meijers-Heijboer H, Lindhout D, Menko F, Vossen S, Moslein G, Tops C, Brocker-Vriends A, Wu Y, Hofstra R, Sijmons R, Cornelisse C, Morreau H, Fodde R. Familial endometrial cancer in female carriers of MSH6 germline mutations. *Nat Genet* 1999;**23**:142-4.
13 Boland CR, Thibodeau SN, Hamilton SR, Sidransky D, Eshleman JR, Burt RW, Meltzer SJ, Rodriguez-Bigas MA, Fodde R, Ranzani GN, Srivastava S. A National Cancer Institute Workshop on Microsatellite Instability for cancer detection and familial predisposition: development of international criteria for the determination of microsatellite instability in colorectal cancer. *Cancer Res* 1998;**58**:5248-57.
14 Wu Y, Berends MJW, Mensink RGJ, Kempinga C, Sijmons RH, van der Zee AGJ, Hollema H, Kleibeuker JH, Buys CHCM, Hofstra RMW. Association of hereditary nonpolyposis colorectal cancer-related tumors displaying low microsatellite instability with MSH6 germline mutations. *Am J Hum Genet* 1999;**65**:1291-8.
15 Caduff RF, Johnston CM, Svoboda-Newman SM, Poy EL, Merajver SD, Frank TS. Clinical and pathological significance of microsatellite instability in sporadic endometrial carcinoma. *Am J Pathol* 1996;**148**:1671-8.
16 Burks RT, Kessis TD, Cho KR, Hedrick L. Microsatellite instability in endometrial carcinoma. *Oncogene* 1994;**9**:1163-6.
17 Risinger JI, Berchuck A, Kohler MF, Watson P, Lynch HT, Boyd J. Genetic instability of microsatellites in endometrial carcinoma. *Cancer Res* 1993;**53**:5100-3.
18 Helland Å, Børresen-Dale AL, Peltomäki P, Hektoen M, Kristensen GB, Nesland JM, de la Chapelle A, Lothe RA. Microsatellite instability in cervical and endometrial carcinomas. *Int J Cancer* 1997;**70**:499-501.
19 Esteller M, Catasus L, Matias-Guiu X, Mutter GL, Prat J, Baylin SB, Herman JG. hMLH1 promoter hypermethylation is an early event in human endometrial tumorigenesis. *Am J Pathol* 1999;**5**:1767-72.
20 Esteller M, Levine R, Baylin SB, Ellenson LH, Herman JG. MLH1 promoter hypermethylation is associated with the microsatellite instability phenotype in sporadic endometrial carcinomas. *Oncogene* 1998;**17**:2413-17.
21 Simpkins SB, Bocker T, Swisher EM, Mutch DG, Gersell DJ, Kovatich AJ, Palazzo JP, Fishel R, Goodfellow PJ. MLH1 promoter methylation and gene silencing is the primary cause of microsatellite instability in sporadic endometrial cancers. *Hum Mol Genet* 1999;**8**:661-6.
22 Herman JG, Umar A, Polyak K, Graff JR, Ahuja N, Issa JPJ, Markowitz S, Willson JKV, Hamilton SR, Kinzler KW, Kane MF, Kolodner RD, Vogelstein B, Kunkel TA, Baylin SB. Incidence and functional consequences of hMLH1 promoter hypermethylation in colorectal carcinoma. *Proc Natl Acad Sci USA* 1998;**95**:6870-5.
23 Zhou XP, Hoang JM, Li YJ, Seruca R, Carneiro F, Sobrinho-Simoes M, Lothe RA, Gleeson CM, Russell SE, Muzeau F, Flejou JF, Hoang-Xuan K, Lidereau R, Thomas G, Hamelin R. Determination of the replication error phenotype in human tumors without the requirement for matching normal DNA by analysis of mononucleotide repeat microsatellites. *Genes Chrom Cancer* 1998;**2**:101-7.
24 de la Chapelle A. Testing tumors for microsatellite instability. *Eur J Hum Genet* 1999;**7**:407-8.
25 Samowitz WS, Slattery ML, Potter JD, Leppert MF. BAT-26 and BAT-40 instability in colorectal adenomas and carcinomas and germline polymorphisms. *Am J Pathol* 1999;**154**:1637-41.
26 Pyatt R, Chadwick RB, Johnson CK, Adebamowo C, de la Chapelle A, Prior TW. Polymorphic variation at the BAT-25 and BAT-26 loci in individuals of African origin. Implications for microsatellite instability testing. *Am J Patho*l 1999;**155**:349-53.
27 Aaltonen LA, Salovaara R, Kristo P, Canzian F, Hemminki A, Peltomäki P, Chadwick RB, Kääriäinen H, Percesepe A, Ahtola H, Härkönen N, Julkunen R, Kangas E, Ojala S, Tulikoura J, Valkamo E, Eskelinen M, Järvinen H, Mecklin JP, de la Chapelle A. Incidence of hereditary nonpolyposis colorectal cancer and the feasibility of molecular screening for the disease. *N Engl J Med* 1998;**338**:1481-7.
28 Tannergard P, Lipford JR, Kolodner R, Frodin JE, Nordenskjold M, Lindblom A. Mutation screening in the hMLH1 gene in Swedish hereditary nonpolyposis colon cancer families. *Cancer Res* 1995;**55**:6092-6.
29 Shimodaira H, Filosi N, Shibata H, Suzuki T, Radice P, Kanamaru R, Friend SH, Kolodner RD, Ishioka C. Functional analysis of human MLH1 mutations in Saccharomyces cerevisiae. *Nat Genet* 1998;**4**:384-9.
30 Liu B, Parsons R, Papadopoulos N, Nicolaides NC, Lynch HT, Watson P, Jass JR, Dunlop M, Wyllie A, Peltomäki P, de la Chapelle A, Hamilton SR, Vogelstein B, Kinzler KW. Analysis of mismatch repair genes in hereditary nonpolyposis colorectal cancer patients. *Nat Med* 1996;**2**:169-74.

31 Brieger A, Trojan J, Raedle J, Roth WK, Zeuzem S. Identification of germline mutations in hereditary nonpolyposis colorectal cancer using base excision sequence scanning analysis. *Clin Chem* 1999;**45**:1564-7.
32 Maliaka YK, Chudina AP, Belev NF, Alday P, Bochkov NP, Buerstedde JM. CpG dinucleotides in the hMSH2 and hMLH1 genes are hotspots for HNPCC mutations. *Hum Genet* 1996;**97**:251-5.
33 Liu T, Stathopoulos P, Lindblom P, Rubio C, Wasteson Arver B, Iselius L, Holmberg E, Gronberg H, Lindblom A. MSH2 codon 322 Gly to Asp seems not to confer an increased risk for colorectal cancer susceptibility. *Eur J Cancer* 1998;**34**:1981.
34 Malkhosyan S, Rampino N, Yamamoto H, Perucho M. Frameshift mutator mutations. *Nature* 1996;**382**:499-500.
35 Souza RF, Appel R, Yin J, Wang S, Smolinski KN, Abraham JM, Zou TT, Shi YQ, Lei J, Cottrell J, Cymes K, Biden K, Simms L, Leggett B, Lynch PM, Frazier M, Powell SM, Harpaz N, Sugimura H, Young J, Meltzer SJ. Microsatellite instability in the insulin-like growth factor II receptor gene in gastrointestinal tumours. *Nat Genet* 1996;**14**:255-7.
36 Swisher EM, Mutch DG, Herzog TJ, Rader JS, Kowalski LD, Elbendary A, Goodfellow PJ. Analysis of MSH3 in endometrial cancers with defective DNA mismatch repair. *J Soc Gynecol Invest* 1998;**5**:210-16.
37 Markowitz S, Wang J, Myeroff L, Parsons R, Sun L, Lutterbaugh J, Fan RS, Zborowska E, Kinzler KW, Vogelstein B, Brattain M, Willson JKV. Inactivation of the type II TGF-beta receptor in colon cancer cells with microsatellite instability. *Science* 1995;**268**:1336-8.
38 Rampino N, Yamamoto H, Ionov Y, Li Y, Sawai H, Reed JC, Perucho M. Somatic frameshift mutations in the BAX gene in colon cancers of the microsatellite mutator phenotype. *Science* 1997;**275**:967-9.
39 Duval A, Gayet J, Zhou XP, Iacopetta B, Thomas G, Hamelin R. Frequent frameshift mutations of the TCF-4 gene in colorectal cancers with microsatellite instability. *Cancer Res* 1999;**59**:4213-15.
40 Riccio A, Aaltonen LA, Godwin AK, Loukola A, Percesepe A, Salovaara R, Masciullo V, Genuardi M, Paravatou-Petsotas M, Bassi DE, Ruggeri BA, Klein-Szanto AJ, Testa JR, Neri G, Bellacosa A. The DNA repair gene MBD4 (MED1) is mutated in human carcinomas with microsatellite instability. *Nat Genet* 1999;**23**:266-8.
41 Chadwick RB, Jiang GL, Bennington GA, Yuan B, Johnson CK, Stevens MW, Niemann TH, Peltomäki PT, Huang S, de la Chapelle A. Candidate tumor suppressor RIZ is frequently involved in colorectal carcinogenesis. *Proc Natl Acad Sci USA* 2000;**97**:2662-7.

website extra

The supplementary data (figs 2–7) can be found on the JMG website

www.jmedgenet.com

Absence of learning difficulties in a hyperactive boy with a terminal Xp deletion encompassing the *MRX49* locus

E S Tobias, G Bryce, G Farmer, J Barton, J Colgan, N Morrison, A Cooke, J L Tolmie

J Med Genet 2001;**38**:466–469

Duncan Guthrie Institute of Medical Genetics, Yorkhill, Glasgow G3 8SJ, UK
E S Tobias
J Colgan
N Morrison
A Cooke
J L Tolmie

Department of Child and Family Psychiatry, Yorkhill NHS Trust, Glasgow G3 8SJ, UK
G Bryce
J Barton

Department of Paediatrics, Raigmore Hospital, Old Perth Road, Inverness IV2 3UJ, UK
G Farmer

Correspondence to: Dr Tobias, gbcv55@udcf.gla.ac.uk

EDITOR—The genetic counselling of a pregnant woman who carries an Xp chromosomal deletion is far from straightforward. While the precise locations of the *CDPX1* (arylsulphatase E), steroid sulphatase (*STS*), and Kallman (*KAL1*) genes are known and FISH probes are available for these well characterised genes, the positions of putative mental retardation genes in this region have not yet been determined. Clinical and molecular studies undertaken over

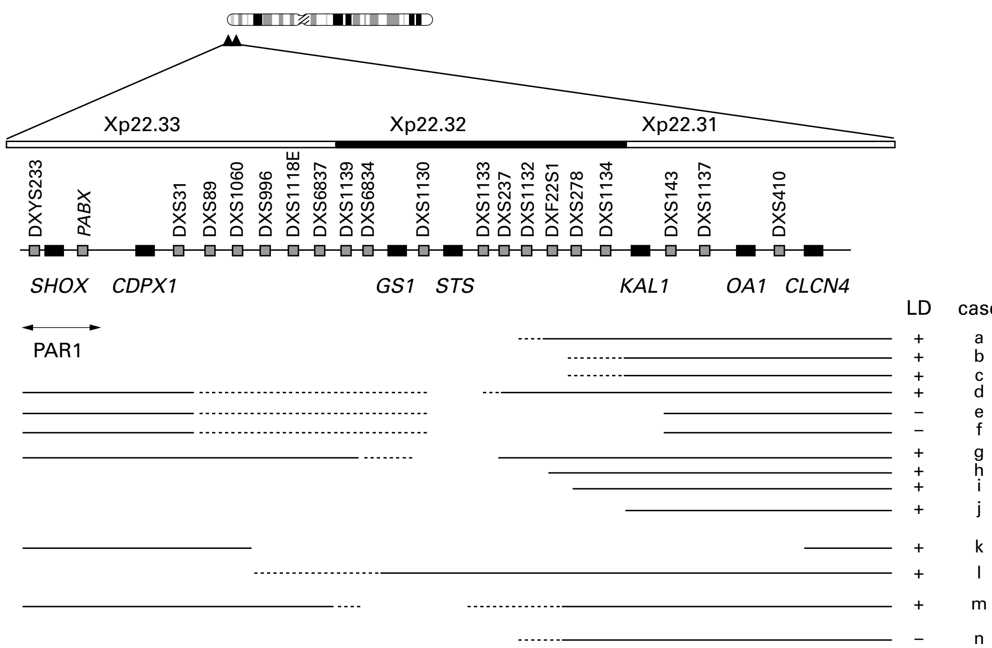

Figure 1 (a) Case 6, (b) case 8, (c) case 9, (d) case 4, (e) case 12, and (f) case 13 of Ballabio et al,[1] (g)-(j) cases BA16, BA20, BA139, and BA75 of Schaefer et al,[3] (k) boy with IQ of 46, short stature, generalised ichthyosis, hypogonadotrophic hypogonadism, nystagmus, and photophobia,[2] (l) boy with aggressive and hyperactive behaviour, myoclonic epilepsy, developmental delay, and no speech aged 4 years 8 months,[4] (m) monozygous male twins with X linked ichthyosis, learning difficulties (LD), and epilepsy,[10] (n) our patient, with short stature, Binder syndrome, and ichthyosis (consistent with the loss of the SHOX, CDPX1, and STS genes, respectively) but no significant learning difficulties. The presence (+) or absence (-) of LD is indicated for each case. A broken line indicates the chromosomal region within which the breakpoint is assumed to lie, while a solid line indicates a retained region.

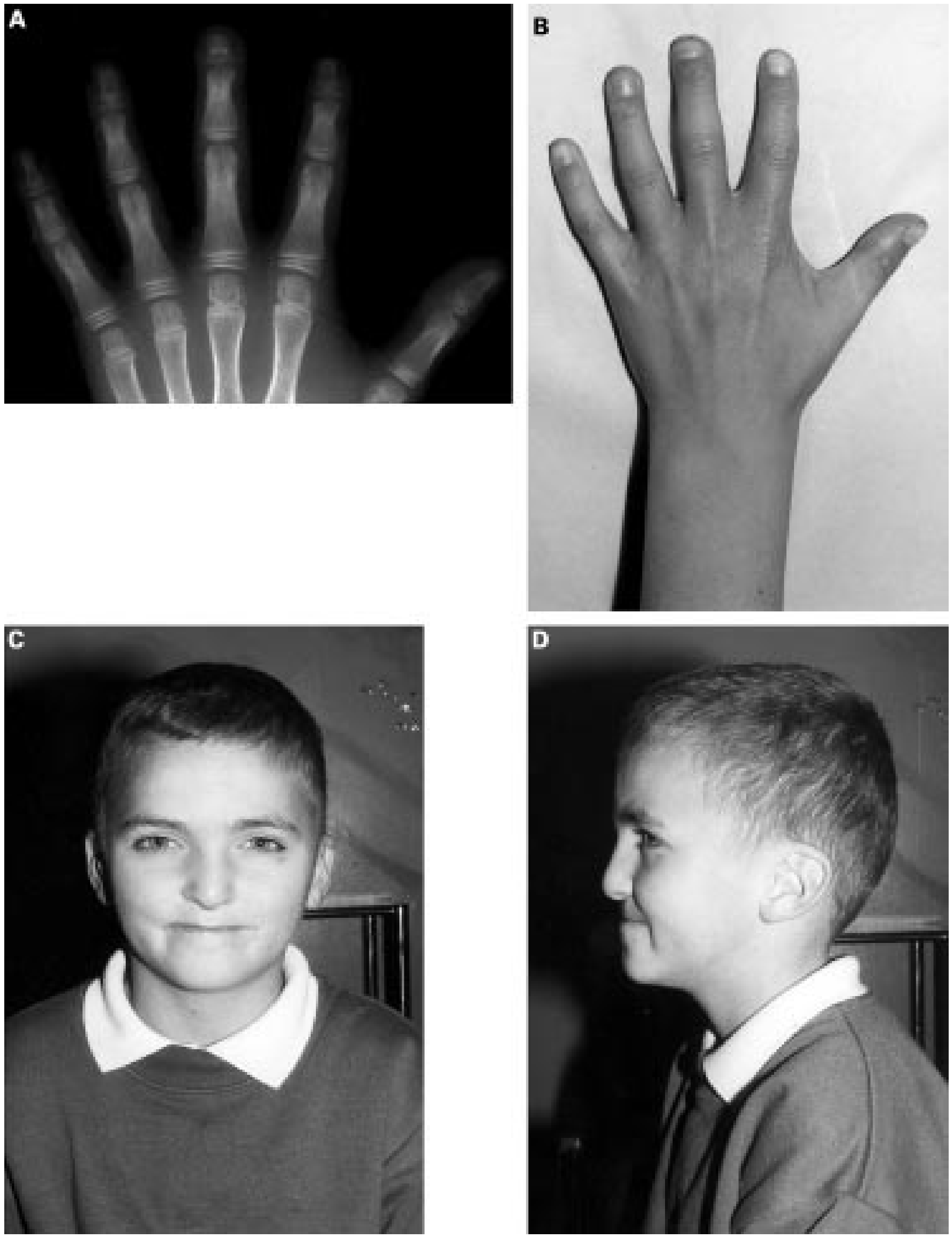

Figure 2 (A) Radiograph of left hand showing shortening of distal phalanx of middle finger. (B) Dorsum of left hand. (C) AP and (D) lateral views of our patient, aged 9, showing facial dysmorphism similar to that in Binder syndrome (see text for description).

the past 10 years on patients with distal Xp deletions imply, however, that the putative X linked mental retardation (XLMR) gene, *MRX49*, lies distal to *GS1* and *STS* but proximal to DXS31 and *CDPX1* (fig 1).[1–4]

Here we describe the clinical, cytogenetic, and molecular features of a boy with an unbalanced X;Y translocation resulting in a deletion of Xp extending from Xptel to the *STS* gene who, intriguingly, does not have learning difficulties (LD), despite the loss of this putative XLMR locus.

Case report

This 9 year old boy was delivered at term by caesarean section on account of fetal distress. He weighed only 2610 g but did not have any significant problems neonatally. His developmental milestones were achieved satisfactorily but he was investigated, aged 21 months, on account of his significant hyperactivity and ichthyosis. He has facial dysmorphism akin to that of Binder syndrome, including a broad nasal bridge and forehead, maxillary hypoplasia, relative prognathism, and dental malocclusion, in addition to terminal phalangeal shortening (fig 2). He suffered from epileptic seizures from the age of around 6 months, requiring prophylactic medication for two years. With the exception of one seizure that lasted 45 minutes, the fits were all brief and associated with pyrexia. His height lies just above the 3rd centile, while his head circumference and weight lie between the 25th and 50th centiles. He was diagnosed by a child

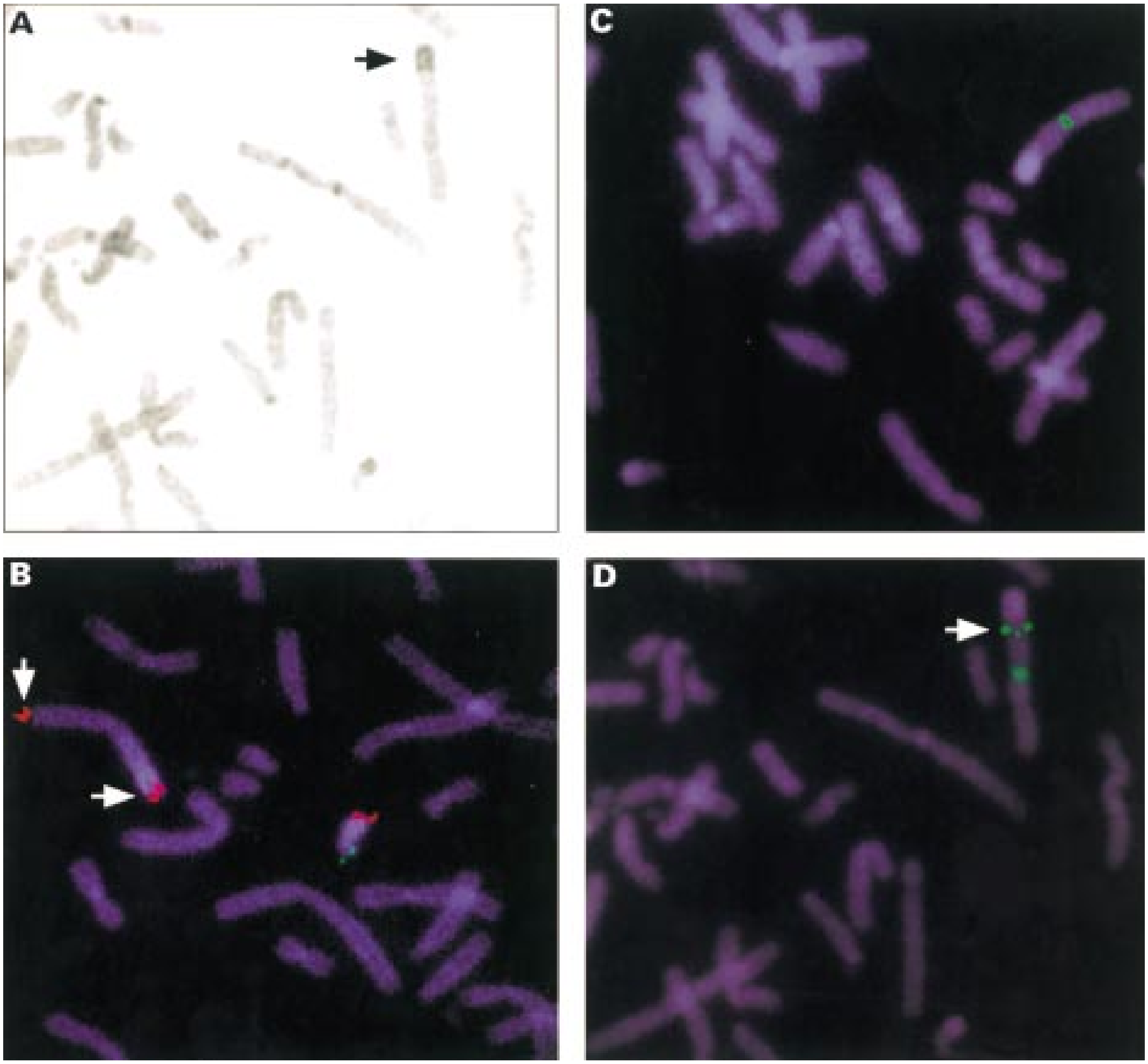

Figure 3 Chromosome analysis of our patient. (A) DAPI stained metaphase spread showing the presence of Y derived heterochromatin (arrow) on Xp. FISH analysis showing (B) the presence of the (red) XYqtel signal (arrow) at the tips of both arms of the derivative X chromosome and the (green) XYptel signal on the Y chromosome only, (C) the absence of STS signal on the derivative X chromosome, and (D) the presence of KAL1 signal (arrow) on the derivative X chromosome.

psychiatrist as having attention deficit hyperactivity disorder (ADHD) and was treated successfully with methylphenidate.

Psychometric testing, done by a senior educational psychologist, in addition to his assessment by his schoolteacher, indicated that he is of average cognitive potential and does not have any innate learning difficulties. His CT

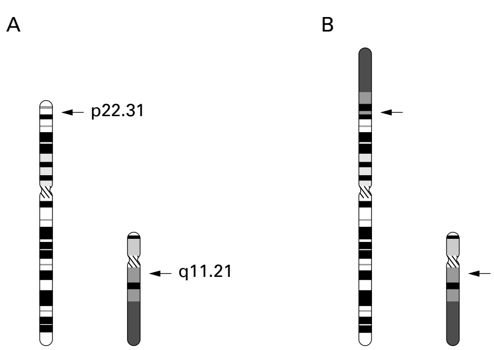

Figure 4 Schematic indication of the origin of the derivative X chromosome showing (A) the X and Y chromosome breakpoints and (B) the derivative X chromosome.

Table 1 Results of molecular (DXYS233, PABX, DXS996, DXS1118E, DXS6837, DXS1139, DXS6834, DXS1130, DXS237, DXS278, and DXS987) and FISH (XYqtel, XYptel, STS and KAL1) analyses undertaken to determine the location of the Xp breakpoint in our patient

Marker	*Result*
XYqtel	+
XYptel	−
DXYS233	−
PABX	−
DXS996	−
DXS1118E	−
DXS6837	−
DXS1139	−
DXS6834	−
DXS1130	−
STS	−
DXS237	−
DXS278	+
KAL1	+
DXS987 (Xp22.2)	+

and EEG proved normal. Cytogenetic analysis, however, showed his karyotype to be 46,Y,der(X)t(X;Y)(p22.31;q11.21). The derivative X chromosome was found to lack the XYptel and *STS* sequences but to contain a large region of Y long arm material, including the heterochromatic region and the XYqtel sequence (figs 3 and 4). Additional FISH and molecular analyses were carried out, localising the Xp breakpoint to between the *STS* and *KAL1* genes (table 1). His mother is a carrier of the derivative X chromosome and has carrier levels of STS activity.

All FISH probes were used essentially according to the manufacturer's instructions. Hybridisations were performed on metaphase chromosomes using *STS* or *KAL1* Xp22.3 region probe with DXZ1 chromosome X control probe (ONCOR)[1 5] or chromoprobe T XYptel/qtel (CYTOCELL).[6]

Discussion

While the boy's short stature, craniofacial abnormalities, and ichthyosis are certainly consistent with the loss of the *SHOX*, *CDPX1*, and *STS* genes, respectively, the severe hyperactivity which he exhibited in his early childhood was not readily predictable from his karyotype. Although both twin and adoption studies suggest that attention deficit and hyperactivity are strongly heritable,[7] these complex disorders are likely to be multifactorial and genetically heterogeneous. The marked hyperactivity observed in this boy and the boy reported by Spranger *et al*[4] might reflect the loss of an unidentified ADHD susceptibility gene in this Xp region, although we cannot exclude the possibility of the ADHD being an unrelated finding.

The results of the mapping studies (fig 1) have hitherto been interpreted as indicating that an XLMR gene is located between *DXS31* and *STS*. These analyses have included a clinical and molecular study of 27 patients with deletions involving the distal short arm of the X chromosome,[1] a description by Schaefer *et al*[3] of several patients with LD and terminal and interstitial Xp deletions,[3] and a two point linkage analysis with X chromosomal markers on a family in which five males in two generations showed mild to moderate LD.[8]

The boy reported by Spranger *et al*,[4] with an Xp terminal deletion with a breakpoint distal to the *STS* gene, was described as having LD in addition to short stature and chondrodysplasia punctata. Their molecular analysis would suggest that the putative MRX gene, *MRX49*, lies distal to *GS1*, which is consistent with the mapping data provided by Ballabio *et al*[1] (fig 1). Furthermore, very recently, a gene which resides between markers DXS1139 and DXS6837, *VCX-A*, was identified by further deletion mapping of 15 males with Xp deletions.[9] This gene was reported to be deleted or retained in all of the subjects who had LD or were of normal intelligence, respectively.[9]

The lack of LD in the boy described here would suggest, however, either that the putative XLMR gene is located more proximally than previously considered or that if such a gene is located distal to *STS*, its deletion is alone insufficient to cause LD. The genotype-phenotype correlation is, therefore, much less straightforward than might have been inferred from previous reports. This has important implications for the accurate counselling of carriers of similar Xp chromosomal deletions.

1 Ballabio A, Bardoni B, Carrozzo R, Andria G, Bick D, Campbell L, Hamel B, Ferguson-Smith MA, Gimelli G, Fraccaro M, Maraschio P, Zuffardi O, Guioli S, Camerino G. Contiguous gene syndromes due to deletions in the distal short arm of the human X chromosome. *Proc Natl Acad Sci USA* 1989;**86**:10001-5.
2 Muroya K, Ogata T, Matsuo N, Nagai T, Franco B, Ballabio A, Rappold G, Sakura N, Fukushima Y. Mental retardation in a boy with an interstitial deletion at Xp22.3 involving STS, KAL1, and OA1: implication for the MRX locus. *Am J Med Genet* 1996;**64**:583-7.
3 Schaefer L, Ferrero GB, Grillo A, Bassi MT, Roth EJ, Wapenaar MC, van Ommen GJB, Mohandas TK, Rocchi M, Zoghbi HY, Ballabio A. A high resolution deletion map of human chromosome Xp22. *Nat Genet* 1993;**4**:272-9.
4 Spranger S, Schiller S, Jauch A, Wolff K, Rauterberg-Ruland I, Hager D, Tariverdian G, Troger J, Rappold G. Leri-Weill syndrome as part of a contiguous gene syndrome at Xp22.3. *Am J Med Genet* 1999;**83**:367-71.
5 Ballabio A, Andria G. Deletions and translocations involving the distal short arm of the human X chromosome: review and hypotheses. *Hum Mol Genet* 1992;**1**:221-7.
6 NIH and Institute of Molecular Medicine Collaboration. A complete set of human telomeric probes and their clinical application. *Nat Genet* 1996;**14**:86-9.
7 Thapar A, Holmes J, Poulton K, Harrington R. Genetic basis of attention deficit and hyperactivity. *Br J Psychiatry* 1999;**174**:105-11.
8 Claes S, Vogels A, Holvoet M, Devriendt K, Raeymaekers P, Cassiman JJ, Fryns JP. Regional localization of two genes for nonspecific X-linked mental retardation to Xp22.3-p22.2 (MRX49) and Xp11.3-p11.21 (MRX50). *Am J Med Genet* 1997;**73**:474-9.
9 Fukami M, Kirsch S, Schiller S, Richter A, Benes V, Franco B, Muroya K, Rao E, Merker S, Niesler B, Ballabio A, Ansorge W, Ogata T, Rappold GA. A member of a gene family on Xp22.3, VCX-A, is deleted in patients with X-linked nonspecific mental retardation. *Am J Hum Genet* 2000;**67**:563-73.
10 Gohlke BC, Haug K, Fukami M, Friedl W, Noeker M, Rappold GA, Haverkamp F. Interstitial deletion in Xp22.3 is associated with X linked ichthyosis, mental retardation, and epilepsy. *J Med Genet* 2000;**37**:600-2.

Identification of a new *TWIST* mutation (7p21) with variable eyelid manifestations supports locus homogeneity of BPES at 3q22

Helene Dollfus, Govindasamy Kumaramanickavel, Partha Biswas, Corinne Stoetzel, Renaud Quillet, Michael Denton, Marion Maw, Fabienne Perrin-Schmitt

J Med Genet 2001;**58**:470–471

LGME du CNRS, INSERM U184, Faculté de Médecine, 11 rue Humann, 67085 Strasbourg, France
H Dollfus
C Stoetzel
R Quillet
F Perrin-Schmitt

Sankara Nethralaya, Medical Research Foundation, 18 College Road, Chennai, India
G Kumaramanickavel

Anandalok, Asutosh Mukherjee Road, Calcutta, India
P Biswas

Biochemistry Department, University of Otago, PO Box 56, Dunedin, New Zealand
M Denton
M Maw

Correspondence to:
Dr Dollfus,
helene.dollfus@medecine.u-strasbg.fr

EDITOR—Blepharophimosis-ptosis-epicanthus inversus syndrome (BPES) is an autosomal dominant disorder of eyelid development defined by small palpebral fissures, epicanthus inversus, and ptosis.[1 2] BPES type I (OMIM 110100) is characterised by female infertility, whereas BPES type II (OMIM 601649) is transmitted by both females and males. Most cases of BPES types I and II map to chromosome 3q22-q23 (*BPES1*).[3–7] However, a second locus (*BPES2*) was reported in the chromosome 7p13-p21 region on the basis of patients presenting with eyelid anomalies carrying chromosomal abnormalities in the 7p21 region[8–11] and the further linkage data of a large Indian family diagnosed initially with BPES type II.[7] The *TWIST* gene, mapped on chromosome 7p21, codes for a transcription factor with a bHLH domain.[12] *TWIST* mutations[13–18] have been reported in the heterozygous state in patients presenting with the Saethre-Chotzen syndrome (SCS, OMIM 101400). This disorder is a common autosomal dominant form of syndromic craniosynostosis defined by craniostenosis, minor limb and ear abnormalities, and frequent ptosis of the eyelids.[19] In the present study, molecular genetic analysis at *TWIST* and subsequent clinical re-evaluation of the Indian family were used to investigate the possibility that prominent eyelid malformations may represent a clinical variant in the spectrum of phenotypes associated with SCS.

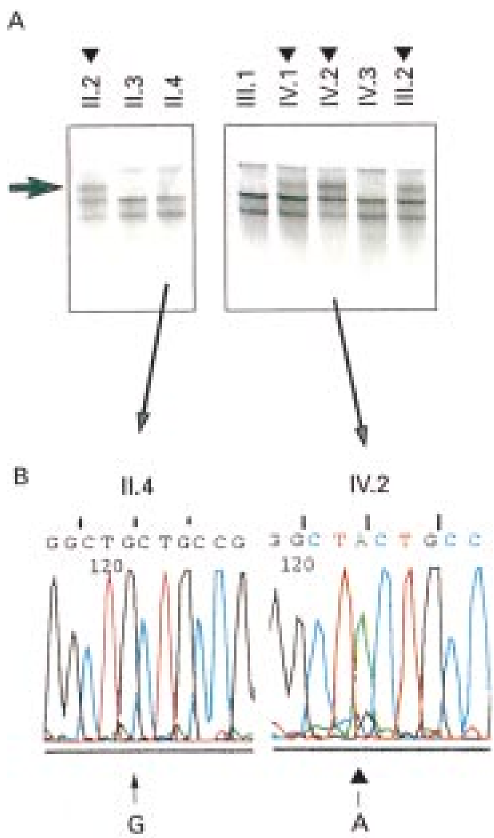

Figure 1 Abnormal SSCP pattern and sequence analysis showing the TWIST mutation (identification of patients was done according to Maw et al[7]). (A) Abnormal SSCP band (arrow) of affected patients (arrow heads) compared to unaffected members of the family. (B) Sequence analysis: antisense sequence of II.4, an unaffected member of the family, compared to IV.2, a patient carrying the mutation. All the patients with an abnormal SSCP band carried the 28 C→T mutation.

The four generation Indian family originates from the Bihar region in the western part of India. The members of the family were initially referred in 1995 because of palpebral anomalies.[7] Clinical re-evaluation of the family took place at the Anandalok Eye Hospital in Calcutta in June 2000. Nineteen members of the family, including 17 affected persons, were examined in detail (photographs and *x* rays available on request for all affected members).

DNA samples, extracted from Guthrie cards, were available from 31 members of the Indian family.[7] These samples were PCR amplified for *TWIST* and PCR products were subjected to single strand sequence conformation polymorphism (SSCP) and direct sequencing analyses. The primer pair that allowed detection of the mutations reported here was forward primer, VB56 (5' - GAG GCGCCCCGCTCTTCTCCTCTG - 3') and reverse primer TQ 53 (5' - CGTCTGAAGAACGGCGCGAA - 3'). A specific migration pattern was observed after amplification of the DNA of all 16 members of the Indian family who were previously reported to have an abnormal clinical examination. In all cases, the abnormal SSCP pattern cosegregated with the previously reported haplotype of linked chromosome 7p markers[7] (fig 1). Direct sequence analyses were performed on the PCR products of all 31 DNA samples. All 16 samples with an abnormal SSCP pattern showed the same heterozygous mutation, namely a C to T transition at position +82, changing a CAG codon to TAG, which is predicted to result in premature termination of the protein at codon 28 (28 C→T) positioned far upstream of the bHLH motif and probably within the recently reported histone acetyltransferase interaction domain.[20] This nonsense *TWIST* mutation probably results in the absence of stable protein synthesis from the

Figure 2 Photographs of two members of the family carrying the mutation showing variable phenotypes. (A) Full face of patient II.1 showing bilateral ptosis and reduced palpebral aperture. (B) Profile of patient II.I. (C) Full face of patient IV.6 showing asymmetrical orbits and narrow forehead. (D) Profile of patient IV.6 with obvious exophthalmos.

mutant allele and suggests that haploinsufficiency at the *TWIST* locus is responsible for the phenotype in this Indian family.

The phenotype of family members carrying the mutation showed very mild clinical features of SCS in some subjects without evidence of obvious craniostenosis but more pronounced eyelid manifestation compared to other subjects with all the clinical and radiographic evidence of craniostenosis as well as brachydactyly and external ear anomalies (fig 2). Collectively, the phenotype of the affected members of this family was compatible with the diagnosis of SCS with variable expressivity and more pronounced eyelid manifestations in some of them.

Variable expressivity in SCS has been extensively underlined as a pitfall in the establishment of the diagnosis.[19 21] In most cases, the details of the dysmorphic gestalt could not be correlated with the functional defects expected from the *TWIST* mutations detected. That the clinical features of some members of the Indian family were easily confused with BPES indicates that palpebral anomalies may be the main manifestation of haploinsufficiency at the *TWIST* locus in some SCS patients.

In conclusion, genetic and phenotypic assessment of the Indian family, previously reported as locus *BPES2*, now suggests that autosomal dominant BPES (types I and II) is probably a homogeneous disorder with a unique locus on chromosome 3q22-q23 (locus *BPES1*).

We are most grateful to RETINA France for supporting this project. We would like to thank Dr M Le Merrer, Dr J Kaplan, and Professor P Chambon for their continued support. We also thank S Vicaire and the oligonucleotide team from the IGBMC. R Quillet is recipient of a grant from le Ministere de l'Enseignement Superieur et de la Recherche. This work was supported by grants from l'Association de la Recherche sur le Cancer (ARC), from the Faculté de Médecine de Strasbourg, from the Centre National de la Recherche Scientifique, from the Institut National de la Santé et de la Recherche Médicale, and from Les Hôpitaux Universitaires de Strasbourg.

1 Townes PL, Muechler EK. Blepharophimosis, ptosis, epicanthus inversus and primary amenorrhoea. *Arch Ophthalmol* 1979;**97**:1664-6.
2 Zlotogora J, Sagi M, Cohen T. The blepharophimosis, ptosis, and epicanthus inversus syndrome: delineation of two types. *Am J Hum Genet* 1983;**35**:1020-7.
3 Lawson CT, Toomes C, Fryer A, Carette MJM, Taylor GM, Fukushima Y, Dixon MJ. Definition of the blepharophimosis, ptosis, epicanthus inversus syndrome critical region at chromosome 3q23 based on the analysis of chromosomal anomalies. *Hum Mol Genet* 1995;**4**:963-7.
4 Amati P, Chomel JC, Nivelon-Chevalier A, Gilgenkrantz S, Kitzis A, Kaplan J, Bonneau D. A gene for blepharophimosis-ptosis-epicanthus inversus syndrome maps to chromosome 3q23. *Hum Genet* 1995;**96**:213-15.
5 Amati P, Gasparini P, Zlotogora J, Zelante L, Chomel JC, Kitzis A, Kaplan J, Bonneau D. A gene for premature ovarian failure associated with eyelid malformation maps to chromosome 3q22-q23. *Am J Hum Genet* 1996;**58**:1089-92.
6 Small KW, Stalvey M, Fisher L, Mullen L, Dickel C, Beadles K, Reimer R, Lessner A, Lewis K, Pericak-Vance MA. Blepharophimosis syndrome is linked to chromosome 3q. *Hum Mol Genet* 1995;**4**:443-8.
7 Maw M, Kar B, Biswas J, Biswas P, Nancarrow D, Denton M, Bridges R, Kumaramanickavel G, Badrinath SS. Linkage of blepharophimosis syndrome in a large Indian pedigree to chromosome 7p. *Hum Mol Genet* 1996;**5**:2049-54.
8 Bianchi DW, Cirillo-Silengo M, Luzzatti L, Greenstein RM. Interstitial deletion of the short arm of chromosome 7 without craniosynostosis. *Clin Genet* 1981;**19**:456-61.
9 Wang C, Maynard S, Glover TW, Biesecker LG. Mild phenotypic manifestation of a 7p15.3p21.2 deletion. *J Med Genet* 1993;**30**:610-12.
10 Carlo B, Lina A, Vincenzo Z. Deletions of the short arm of chromosome 7 without craniostenosis. *Clin Genet* 1982;**21**:348-9.
11 Cartwright MJ, Hassan TS, Frueh BR. Microdeletion of chromosome 7p syndrome with ocular manifestations. *Ophthal Plast Reconstr Surg* 1995;**11**:139-41.
12 Bourgeois P, Stoetzel C, Bolcato-Bellemin AL, Mattei MG, Perrin-Schmitt F. The human *H-twist* gene is located at 7p21 and encodes a b-HLH protein which is 96% similar to its murine counterpart. *Mamm Genome* 1996;**7**:915-91.
13 El Ghouzzi V, Le Merrer M, Perrin-Schmitt F, Lajeunie E, Benit P, Renier D, Bourgeois P, Bolcato-Bellemin AL, Munnich A, Bonaventure J. Mutations of the *TWIST* gene in the Saethre-Chotzen syndrome. *Nat Genet* 1997;**15**:42-6.
14 Howard TD, Paznekas W A, Green ED, Chiang LC, Ma N, Ortiz De Luna RI, Delgado CG, Gonzalez-Ramos M, Kline AD, Jabs EW. Mutations in *TWIST,* a basic helix-loop-helix transcription factor, in Saethre-Chotzen syndrome. *Nat Genet* 1997;**15**:36-41.
15 Rose CSP, Reardon W, Malcolm S, Winter RM. The *TWIST* gene, although not disrupted in Saethre-Chotzen patients with apparently balanced translocations of 7p21, is mutated in familial and sporadic cases. *Hum Mol Genet* 1997;**8**:1369-73.
16 Zackai EH, Stolle CA. A new twist: some patients with Saethre-Chotzen syndrome have a microdeletion syndrome. *Am J Hum Genet* 1998;**63**:1277-81.
17 Johnson D, Horsley SW, Moloney DM, Oldridge M, Twigg SRF, Walsh S, Barrow M, Njolstad PR, Kunz J, Ashworth GJ, Wall SA, Kearney L, Wilkie AOM. A comprehensive screen for *TWIST* mutations in patients with craniosynostosis identifies a new microdeletion syndrome of chromosome band 7p21.1. *Am J Hum Genet* 1998;**63**:1282-93.
18 Gripp KW, Zackai EH, Stolle C. Mutations in the human *TWIST* gene. *Hum Mutat* 2000;**15**:150-5.
19 Reardon W, Winter RM. Saethre-Chotzen syndrome. *J Med Genet* 1994;**31**:393-6.
20 Harnarnori Y, Sartorelli V, Ogryzko V, Purl PL, Wu HU, Wang JYJ, Nakatani Y, Kedes L. Regulation of histone acetyltransferases p300 and PCAF by the bHLH protein twist and adenoviral oncoprotein EIA. *Cell* 1999;**96**:405-13.
21 Pantke OA, Cohen MM, Witkop CJ, Feingold M, Schaumann B, Pantke HC, Gorlin RJ. The Saethre-Chotzen syndrome. *Birth Defects* 1975;**XI**(2):190-225.

Association between the defective Pro369Ser mutation and in vivo intrahepatic α1-antitrypsin accumulation

Susana Seixas, Ana Isabel Lopes, Jorge Rocha, Lídia Silva, Carlos Salgueiro, Jaime Salazar-de-Sousa, Amélia Batista

EDITOR—α1-antitrypsin (PI), the major inhibitor of neutrophil elastase in the lower respiratory tract, is a highly polymorphic glycoprotein synthesised in the liver that has several rare gene products in which serum protein levels are reduced or even undetectable.[1] Early onset pulmonary emphysema, resulting from unopposed elastase activity, and neonatal cholestasis probably resulting from the retention of the defective protein in the liver,[2] are the two most common clinical manifestations of PI deficiency and are mainly associated with PI*Z, the most common deficient allele. In addition, other rare alleles occasionally associated with liver injury have been shown to share with PI*Z an increased tendency for intracellular accumulation. Recently, a complete intracellular transport block has been reported for a newly identified[3 4] defective Pro369Ser allele (Mwürzburg) by in vitro expression studies in human cell cultures. Adenovirus mediated transfer of the mutant gene into the mouse reproduced the consequences of this block and no traceable amounts of the variant protein could be detected in the plasma after in vivo recombinant expression.[3] However, no detectable intrahepatocytic PI inclusions were found in the mice expressing the Mwürzburg mutant[3] and no liver biopsy material has yet been presented from patients with this defective allele.

Case report

We report a carrier of the Mwürzburg allele with evidence for in vivo intrahepatic accumulation of PI. The patient is a white Portuguese boy who presented at the age of 1.5 months with cholestasis associated with a recent cytomegalovirus (CMV) infection. A percutaneous liver biopsy performed at the age of 2.5 months showed significant portal fibrosis with porto-portal bridging, giant cell transformation, moderate cholestasis, and an intense portal-acinar inflammatory infiltrate. Periodic acid-Schiff staining after diastase treatment (PAS-D) additionally showed the presence of positive, diastase resistant, intracellular inclusions. Immunoperoxidase staining specific for PI was positive (fig 1). Serum PI concentration, determined by automated nephelometry (Behring), was found to be 92% of normal on admission and dropped to 45% of normal at the age of 24 months, after CMV serology (IgM) and antigens became negative and following progressive decline of transaminase levels to their normal upper limit. The PI

J Med Genet 2001;**38**:472–474

Instituto de Patologia e Imunologia Molecular, Universidade do Porto (IPATIMUP), R Dr Roberto Frias s/n, 4200 Porto, Portugal
S Seixas
J Rocha

Faculdade de Ciências, Universidade do Porto, Portugal
S Seixas
J Rocha

Unidade de Gastrenterologia Pediátrica, Hospital de Santa Maria, Lisboa, Portugal
I A Lopes
J Salazar de Sousa

Serviço de Pediatria, Hospital do Barreiro, Barreiro, Portugal
L Silva
C Salgueiro

Serviço de Anatomia Patológica, Hospital de Santa Maria, Lisboa, Portugal
A Batista

Correspondence to: Dr Rocha, jrocha@ipatimup.pt

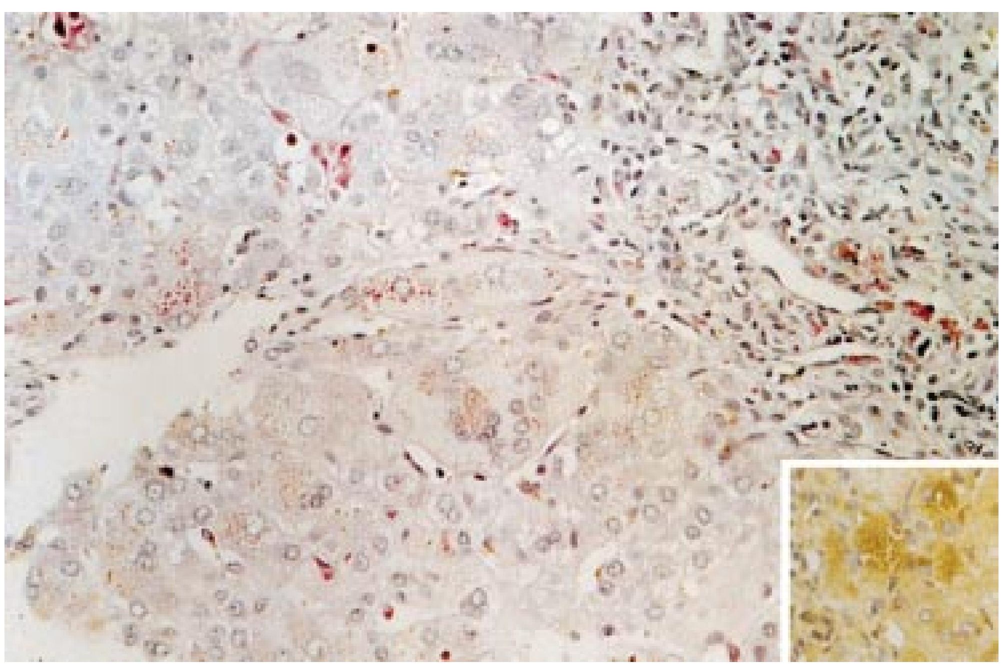

Figure 1 Tissue section from the patient's percutaneous liver biopsy. PAS positive diastase resistant inclusions were found in the cytoplasm of several hepatocytes (PAS-D). PI is identified by immunoperoxidase in inset (immunoperoxidase staining).

Figure 2 PI patterns after polyacrylamide gel hybrid isoelectric focusing (pH range of 4.3 to 4.8) and Coomassie blue staining.[5] *From left (1) M2/S = patient's mother, (2) Mwürzburg/S = patient, (3) Mwürzburg/M3 = patient's father, (4) M1 = control. The major band corresponding to the Mwürzburg gene product is indicated with an arrow.*

concentration in the patient's father was 49% of normal.

Isoelectric focusing analysis of PI types showed that the patient was heterozygous for the S allele and for a deficient variant gene product, inherited from his father, which has an isoelectric point identical to M1 and a band with decreased intensity (fig 2). These patterns were confirmed by print immunofixation (not shown). DNA sequencing of all PI coding exons (II-V), performed as previously described,[6 7] has shown that the patient and his father shared a C to T transition leading to a 369Pro (CCC)→Ser (TCC) substitution in the common M1Val213 allele, as in the variant Mwürzburg.[3 4] The presence of the Mwürzburg allele was also confirmed by partial PCR amplification of exon V with a mismatched primer that generates an 118 bp fragment: 5'-CCCGAGGTCAAGTTCAA CAgA-3' (bases 10049-10069, mismatched base in lower case); 5'- GAGGAGCGAGAGG CAGTTATT-3' (bases 10166-10146). Thirty five cycles of PCR were performed for one minute at 94°C, one minute at 58°C, and one minute at 72°C. The mismatched primer artificially introduces a *Nde*II restriction site in the mutated Pro369Ser allele during PCR amplification (fig 3, lanes 1 and 2). In addition, the primer also generates a further *Hin*fI restriction site in the presence of the Pro369Leu mutation (fig 3, lanes 3 and 4), which characterises the severely deficient variant Mheerlen.[8]

Discussion

To our knowledge the present case represents the first reported association between the defective α1-antitrypsin Pro369Ser mutation and in vivo intrahepatic protein accumulation. Although the S variant has been found to show increased intracellular retention and the ability to form heteropolymers with Z,[9–11] this increase is only marginal and no evident inclusions of S α1-antitrypsin have been found in most pathology samples observed so far. Therefore, the observation of PI liver inclusions in the Mwürzburg/S patient is most likely to be predominantly caused by the Mwürzburg variant and provides further in vivo evidence that the severe deficiency resulting from the Pro369Ser mutation is caused by protein accumulation, as in the case of the Z allele.

Since the patient's PI type would be expected to be similar to SZ, which is not associated with increased risk of liver disease in infancy, his liver injury is probably related more to the CMV infection than to the Mwürzburg variant. However, the similar behaviour of Mwürzburg and Z both in vitro and in vivo indicates that it may lead to liver disease in Mwürzburg homozygotes or in Mwürzburg/Z heterozygous combinations.

Contrary to previous observations,[3] the present detection of a faint PI band with the same isoelectric point of M1, both in the patient and his father, indicates that Mwürzburg can still be secreted in limited amounts into the plasma. However, since the variant will remain unidentified in combination with the common normal M1 allele, the PCR introduction of a *Nde*II restriction site is a simple alternative tool

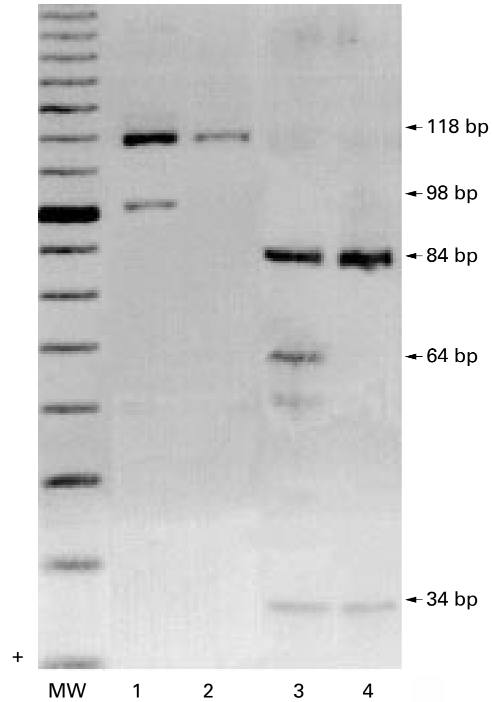

Figure 3 Detection of the Pro369Ser and Pro369Leu mutations after PCR amplification with a mismatched primer. (Lanes 1 and 2) NdeII digested fragments from the Mwürzburg/S patient (1) and from a normal M1 control (2). The Pro369Ser mutated sequence generates one 98 bp fragment and one 20 bp fragment (not visible). (Lanes 3 and 4) HinfI digested fragments from a M2/Mheerlen subject (3) and from a normal M1 control (4). The normal sequence produces one 84 bp fragment and one 34 bp fragment. The Pro369Leu mutated sequence generates an additional restriction site and 64 bp, 34 bp, and 20 bp (not visible) fragments are produced. MW= molecular weight marker. DNA fragments were visualised by silver staining after non-denaturing electrophoresis on 9% polyacrylamide gels.

to detect the Pro369Ser mutation, especially in cases where no unusual isoelectric focusing patterns are associated with decreased PI serum levels or with intrahepatic protein accumulation.

We thank Ms Lúcia Ramires and Ms Piedade Mendonça for technical assistance. This work was supported in part by Conselho de Prevenção do Tabagismo. Susana Seixas is supported by grant BD/13885/97 from Praxis XXI.

1 Cox DW. α1-antitrypsin deficiency. In: Scriver CH, Beaudet AL, Sly WS, Valle D, eds. *The metabolic and molecular bases of inherited disease*. Vol 3. New York: McGraw-Hill, 1995:4125-58.
2 Permultter DH. The cellular basis for liver injury in α1-antitrypsin deficiency. *Hepatology* 1991;**13**:172-85.
3 Poller W, Merklein F, Schneider-Rasp S, Haack A, Fechner H, Wang H, Anagostopoulos I, Weidinger S. Molecular characterisation of the defective α1-antitrypsin alleles PI Mwürzburg (Pro369Ser), Mheerlen (Pro369Leu), and Q0lisbon (Thr68Ile). *Eur J Hum Genet* 1999;**7**:321-31.
4 Rocha J, Seixas S, Lopes AI, Silva L, Salgueiro C, Salazar-de-Sousa J, Batista A. Human gene mutation report. *Hum Genet* 1999;**104**:114.
5 Rocha J, Pinto D, Santos MT, Amorim A, Amil-Dias J, Cardoso-Rodrigues F, Aguiar A. Analysis of the allelic diversity of a (CA)n repeat polymorphism among α1-antitrypsin gene products from northern Portugal. *Hum Genet* 1997;**99**:194-8.
6 Graham A, Kalsheker NA, Bamforth FJ, Newton CR, Markham AF. Molecular characterization of two alpha-1-antitrypsin deficiency variants: proteinase inhibitor (Pi) Nullnewport (Gly115→Ser) and (Pi) Zwrexham (Ser-19→Leu). *Hum Genet* 1990;**85**:537-40.
7 Seixas S, Garcia O, Amorim A, Rocha J. A novel alpha-1-antitrypsin R281del variant found in a population sample from the Basque Country. *Hum Mutat* 2000;**15**:121-2.

8 Hofker MH, Nukiwa T, van Paassen, Nelen M, Kramps JA, Klasen EC, Frants RR, Crystal RG. A Pro→Leu substitution in codon 369 of the alpha-1-antitrypsin deficiency variant PI Mheerlen. *Hum Genet* 1989;**81**:264-8.
9 Teckman JH, Permulter DH. The endoplasmatic reticulum degradation pathway for mutant secretory proteins α1-antitrypsin Z and S is distinct from that for an unassembled membrane protein. *J Biol Chem* 1996;**271**:13215-20.
10 Elliot PR, Stein PE, Bilton D, Carrell RW, Lomas DA. Structural explanation for the deficiency of S α1-antitrypsin. *Nat Struct Biol* 1996;**3**:910-11.
11 Mahadeva R, Chang WSW, Dafforn TR, Oakley DJ, Foreman RC, Calvin J, Wight DGD, Lomas DA. Heteropolymerization of S, I an Z α1-antitrypsin and liver cirrhosis. *J Clin Invest* 1999;**103**:999-1006.

The androgen receptor and DXS15-134 markers show a high rate of discordance for germline X chromosome inactivation

Vikas Mahavni, Seung C Kim, Teresa A Benda, Linda Sanders, Richard E Buller

EDITOR—The process of X chromosome inactivation was identified as early as 1960 when Ohno and Hauschka[1] described the presence of a pyknotic X chromosome in both benign and malignant cell lines. Mary Lyon formalised the role of X inactivation and its relationship to dosage compensation of X chromosome genetic material in a letter to *Nature* in 1961.[2] This phenomenon, now known as the Lyon hypothesis, states that only one X chromosome is transcriptionally active in a given female cell. While the Lyon hypothesis dictates that the X inactivation process is random, skewing of this process to the point of non-random X chromosome inactivation is a known mechanism associated with the development of X linked genetic diseases in females.[3]

Our laboratory has been interested in the association of non-random X chromosome inactivation (NRXI) with ovarian cancer.[4] Not only does this process violate a basic biological principle, the Lyon hypothesis, but it also provides a mechanism to bypass one of two steps generally accepted as necessary for the development of a cancer phenotype, dictated by the Knudson two hit model.[5] The process of X inactivation silences one of two alleles for a particular gene and hence creates a state of functional loss of heterozygosity. Thus, X linked tumour suppressor genes can require only a single mutational event (or "hit") to contribute to the process of carcinogenesis. Furthermore, with NRXI, hypothetical germline mutation of tumour suppressor genes could contribute to early onset disease. We have hypothesised that the process of NRXI may provide a mechanism for some hereditary breast or ovarian cancers independent of *BRCA1*/*BRCA2* associated disease because of its strong association with invasive ovarian cancers.[4] More recently, data from our group suggest that this association extends to breast and endometrial, but not cervical or vulvar cancers.[6]

The gold standard for assessment of X chromosome inactivation status has been an evaluation of the androgen receptor (AR) gene polymorphism(s). The AR gene, localised to Xq13, is characterised by a highly polymorphic trinucleotide repeat $(CAG)_n$ in the coding region of its first exon. This repeat sequence is preceded by target sequences for the methylation sensitive restriction enzymes *Hha*I and *Hpa*II. The X chromosome inactivation mechanism results in site specific cytosine methylation of the inactive chromosome. This renders the methylated chromosome resistant to restriction enzyme digestion. In contrast, the active (unmethylated) X chromosome is sensitive to digestion by methylation specific restriction enzymes. Polymerase chain reaction (PCR) amplification of restriction digest can therefore be used to identify the active X chromosome. The majority of papers relating to X chromosome inactivation use the AR model. While other loci have been proposed, other potentially useful loci have primarily been studied only in small cohorts and these studies have been lacking in comparative analysis between the AR and the test locus.

In order better to understand NRXI and the extent to which it may occur throughout a given X chromosome, it would be useful to evaluate the degree of methylation of multiple X chromosome markers. In 1998, Okamoto *et al*[7] published a report of 110 Japanese females evaluated for mononuclear cell clonality, using a unique short tandem repeat (STR) site at DXS15-134.[7] This marker has been localised distal to the AR locus at Xq28 and is characterised by a pentameric repeat pattern flanked by *Hha*I and *Hpa*II restriction enzyme target sequences. These authors reported the results of AR and DXS15-134 PCR analysis of germline DNA in 91 women. Eighteen of these 91 females were heterozygous at both loci. The results of the AR and DXS15-134 PCR analysis were completely concordant. We have therefore chosen to perform a similar comparative analysis at the AR and DXS loci using germline DNA samples from probands with breast or ovarian cancer and a cohort of healthy cancer free controls.

Material and methods

Blood samples were obtained in accordance with guidelines set forth by the Committee on Human Subjects at the University of Iowa Hospitals and Clinics (UIHC). Case selection was from the Surgical (breast cancer) and

J Med Genet 2001;**38**:474–478

Division of Gynecologic Oncology, Department of Obstetrics and Gynecology, The University of Iowa Hospitals and Clinics (UIHC), 200 Hawkins Drive, 4630 JCP, Iowa City, Iowa 52242-1009, USA
V Mahavni
S C Kim
T A Benda
L Sanders
R E Buller

Correspondence to:
Dr Buller,
richard-buller@uiowa.edu

Gynecologic (ovarian cancer) Oncology Clinics at UIHC Clinical Cancer Center. Healthy controls were consenting paid volunteers. The cancer probands were selected based on consecutive patient visits to the clinic and were not enriched for known *BRCA1*/*BRCA2* status or family history of breast/ovarian cancer. We used mononuclear cell DNA from 139 probands (76 healthy controls, 20 breast cancer, 43 ovarian cancer). Personnel trained in the collection and construction of cancer family pedigrees obtain all pedigrees at the UIHC.

DNA extractions followed a standard phenol/chloroform/isoamyl alcohol extraction protocol we have previously reported.[8 9] Germline mononuclear cell DNA was subjected to restriction enzyme digestion by a combination of *Hha*I and *Hpa*II (New England Biolabs, Boston, MA). Each sample was aliquotted to paired, digested, and sham digests (controls). Ten µl of germline DNA (40-80 ng of DNA) were combined with 13.7 µl of double deionised water (ddH$_2$O), 3 µl of 10 × concentration NEB4 buffer (New England Biolabs, Boston, MA), 0.3 µl of bovine serum albumin (New England Biolabs, Boston, MA), 1 µl (2 units) of *Hha*I, 2 µl (2 units) *Hpa*II (New England Biolabs, Boston, MA) for a total volume of 30 µl. In the sham digest reaction, the combined volumes of restriction enzymes were substituted with a 50% glycerol solution (Fisher Scientific, Fairlawn, NJ). Samples were digested to completion at 37°C for 16 hours followed by heat inactivation of the restriction enzyme at 95°C for 30 minutes.

Both active and sham digested DNA (1.5 µl) were amplified at AR and DXS15-134 loci in 10 µl PCR reactions. Included in the reaction was 4.8 µl of ddH$_2$O, 1 µl of 10 × PCR buffer (Boehringer Mannheim, Germany), 1 µl dNTP (2 µmol/l), 0.5 pmol M$_{13}$ forward 29/IRD 700 dye tailed primer (LI-COR®, Lincoln, NE), 1 unit of *Taq* polymerase (Boehringer-Mannheim, Germany), and 0.5 µl each of the following primers: AR-F: 5'-CACGACGTTG TAAAACGACTGCGCGAAGTGATCCAG AAC, AR-R: 5'-TACGATGGGCTTGGGGA GAA. In the DXS15-134 reaction, the M$_{13}$ tailed DXS15-134 primers were: DXS15-134F: 5'-CACGACGTTGTAAAACGACGA ATTCTTTGCCTAGACCGG, DXS15-134R: 5'-TTGGAGCCAGGAGAATCGCTTGAAC.

Thermal cycler conditions followed a modified step down protocol. After an initial denaturing step at 95°C for five minutes, subsequent cycles included 45 second denaturation steps at this temperature. For the first five cycles, a five minute annealing step at 68°C was used to increase early amplification specificity. Next, a single 58°C step down with a two minute annealing time was followed by 25 cycles at 56°C steps with 60 second annealing time. All extensions were at 72°C for 60 seconds. The programme was completed by a final two minute extension time at 72°C. This unusual programme has been very useful in amplifying many different markers particularly in multiplex PCR reactions.

Two µl of PCR product were combined with 8 µl of LI-COR® IR 2 STOP solution (LI-COR®, Lincoln, NE). The combination was heated to 95°C for four minutes before loading onto a 25 cm, 7% Long Ranger™ (FMC Bioproducts, Rockland, ME) acrylamide gel.

The samples were electrophoresed at 50°C, 40 volts, and 40 mA for 90 minutes (AR) to 120 minutes (DXS15-134) based on fragment size. Internal size standards (LI-COR®, Lincoln, NE) were loaded in every tenth well for base pair length determination. Electrophoresis gels were evaluated using LI-COR® based ImagIR 4.0 data collection software and image manipulator software (LI-COR®, Lincoln, NE).

LI-COR® sample interpretation was based on comparison of allele banding patterns and relative intensities from the gel image files. Informative samples contained two alleles in the control lanes. Non-random X chromosome inactivation was defined as a relative loss of one allele band intensity in the digested DNA lane while the second band was unchanged relative to the control. Confirmation of the NRXI designation was via interpretation of relative band optical densities as determined by the Scanalytics GeneImagIR software (Scanalytics, Billerica, MA). An optical density differential of ⩾3:1 or ⩽0.33 between bands as defined by Mutter *et al*[10 11] was accepted as sufficient for defining NRXI. A designation of random X inactivation (RXI) was assigned when the two allele band intensities in the digest amplification maintained the same relative 1:1 ratio seen in the undigested control amplification. Occasional small differences (differential amplification) in allele intensity in the controls did not alter assignment in a sample with RXI. A reversal of the differential pattern between digest and controls necessitated a comparison of ratios between digested and control samples to determine X inactivation status in <5% of cases.

All statistical measures were performed using SPSS® 10.0 statistical software (SPSS® Inc, Chicago, IL). Comparisons of NRXI rates were performed using the chi-square test. Pearson's r was used to measure correlation between the two loci and Cohen's kappa (κ) was applied to assess agreement between the two loci. Comparison of mean optical density ratio for consistency analysis incorporated analysis of variance (ANOVA) with Bonferroni correction for multiple comparisons.

In order to validate the consistency of the assay, aliquots of DNA showing SXI from a single proband was subjected to five separate restriction digests. Multiple portions of each of these digested samples were then PCR amplified at the AR locus. These reactions generated 19 separate assays on DNA from the same proband. Analysis of the band ratios confirmed the reproducibility of the assay. The mean ratio and 95% confidence intervals were 3.7479 (3.5892-3.9065). The ratios were compared among groups via ANOVA analysis. There were no significant differences detected ($0.248 \leq p \leq 1.0$) between either the varying

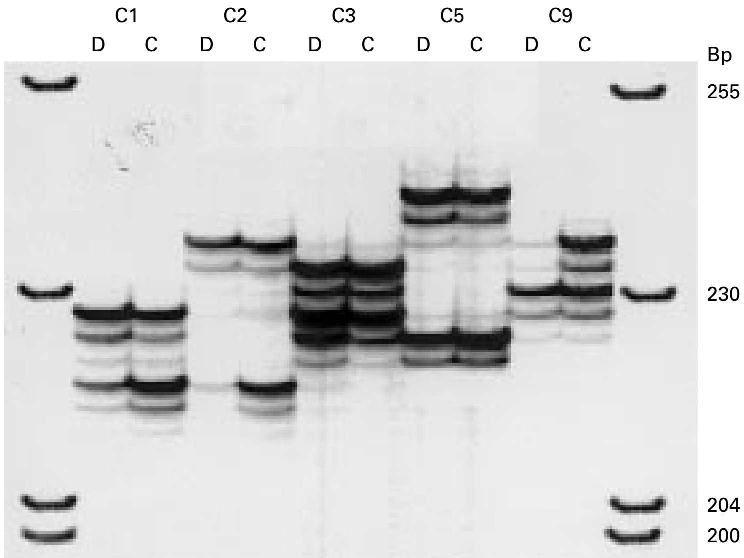

Figure 1 *Amplification of the AR locus. Proband identification is provided along the top of the image (for example, C1, C2). Lanes are labelled as D for digested DNA and C for control or sham digested DNA. Band markers flank the gel to provide reference for base pair length determination. This image shows examples of random X inactivation for probands C1, C2, and C5 with equal numbers and intensities of bands seen in both the digest and control lanes. Probands C2 and C9 show examples of non-random X chromosome inactivation with loss of the lower allelic band for C2 and the upper band for C9 in the digest lane as a result of preferential restriction digestion of the active (unmethylated) X chromosome.*

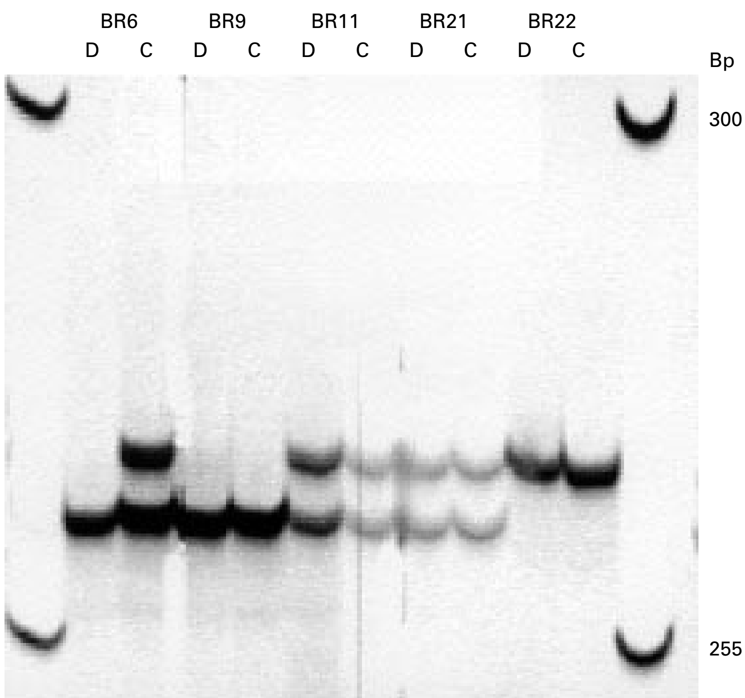

Figure 2 *Amplification of the DXS15-134 locus. Proband identification (for example, BR6, BR9) and base pair ladders are provided for reference. Generally, only two alleles were amplified at DXS15-134 compared to approximately 18 allelotypes for the AR locus. Random X inactivation patterns are seen for probands BR11 and BR21 while uninformative results are shown for probands BR9 and BR22. Only BR6 shows NRXI.*

Table 1 *Comparison of X inactivation patterns*

AR locus	*DXS15-134 locus* Non-random	Random	Non-informative	*Total*
Non-random	1 (4.5%)	21 (95.5%)	23	45
Random	—	32 (100%)	45	77
Non-informative	—	9 (100%)	8	17
Totals	1 (1.6%)	62 (98.4%)	76	139

digest or amplifying identical aliquots of DNA from a single digest.

Germline DNA from a total of 139 subjects was evaluated at both the AR and DXS15-134 loci. These included samples from 76 healthy, cancer free controls, 20 breast cancer probands, and 43 ovarian cancer probands. Results for X inactivation studies were considered informative if the DNA was heterozygous at the locus, that is, there were two alleles in the control lane.

Results

Fig 1 shows a LI-COR® gel image of five DNA samples from subjects analysed at the AR locus for X inactivation. All five were informative at this locus. The upper and lower bands are of equal intensity in both the control and digest lanes reflecting random X chromosome inactivation for subjects C3 and C5. This relationship is clear to the naked eye. Software analysis of these respective samples yielded optical density ratios of 1.94 and 1.13 for these subjects. These ratios confirmed classification of these samples to the random X inactivation group. For subjects C1, C2, and C9 the ratio of optical densities between the control and digest lanes are 3.02, >100, and 3.57, respectively. Hence, since these ratios were ⩾3:1, the samples were designated examples of non-random X inactivation. At this locus, 122 (88%) DNA samples were informative. Seventeen (12.2%) of the DNA samples were homozygous at the AR locus and therefore were considered uninformative. Of the informative samples, 45 (37%) showed non-random X inactivation patterns, while 77 (63%) showed random X inactivation.

Fig 2 shows a LI-COR® gel image of five DNA samples from probands analysed at the DXS15-134 locus for X inactivation. Three of these five subjects (BR6, BR11, and BR21) were informative at this locus. Non-random X inactivation is seen for proband BR6 while random X inactivation is seen for probands BR11 and 21. Generally, the gel images at this locus are much clearer than for the AR locus, hence software analysis was unnecessary. Probands BR9 and 22 are homozygous at this locus and therefore were considered uninformative. Overall, 63 (45.3%) DNA samples were informative. Seventy six (54.7%) samples were homozygous at the DXS15-134 locus and therefore were uninformative at this locus for X inactivation. Of the informative samples, only one (1.6%) showed a non-random X inactivation pattern, while 62 (98.4%) showed random X inactivation.

Table 1 compares the X inactivation data between the two study loci. For informative samples, agreement between the two assays was achieved in only 33 of 54 cases for a concordance rate of 61.1%. Further, Pearson's r calculation of correlation between loci was not significant (r=0.024, p=0.775). Interassay agreement was tested using Cohen's kappa and was also found to be insignificant at κ=–0.031 (p=0.475). Comparing the utility of the DXS15-134 assay to the AR result, the sensitivity of the DXS15-134 locus to detect NRXI was only 4.5% while the negative predictive value of the test was 39.6%.

Discussion

The process of X chromosome inactivation occurs as early as the blastocyst stage of embryonic life and the inactive state of the chromosome is stably maintained through subsequent cell divisions.[2] X inactivation results in equalisation of X chromosome gene expression between male and female cells and is therefore considered a mechanism for dosage compensation. The inactivation process has been well documented in mice[12–14] and is beginning to be understood in humans.[15] A *cis* acting RNA transcript known as XIST (X inactivation sequence transcript) is coded from the XIC (X inactivation centre) localised to Xq13. The XIST molecule is not translated to a protein product, but rather is distributed along the length of the X chromosome to form a complex with DNA and the histone variant MacroH2A conformational shape changes to the DNA in proximity to XIST. The final step of inactivation is site specific methylation of cytosine bases.[15–17]

The end result of the inactivation process is to abrogate gene expression from the inactive X chromosome. This mechanism does not inactivate all genes on the inactive X chromosome. A number of genes localised to a limited number of sites have been shown to escape the inactivation process; these include *ARSD*, *ARSE*, *GS1*, *STS*, *KAL*, *ANT3*, *XE7*, *MIC2*, and others.[18] Initially, loci shown to escape X inactivation were localised to the pseudoautosomal region of the X chromosome, frequently had Y chromosome homologues, and appeared to cluster on the p arm of the X chromosome. Now it is known that additional genes, both with and without Y chromosome homologues, and on the q arm of the X chromosome can also escape inactivation.[18 19]

Studies of X chromosome inactivation were initially based upon electrophoretic analysis of the glucose-6-phosphate dehydrogenase protein. This technique pioneered by Fialkow[20] was unfortunately limited by its lack of informative results. Other markers and techniques were also limited by a lack of informative sites.[21 22] However, since the development of the AR assay by Allen *et al*,[23] this technique has gained widespread acceptance and has been used in many studies of tumour clonality as well as X chromosome inactivation. The AR gene $(CAG)_n$ trinucleotide repeats fall within exon 1 and are polymorphic in 90% of females from all racial groups.[24] The utility of the AR assay is occasionally limited by difficulty in interpretation of results owing to stutter bands (as in fig 1) and software problems associated with optical scanning of gels using isotopic methods.[4] Although trinucleotide repeats are usually much clearer on gel electrophoresis than dinucleotide repeats, the relatively high GC content of the AR repeat can potentially result in amplification difficulties. There is also a fair amount of subjectivity in the interpretation of the banding patterns that determine inactivation status. In contrast, the pentameric character of the DXS15-134 locus contributed to the ease of amplification of two unique alleles with clear and distinct banding patterns. Theoretically, DXS15-134 X inactivation patterns should supplement an AR analysis. Unfortunately, we found that results from the two assays were discordant in 38.9% of cases.

At present, it is difficult to know which of the assays is more reliable. The overall incidence of NRXI, 37% of the informative cases, as determined by the AR assay was driven by the difference in rates between cancer probands (52.7%) and healthy controls (23.9%). Comparison of NRXI rates between several different cancers, and the influence of age on this process forms the basis of another study (Mahavni *et al*, unpublished data). Results from several cases of X linked diseases, expressed in females, can readily be explained by and are consistent with NRXI results obtained at the AR locus. Correlative studies of other X linked loci including the *MAOA* locus[25] and several single nucleotide polymorphisms (SNPs) are currently under way in our laboratory. One possible explanation of our results is that the DXS15-134 locus escapes X inactivation.

Three lines of evidence support the concept that the DXS15-134 locus is transcribed: (1) the study of Okamoto *et al*,[7] (2) the single case (BR6) with NRXI, and (3) our laboratory has been able to apply our current DXS15-134 primers to a cDNA template and obtain PCR products, suggesting that the DXS15-134 locus is transcribed (data not shown). The poor sensitivity and predictive value of the locus to detect NRXI probably limit its use as a marker for X inactivation studies. Additional support for the hypothesis that the Xq28 region containing DXS15-134 escapes X inactivation was presented by Bailey *et al*[17] who reported on the variable clustering of Line-1 (L1) elements in selected human chromosomes. The L1 content of genomic segments that carry genes capable of escaping X inactivation was significantly lower ($p=4.8 \times 10^{-5}$) than the X chromosome average of those genes subject to inactivation (p=0.004). The region of Xq28 contained a relatively low base pair fraction (0.2%) of L1 elements. This may provide support to the idea of DXS15-134 generally escaping the X inactivation process, but clearly additional studies will be required to resolve these questions.

This research was supported in part by the Florence and Marshall Schwid Award to Dr Richard E Buller from the Gynecologic Cancer Foundation. Dr Vikas Mahavni was supported by a Department of Health and Human Services, Public Health Service-National Institute of Health training grant T32 HL07344.

1 Ohno S, Hauschka TS. Allocycly of the X chromosome in tumors and normal tissue. *Cancer Res* 1960;**20**:541-5.
2 Lyon MF. Gene action in the X chromosome of the mouse (Mus musculus L) *Nature* 1961;**190**:372-3.
3 Puck JM, Willard HF. X inactivation in females with X-linked disease. *N Engl J Med* 1998;**338**:325-8.
4 Buller RE, Sood AK, Lallas TA, Beukers TE, Skilling JS. Association between nonrandom X-chromosome inactivation and BRCA 1 mutation in germline DNA of patients with ovarian cancer. *J Natl Cancer Inst* 1999;**91**:339-46.
5 Knudson AG Jr. Mutation and cancer: statistical study of retinoblastoma. *Proc Natl Acad Sci USA* 1971;**68**:820-3.

6 Mahavni V, Buller RE. Hormone and smoking related cancers further define a role for nonrandom X-chromosome inactivation in carcinogenesis. Poster presented at 91st Annual Meeting of the American Association of Cancer Research, San Francisco, CA, 1-5 April 2000.
7 Okamoto T, Okada M, Wada H, Kanamaru A, Kakishita E, Hashimoto T, Furuyama J. Clonal analysis of hematopoietic cells using a novel polymorphic site of the X chromosome. *Am J Hematol* 1998;**58**:263-6.
8 Buller RE, Skilling JS, Kaliszewski S, Niemann T, Anderson BA. Absence of significant germline p53 mutations in ovarian cancer patients. *Gynecol Oncol* 1995;**58**:368-74.
9 Skilling JS, Powills K, Lager DJ, Anderson BA, Sorosky JI, Buller RE. p53 allelotypes and enhanced detection of allelic loss on ovarian cancer: lack of correlation with familial and clinical factors. *Gynecol Oncol* 1996;**61**:180-8.
10 Mutter GL, Chaponot ML, Fletcher JA. A polymerase chain reaction assay for non-random X chromosome inactivation identifies monoclonal endometrial cancers and precancers. *Am J Pathol* 1995;**146**:501-8.
11 Mutter GL, Boyton KA. PCR bias in amplification of androgen receptor alleles, a trinucleotide repeat marker used in clonality studies. *Nucleic Acids Res* 1995;**23**:1411-18.
12 Lee TL, Jaenisch R. Long range cis effects of ectopic X-inactivation centres on a mouse autosome. *Nature* 1997; **386**:275-9.
13 Brockdorf N, Duthie SM. X Chromosome inactivation and the XIST gene. *Cell Mol Life Sci* 1998;**54**:104-12.
14 Marahrens Y, Loring J, Jaenisch R. Role of the Xist gene in X chromosome choosing. *Cell* 1998;**92**:657-64.
15 Brown CJ, Hendrich BD, Rupert JL, Lafreniere RG, Xing Y, Lawrence J, Willard HF. The human XIST gene; analysis of a 17 kb inactive X specific RNA that contains conserved repeats and is highly conserved within the nucleus. *Cell* 1992;**71**:527-42.
16 Herzing LBK, Romer JT, Horn JM, Ashworth A. Xist has properties of the X- chromosome inactivation centre. *Nature* 1997;**386**:272-4.
17 Bailey JA, Carrel L, Chakravarti A, Eichler EE. Molecular evidence for a relationship between LINE-1 elements and X chromosome inactivation: the Lyon repeat hypothesis. *Proc Natl Acad Sci USA* 2000;**97**:6634-9.
18 Brown CJ, Carrel L, Willard HF. Expression of genes from the human active and inactive X chromosome. *Am J Hum Genet* 1997;**60**:1333-43.
19 Brown CJ. Role of the X chromosome in cancer. *J Natl Cancer Inst* 1996;**88**:480-2.
20 Fialkow PJ. X-chromosome inactivation and the Xg locus. *Am J Hum Genet* 1970;**22**:460-3.
21 Gale RE, Wheadon H, Linch DC. X chromosome inactivation patterns using HPRT and PGK polymorphisms in haematologically normal and post-chemotherapy females. *Br J Haematol* 1991;**79**:193-7.
22 Vogelstein B, Fearon ER, Hamilton SR, Preisinger AC, Willard HF, Michelson AM, Riggs AD, Orkin SH. Clonal analysis using recombinant DNA probes from the X-chromosome. *Cancer Res* 1987;**47**:4806-13.
23 Allen RC, Zoghbi HY, Moseley AB, Rosenblatt HM, Belmont JW. Methylation of HpaII and HhaI sites near the polymorphic CAG repeat in the human androgen receptor gene correlates with X chromosome inactivation. *Am J Hum Genet* 1992;**51**:1229-39.
24 Edwards A, Hammond HA, Jin L, Casey T, Chakraborty R. Genetic variation at five trimeric and tetrameric repeat loci in four human population groups. *Genomics* 1992;**12**:241-53.
25 Peng H, Du M, Diss TC, Isaacson PG, Pan L. Clonality analysis in tumours of women by PCR amplification of X-linked genes. *J Pathol* 1997;**181**:223-2.

Evaluation of the *ELOVL4* gene in families with retinitis pigmentosa linked to the *RP25* locus

Yang Li, Irene Marcos, Salud Borrego, Zhengya Yu, Kang Zhang, Guillermo Antiñolo

J Med Genet 2001;**38**:478–480

Cole Eye Institute, Cleveland Clinic Foundation, Cleveland, Ohio, USA
Y Li
Z Yu
K Zhang

Unidad de Genética Médica y Diagnóstico Prenatal, Hospitales Universitarios "Virgen del Rocío", Avda Manuel Siurot s/n, 41013 Sevilla, Spain
I Marcos
S Borrego
G Antiñolo

Correspondence to: Dr Antiñolo, gantinolo@hvr.sas.cica.es

EDITOR—Retinitis pigmentosa (RP) is the most common form of retinal dystrophy. Patients present with night blindness and progressive narrowing of the visual field, eventually leading to central vision loss. Fundus examination usually shows bone spicula pigmentation, attenuation of blood vessels in the retina, and waxy pallor of the optic disc. Typically, the electroretinogram is notably diminished or even abolished.[1]

RP shows important allelic and non-allelic genetic heterogeneity (RET-GEN-NET) with different modes of inheritance, including autosomal dominant (AD), autosomal recessive (AR), X linked, and digenic.

ARRP is the most common form of RP. A locus for ARRP, *RP25*, was mapped in 1998 to the long arm of chromosome 6 between microsatellite markers D6S257 and D6S1644 (MIM 602772).[2] Recently, we have excluded two candidates, *GABRR1* and *GABRR2,* as the disease causing gene.[3]

Several loci with retinal dystrophy phenotypes have been mapped to the pericentromeric region of chromosome 6. They include autosomal dominant Stargardt-like disease (*STGD3*),[4] autosomal dominant macular atrophy (*ADMD*),[5] autosomal dominant cone-rod dystrophy (*CORD7*),[6] and Leber congenital amaurosis (*LCA5*).[7]

Recently, the gene responsible for *STGD3* and *ADMD* has been identified.[8] All affected members in four independent families with STGD3 and one family with ADMD shared a common founder haplotype, indicating a single ancestral disease specific mutation. A single 5 bp deletion of a novel gene called *ELOVL4* was identified, which segregates with all affected members of the STGD3 and ADMD families. *ELOVL4* shows cone and rod photoreceptor expression in the eye, is composed of six exons, and encodes a putative transmembrane protein of 314aa with similarities to the ELO family of proteins involved in elongation of very long chain fatty acids. Based on its similarity, it has been suggested that this protein is involved in synthesis of polyunsaturated fatty acids (PUFA) in the retina, such as DHA (docosahexaenoic acid). DHA represents 50% of PUFA in the outer segment of the photoreceptor cells and plays a crucial role in photoreceptor cell functions.

It is well known that one gene can cause distinct disease phenotypes with retinal degeneration.[9–19] For example, *ABCR* (also called *ABCA4*), the gene responsible for recessive Stargardt macular dystrophy (STGD1), can cause either ARRP or autosomal recessive cone-rod dystrophy.[17 20–23]

It has been known for a long time that the retina possesses unique properties in lipid metabolism. The high level of PUFA, such as DHA, in the photoreceptors is thought to form an essential lipid environment for the phototransduction function. In addition, DHA is known to be lower in the serum of patients with retinitis pigmentosa. This evidence suggests that lipid metabolism may play a role in the pathogenesis of RP.[24–28]

Table 1 PCR amplification of individual exons of the ELOVL4 gene

Exon	*Forward primers 5'→3'*	*Reverse primers 5'→3'*	*bp*	*°C*
1	*tctctctgggtctccgctt	†gaggggaggccttaacattc	347	58
2	*agccacttgcaggagtcagt	†tgatggttttacacattctcattttt	452	64
3	*agcaatcggaatgcatgaaa	†ttttcacagactggggccta	306	58
4	*tccatgccttgtacattttgtg	†tccactgaacacatatatgcaat	348	60
5	*acatctcagtggcttactgcc	†gaaaattgtctaaaatgacattgcac	291	66
6	*gaagatgccgatgttgttaaaag	†gtcaacaacagttaaggccca	376	62

All the primers had the universal M13 primers attached 5'.
*M13F: cgccagggttttcccagtcacgac and †M13R: tttcacacaggaaacagctatgac.

ELOVL4 maps within the critical *RP25* region and has a potential role in DHA synthesis. We therefore considered *ELOVL4* to be a good candidate for the *RP25* gene and performed mutational analysis of *ELOVL4* in RP families linked to this locus. Eight families with 18 patients were included in these studies.

Each exon of the *ELOVL4* gene was amplified from genomic DNA derived from the index patients of the eight families using intronic primers (table 1). These PCR products were purified, analysed by EMD (enzymatic mutation detection),[29] and automatically sequenced as previously described.[3]

Only two heterozygous variations were identified, both of which (IVS2-99T→C and M299V) have been previously described by Zhang *et al*[8] as non-pathogenic polymorphisms. These variants have been found in one family linked to *RP25*. In this particular family, there are two patients, both heterozygous for IVS2-99T→C and M299V. However, we did not detect any pathogenic variation in the *ELOVL4* gene in the RP patients. Therefore, we excluded *ELOVL4* as the gene responsible for *RP25*. Thus, our data indicate that at least two different genes involved in retinal degeneration are located in this region of the long arm of chromosome 6.

In conclusion, we have conducted a mutational screen in *ELOVL4*, the gene responsible for STGD3 and ADMD in ARRP families linked to *RP25*. After direct molecular analysis of the coding sequence and the intron-exon boundaries of *ELOVL4*, we did not find any pathogenic variant. Our results indicate that the *ELOVL4* gene seems not to be involved in the pathogenesis of *RP25* and *STGD3*/*ADMD* and *RP25* are not allelic variants of the same gene. Nevertheless, a role for *ELOVL4* in other inherited forms of RP needs to be elucidated.

Data access: RET-GEN-NET, http://www.sph.uth.tm.edu/Retnet/home.html Online Mendelian Inherited in Man (OMIN), http://www.ncbi.nlm.nih/htbin-post/OMIN

The first two authors contributed equally to this work. We would like to express our gratitude to all those affected by RP for their cooperation, essential for the completion of this study. This study was supported by Helen Keller Eye Research Foundation (YL), Grant Ritter Fund and NIH EY00401 (KZ), Fondo de Investigaciones Sanitarias (99/0010-02) (SB, GA), the Fundación ONCE, and the Asociación Andaluza de Retinosis Pigmentaria. IM is recipient of a fellowship from the Instituto de Salud Carlos III (99/4250, Ministerio de Sanidad y Consumo, Spain).

1 Jiménez-Sierra JM, Ogden TE, van Boemel GB. *Inherited retinal diseases: a diagnostic guide*. St Louis: Mosby, 1989.
2 Ruiz A, Borrego S, Marcos I, Antinolo G. A major locus for autosomal recessive retinitis pigmentosa on 6q, determined by homozygosity mapping of chromosomal regions that contain gamma-aminobutyric acid-receptor clusters. *Am J Hum Genet* 1998;**62**:1452-9.
3 Marcos I, Ruiz A, Blaschak CJ, Borrego S, Cutting GR, Antiñolo G. Mutation analysis of *GABRR1* and *GABRR2* in autosomal recessive retinitis pigmentosa (*RP25*). *J Med Genet* 2000;**37**:*e*5.
4 Stone EM, Nichols BE, Kimura AE, Weingeist TA, Drack A, Sheffield VC. Clinical features of a Stargardt-like dominant progressive macular dystrophy with genetic linkage to chromosome 6q. *Arch Ophthalmol* 1994;**112**:765-72.
5 Griesinger IB, Sieving PA, Ayyagari R. Autosomal dominant macular atrophy at 6q14 excludes CORD7 and MCDR1/PBCRA loci. *Invest Ophthalmol Vis Sci* 2000;**41**:248-55.
6 Kelsell RE, Gregory-Evans K, Gregory-Evans CY, Holder GE, Jay MR, Weber BH, Moore AT, Bird AC, Hunt DM. Localization of a gene (CORD7) for a dominant cone-rod dystrophy to chromosome 6q. *Am J Hum Genet* 1998;**63**:274-9.
7 Dharmaraj S, Li Y, Robitaille JM, Silva E, Zhu D, Mitchell TN, Maltby LP, Baffoe-Bonnie AB, Maumenee IH. A novel locus for Leber congenital amaurosis maps to chromosome 6q. *Am J Hum Genet* 2000;**66**:319-26.
8 Zhang K, Kniazeva M, Han M, Li W, Yu Z, Yang Z, Li Y, Metzker ML, Allikmets R, Zack DJ, Kakuk LE, Lagali PS, Wong PW, MacDonald IM, Sieving PA, Figueroa D, Austin CP, Gould RJ, Ayyagari R, Petrukhin K. A five base-pair deletion in the ELOVL4 gene is associated with two related forms of autosomal dominant macular dystrophy. *Nat Genet* 2001;**27**:89-93.
9 Nichols BE, Sheffield VC, Vandenburgh K, Drack AV, Kimura AE, Stone EM. Butterfly-shaped pigment dystrophy of the fovea caused by a point mutation in codon 167 of the RDS gene. *Nat Genet* 1993;**3**:202-7.
10 Weleber RG, Carr RE, Murphey WH, Sheffield VC, Stone EM. Phenotypic variation including retinitis pigmentosa, pattern dystrophy, and fundus flavinomaculatus in a single family with a deletion of codon 153 or 154 of the peripherin/RDS gene. *Arch Ophthalmol* 1993;**111**:1531-42.
11 Wells J, Wroblewski J, Keen J, Inglehearn C, Jubb C, Eckstein A, Jay M, Arden G, Bhattacharya S, Fitzke F, Bird A. Mutations in the human retinal degeneration slow (RDS) gene can cause either retinitis pigmentosa or macular dystrophy. *Nat Genet* 1993;**3**:213-18.
12 Nakazawa M, Kikawa E, Chida Y, Tamai M. Asn244His mutation of the peripherin/RDS gene causing autosomal dominant cone-rod degeneration. *Hum Mol Genet* 1994;**3**:1195-6.
13 Reig C, Serra A, Gean E, Vidal M, Arumi J, De la Calzada MD, Antich J, Carballo M. A point mutation in the RDS-peripherin gene in a Spanish family with central areolar choroidal dystrophy. *Ophthal Genet* 1995;**16**:39-44.
14 Kohl S, Christ-Adler M, Apfelstedt-Sylla E, Kellner U, Eckstein A, Zrenner E, Wissinger B. RDS/peripherin gene mutations are frequent causes of central retinal dystrophies. *J Med Genet* 1997;**34**:620-6.
15 Allikmets R, Singh N, Sun H, Shroyer NF, Hutchinson A, Chidambaram A, Gerrard B, Baird L, Stauffer D, Peiffer A, Rattner A, Smallwood P, Li Y, Anderson KL, Lewis RA, Nathans J, Leppert M, Dean M, Lupski JR. A photoreceptor cell-specific ATP-binding transporter gene (ABCR) is mutated in recessive Stargardt macular dystrophy. *Nat Genet* 1997;**15**:236-46.
16 Martinez-Mir A, Paloma E, Allikmets R, Ayuso C, del Rio T, Dean M, Vilageliu L, Gonzalez-Duarte R, Balcells S. Retinitis pigmentosa caused by homozygous mutation in the Stargardt disease gene ABCR. *Nat Genet* 1998;**18**:11-12.
17 Cremers FP, van de Pol DJ, van Driel M, den Hollander AI, van Haren FJ, Knoers NV, Tijmes N, Bergen AA, Rohrschneider K, Blankenagel A, Pinckers AJ, Deutman AF, Hoyng CB. Autosomal recessive retinitis pigmentosa and cone-rod dystrophy caused by splice site mutations in the Stargardt's disease gene ABCR. *Hum Mol Genet* 1998;**7**:355-62.
18 Sohocki MM, Sullivan LS, Mintz-Hittner HA, Birch D, Heckenlively JR, Freund CL, McInnes RR, Daiger SP. A range of clinical phenotypes associated with mutations in CRX, a photoreceptor transcription-factor gene. *Am J Hum Genet* 1998;**63**:1307-15.
19 Morimura H, Fishman GA, Grover SA, Fulton AB, Berson EI, Dryja TP. Mutations in the RPE65 gene in patients with autosomal recessive retinitis pigmentosa or Leber congenital amaurosis. *Proc Natl Acad Sci USA* 1998;**95**:3088-93.
20 Martinez-Mir A, Bayes M, Vilageliu L, Grinberg D, Ayuso C, del Rio T, Garcia-Sandoval B, Bussaglia E, Baiget M, Gonzalez-Duarte R, Balcells S. A new locus for autosomal recessive retinitis pigmentosa (RP19) maps to 1p13-1p21. *Genomics* 1997;**40**:142-6.
21 Rozet JM, Gerber S, Souied E, Perrault I, Chatelin S, Ghazi I, Leowski C, Dufier JL, Munnich A, Kaplan J. Spectrum of ABCR gene mutations in autosomal recessive macular dystrophies. *Eur J Hum Genet* 1998;**6**:291-5.
22 van Driel MA, Maugeri A, Klevering BJ, Hoyng CB, Cremers FP. ABCR unites what ophthalmologists divide. *Ophthal Genet* 1998;**19**:117-22.
23 Maugeri A, van Driel MA, van de Pol DJ, Klevering BJ, van Haren FJ, Tijmes N, Bergen AA, Rohrschneider K, Blankenagel A, Pinckers AJ, Dahl N, Brunner HG, Deutman AF, Hoyng CB, Cremers FP. The 2588G→C mutation in the ABCR gene is a mild frequent founder mutation in the western European population and allows the classification of ABCR mutations in patients with Stargardt disease. *Am J Hum Genet* 1999;**64**:1024-35.
24 Schaefer EJ, Robins SJ, Patton GM, Sandberg MA, Weigel-DiFranco CA, Rosner B, Berson EL. Red blood cell membrane phosphatidylethanolamine fatty acid content in various forms of retinitis pigmentosa. *J Lipid Res* 1995;**36**:1427-33.

25 Hoffman DR, Uauy R, Birch DG. Red blood cell fatty acid levels in patients with autosomal dominant retinitis pigmentosa. *Exp Eye Res* 1993;**57**:359-68.
26 Hoffman DR, Birch DG. Docosahexaenoic acid in red blood cells of patients with X-linked retinitis pigmentosa. *Invest Ophthalmol Vis Sci* 1995;**36**:1009-18.
27 Hoffman DR, Uauy R, Birch DG. Metabolism of omega-3 fatty acids in patients with autosomal dominant retinitis pigmentosa. *Exp Eye Res* 1995;**60**:279-89.
28 Gong J, Rosner B, Rees DG, Berson EL, Weigel-DiFranco CA, Schaefer EJ. Plasma docosahexaenoic acid levels in various genetic forms of retinitis pigmentosa. *Invest Ophthalmol Vis Sci* 1992;**33**:2596-602.
29 Del Tito BJ, Poff HE, Novotny MA, Cartledge DM, Walker RI, Earl CD, Bailey AL. Automated fluorescent analysis procedure for enzymatic mutation detection. *Clin Chem* 1998;**44**:731-9.

PTEN mutations are uncommon in Proteus syndrome

K Barker, A Martinez, R Wang, S Bevan, V Murday, J Shipley, R Houlston, J Harper

J Med Genet 2001;**38**:480–481

Cancer Genetics Section, Institute of Cancer Research, 15 Cotswold Road, Sutton, Surrey SM2 5NG, UK
K Barker
S Bevan
V Murday
R Houlston

Department of Dermatology, Great Ormond Street Hospital for Children NHS Trust, Great Ormond Street, London WC1N 3JH, UK
A Martinez
J Harper

Molecular Carcinogenesis Section, Institute of Cancer Research, 15 Cotswold Road, Sutton, Surrey SM2 5NG, UK
R Wang
J Shipley

Correspondence to:
K Barker, karenb@icr.ac.uk

EDITOR—Proteus syndrome (MIM 176920) is a rare, congenital, hamartomatous disorder, which is a member of a group of local overgrowth diseases. Happle[1] proposed that some of these disorders are the result of the action of a lethal gene that can only survive in the mosaic state, which arises from an early somatic mutation or from a half chromatid mutation. Such a mechanism has been shown to be the underlying basis of McCune-Albright syndrome (MIM 174800).[2] One of the mandatory diagnostic criteria for Proteus syndrome is a mosaic distribution of lesions and sporadic occurrence, entirely consistent with Happle's hypothesis.

Currently, little is known about the molecular causes of Proteus syndrome. It is, however, likely that the overgrowth of tissue involves all germ layers. This may be because of hyperproliferation, an absence of appropriate apoptosis, or alternatively cellular hypertrophy. There have been few investigations into the molecular basis of Proteus syndrome. Zhou *et al*[3] recently identified *PTEN* mutations in a patient with a Proteus-like syndrome. Germline *PTEN* mutations are found in a high proportion of patients with Cowden (MIM 158350) and Bannayan-Riley-Ruvalcaba (BRR) syndromes (MIM 153480),[4–7] which share many features of Proteus syndrome. These observations make *PTEN* a strong candidate for a gene mutated in Proteus syndrome. To investigate this possibility, we examined eight patients with Proteus syndrome for *PTEN* mutations. All were unrelated and had classical Proteus syndrome using published diagnostic criteria.[8] Samples were obtained with informed consent and local ethical review board approval. Fibroblasts were cultured from skin biopsies obtained from normal tissue and from regions of overgrowth. Genomic DNA was extracted from cultured cells using a standard sucrose lysis technique. *PTEN* mutational analysis was performed by PCR based conformational specific gel electrophoresis using published oligonucleotides[9] and semi-automated sequencing using an ABI 377 Prism sequencer. A common exon 4 polymorphism was observed in three of the patients, but no missense or truncating mutations in any of the eight samples were detected, suggesting that mutation in *PTEN* is unlikely to be a common cause of Proteus syndrome.

We evaluated *PTEN* as a candidate gene because of its role in the overgrowth syndrome Cowden disease and the recent report of a *PTEN* mutation in a boy with Proteus-like syndrome.[3] PTEN plays a role in the regulation of PI3 kinase signalling, which is involved in the control of apoptosis and cell cycle progression.[10] Hence, by removing the regulatory effects of PTEN on PI3 kinase signalling, deregulated cellular growth could occur. PTEN also appears to play a role in the regulation of cell size and a role for the PI3 kinase signalling pathway in the determination of organ size in mammals has been reported.[11] The boy reported by Zhou *et al*[3] with Proteus-like syndrome had a germline single base transversion resulting in an Arg 335 to Ter substitution in *PTEN*. A second *PTEN* mutation resulting in Arg 130 to Ter was found in DNA from a naevus, lipoma, and an arteriovenous mass. The authors postulated that the first germline mutation gave rise to many of the features of BRR and that the second hit occurred early in embryogenesis causing mosaicism. In our study we did not detect *PTEN* mutations in any of the Proteus syndrome patients we examined. Zhou *et al*[3] similarly failed to detect any *PTEN* mutations in five patients with classical Proteus syndrome; their patient with *PTEN* mutations did not fulfil the stringent diagnostic criteria for Proteus syndrome.

Mutations in the coding region of *PTEN* do not appear to be implicated in classical Proteus syndrome. *PTEN* may still be involved, as our finding does not preclude the possibility that it may be aberrantly imprinted in Proteus syndrome, for example by promoter methylation,[12] leading to reduced PTEN expression. Given the innumerable possibilities for a molecular basis of Proteus syndrome, the identification of which genes are disrupted will prove difficult. One strategy for dissecting the molecular pathways of Proteus and other overgrowth syndromes is through examining the expression patterns of genes in affected and unaffected tissues, which is becoming feasible with the advent of microarray technology.[13]

The first two authors contributed equally to the study. Part of this work was undertaken in The Cancer Gene Cloning Laboratory. We would like to thank the patients who took part in this study.

1 Happle R. Lethal genes surviving by mosaicism: a possible explanation for sporadic birth defects involving the skin. *J Am Acad Dermatol* 1987;**16**:899-906.
2 Schwindinger WF, Francomano CA, Levine MA. Identification of a mutation in the gene encoding the alpha subunit of the stimulatory G protein of adenylyl cyclase in McCune-Albright syndrome. *Proc Natl Acad Sci USA* 1992;**89**:5152-6.
3 Zhou XP, Marsh DJ, Hampel H, Mulliken JB, Gimm O, Eng C. Germline and germline mosaic PTEN mutations associated with a Proteus-like syndrome of hemihypertrophy, lower limb asymmetry, arteriovenous malformations and lipomatosis. *Hum Mol Genet* 2000;**9**:765-8.
4 Marsh DJ, Dahia PL, Zheng Z, Liaw D, Parsons R, Gorlin RJ, Eng C. Germline mutations in PTEN are present in Bannayan-Zonana syndrome. *Nat Genet* 1997;**16**:333-4.
5 Marsh DJ, Dahia PL, Caron S, Kum JB, Frayling IM, Tomlinson IP, Hughes KS, Eeles RA, Hodgson SV, Murday VA, Houlston R, Eng C. Germline PTEN mutations in Cowden syndrome-like families. *J Med Genet* 1998;**35**:881-5.
6 Liaw D, Marsh DJ, Li J, Dahia PL, Wang SI, Zheng Z, Bose S, Call KM, Tsou HC, Peacocke M, Eng C, Parsons R. Germline mutations of the PTEN gene in Cowden disease, an inherited breast and thyroid cancer syndrome. *Nat Genet* 1997;**16**:64-7.
7 Longy M, Coulon V, Duboue B, David A, Larregue M, Eng C, Amati P, Kraimps JL, Bottani A, Lacombe D, Bonneau D. Mutations of PTEN in patients with Bannayan-Riley-Ruvalcaba phenotype. *J Med Genet* 1998;**35**:886-9.
8 Biesecker LG, Happle R, Mulliken JB, Weksberg R, Graham JM Jr, Viljoen DL, Cohen MM Jr. Proteus syndrome: diagnostic criteria, differential diagnosis, and patient evaluation. *Am J Med Genet* 1999;**84**:389-95.
9 Steck PA, Pershouse MA, Jasser SA, Yung WK, Lin H, Ligon AH, Langford LA, Baumgard ML, Hattier T, Davis T, Frye C, Hu R, Swedlund B, Teng DH, Tavtigian SV. Identification of a candidate tumour suppressor gene, MMAC1, at chromosome 10q23.3 that is mutated in multiple advanced cancers. *Nat Genet* 1997;**15**:356-62.
10 Di Cristofano A, Pandolfi PP. The multiple roles of PTEN in tumor suppression. *Cell* 2000;**100**:387-90.
11 Shioi T, Kang PM, Douglas PS, Hampe J, Yballe CM, Lawitts J, Cantley LC, Izumo S. The conserved phosphoinositide 3-kinase pathway determines heart size in mice. *EMBO J* 2000;**19**:2537-48.
12 Whang YE, Wu X, Suzuki H, Reiter RE, Tran C, Vessella RL, Said JW, Isaacs WB, Sawyers CL. Inactivation of the tumor suppressor PTEN/MMAC1 in advanced human prostate cancer through loss of expression. *Proc Natl Acad Sci USA* 1998;**95**:5246-50.
13 Schena M, Heller RA, Theriault TP, Konrad K, Lachenmeier E, Davis RW. Microarrays: biotechnology's discovery platform for functional genomics. *Trends Biotechnol* 1998;**16**:301-6.

Limited contribution of interchromosomal gene conversion to *NF1* gene mutation

M Luijten, R Fahsold, C Mischung, A Westerveld, P Nürnberg, T J M Hulsebos

J Med Genet 2001;**38**:481–484

Department of Human Genetics, Academic Medical Center, University of Amsterdam, Meibergdreef 15, 1105 AZ Amsterdam, The Netherlands
M Luijten
A Westerveld
T J M Hulsebos

Gemeinschaftspraxis B Prager & A Junge, Dresden, Germany
R Fahsold

Institut für Medizinische Genetik, Universitätsklinikum Charité, Berlin, Germany
C Mischung
P Nürnberg

Correspondence to: Dr Luijten, m.luijten@amc.uva.nl

EDITOR—Neurofibromatosis type 1 (NF1) is one of the most common autosomal dominant disorders with a population frequency of 1 in 3500.[1] The disease is clinically characterised by multiple neurofibromas, café au lait spots and Lisch nodules of the iris. The *NF1* gene, a tumour suppressor gene, resides on the proximal long arm of chromosome 17 (17q11.2). It spans approximately 350 kb of genomic DNA and, comprising 60 exons, encodes the protein neurofibromin.[2] This protein, consisting of 2818 amino acids, contains a central domain that has homology with GTPase activating proteins (GAPs).[3]

A distinct feature of the *NF1* gene is the very high spontaneous mutation rate (1×10^{-4} per gamete per generation), which is about 100-fold higher than the usual mutation rate for a single locus.[1] Up to 50% of all NF1 cases are thought to result from de novo mutations. The *NF1* gene provides a large target for mutations because of its relatively large size, but this may only account for a factor of 10 in terms of increase in mutation rate.[4] The presence of numerous *NF1* pseudogenes has been proposed as an explanation for the high mutation rate in NF1.[5] In the human genome, at least 12 different *NF1* related sequences have been identified on chromosomes 2, 12, 14, 15, 18, 21, and 22.[5–13] Most of the *NF1* pseudogenes have been mapped in pericentromeric regions. The chromosome 2 *NF1* pseudogene has been localised to region 2q21, which is known to contain the remnant of an ancestral centromere.[14] Owing to the absence of selective pressure, mutations may accumulate in the *NF1* pseudogenes. Consequently, the pseudogenes could act as reservoirs of mutations, which might be crossed into the functional *NF1* gene by interchromosomal gene conversion.[5] Gene conversion, the non-reciprocal transfer of genetic information between two related sequences, has been recognised as a mutational mechanism for several human genes.[15–17] In all these cases, the conversions occurred between gene and pseudogene on the same chromosome. For NF1, interchromosomal gene conversion is required as none of the *NF1* pseudogenes is located on chromosome 17. Interchromosomal gene conversion has been reported to occur between the von Willebrand factor gene on chromosome 12 and the von Willebrand pseudogene on chromosome 22.[18]

Gene conversion requires close contact between the functional gene and the corresponding pseudogene. The pericentromeric location of the functional *NF1* gene and its pseudogenes may enable this close contact since centromeres tend to associate with each other in a non-random fashion.[19 20] This is underlined by our finding that the *NF1* pseudogenes on chromosomes 2, 14, and 22 have arisen by repeated transposition events between (peri)centromeric locations on these chromosomes (Luijten *et al*, submitted).[13] However, the high mutation rate in NF1 cannot be explained exclusively by interchromosomal gene conversion. Only a small part of the functional *NF1* gene is represented in the *NF1* pseudogenes (see below), while *NF1* gene mutations are scattered over the entire gene. In this study, we investigated whether interchromosomal gene conversion contributes to the mutation rate in NF1.

Table 1 Publicly accessible NF1 pseudogene sequences

Chromosome	*Variant*	*Exons*	*Accession No*	*Reference*
2		10b, 12a–19a, 27b	AF232292-AF232302	13
2		12b–19a, 27b	AC0009477	23
2		13–15*	Y07858	12
2		13	U35697	8
12		16†	U35686	8
12		16, 17	AC024000	Birren *et al*, unpublished‡
14	A	10b, 12a–19a, 27b	AF232248-AF232258	13
14	B	10b, 12a–19a, 27b	AF232259-AF232269	13
14	C	10b, 12a–19a, 27b	AF232270-AF232280	13
14	D	10b, 12a–19a, 27b	AF232281-AF232291	13
14	E	10b, 12a–19a, 27b	AL512624	Genoscope§
14	F	12b–19a, 27b	AL512310	Genoscope§
14	A, B	13–15*	Y07854, Y07855	12
14		13, 15, 16†, 18	U35696, U35684, U35687, U35690	8
15		13–15*	Y07856, Y07857	12
15		14	AF011743	11
15		15	U35685	8
15		15	AF011746, AF011744	11
15		18	U35691	8
15		19b	U35693	8
15		20–22	M84131	6
15		21	AF011748	11
15		23-1	U35694	8
15		24	U35695	8
15		24	AF011747, AF011745, AF011749	11
15		25–27b	M84131	6
15		13–23-1, 24–27b	AC021585, AC023191, AC037471	Birren *et al*, unpublished‡
15		13–23-1, 24–27b	AC020679	Birren *et al*, unpublished‡
15		24–27b	AC060814	Birren *et al*, unpublished‡
18		7–9, 11	AP001004	Hattori *et al*, unpublished¶
18		8	U35688	8
18		9	U35689	8
21		7–9, 11	D26141, AC004527	7; Weiss *et al*, unpublished**
22		10b, 12a–19a, 27b	AC002471, AC003064, AC005374	13
22		13–15*	Y07859	12
22		18	U35692	8

*Sequences of the last part of exon 13, of the complete exon 14, and of the first part of exon 15 have been determined.
†The sequence of only part of exon 16 has been determined.
‡Birren B, Linton L, Nusbaum C, Lander E, unpublished data.
§Genoscope, Centre National de Sequencage (www.genoscope.cns.fr).
¶Hattori M, Ishii K, Toyoda A, Taylor TD, Hong-Seog P, Fujiyama A, Yada T, Totoki Y, Watanabe H, Sakaki Y, unpublished data.
**Weiss RB, Dunn DM, Aoyagi A, Banks L, Duval B, Hamil C, Holmes C, Mahmoud M, Rose R, Stokes R, Stump MD, Yu P, Zhou L, Gitin Y, Nelson J, von Niederhausen A, unpublished data.

First, we inventoried all available *NF1* pseudogene sequences (table 1). These included not only the published *NF1* pseudogene sequences, but also so far unidentified *NF1* pseudogene sequences present in the first draft sequence of the human genome. The latter were detected by performing a BLAST search using the complete cDNA sequence of the *NF1* gene (http://www.nf.org/nf1gene/nf1gene.cDNAtext.html). In a previous study, we elucidated the complete nucleotide sequence of the *NF1* pseudogene on chromosome 22.[13] Analysis of this sequence showed that sequences homologous to exons 10b, 12a-19a, and 27b

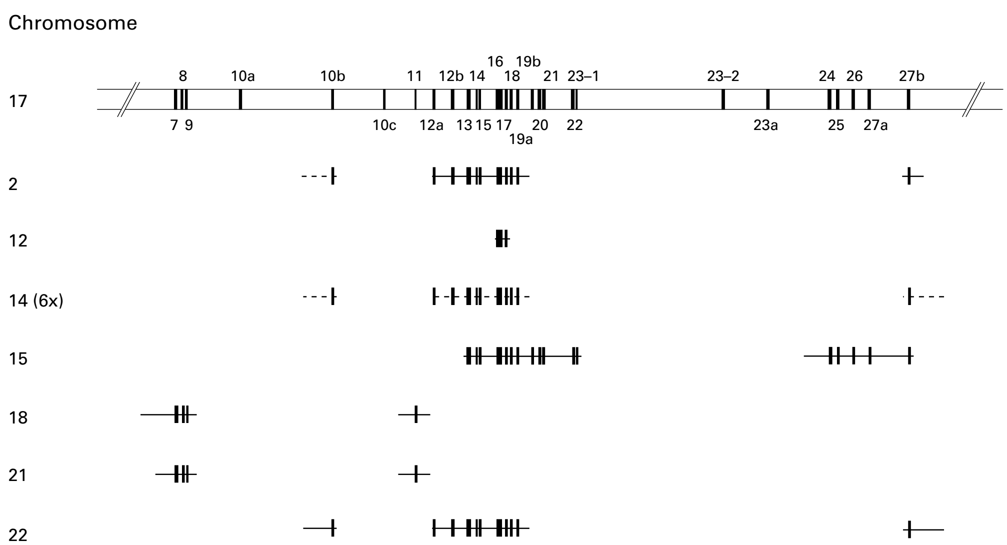

Figure 1 Overview of the exons maximally represented in the various NF1 pseudogenes. Exons and introns of the functional NF1 gene are denoted by black and white boxes, respectively. For the NF1 pseudogenes, black boxes indicate exons that have been sequenced. The maximum length of the corresponding segments of the functional gene of the NF1 pseudogenes on chromosomes 2 and 14 is denoted by a dashed line. The actual size of the represented segment of the chromosome 12, 15, 18, 21, and 22 NF1 pseudogenes is indicated by an unbroken line. The multiple variants of the chromosome 14 and 15 NF1 pseudogenes have the same genomic organisation.

Table 2 Disease causing NF1 gene mutations congruous to NF1 pseudogene sequences

Location	*Mutation*	*Reference*	*Pseudogene*	*NF1 gene in patient—NF1 pseudogene‡*
Exon 7	910C>T*†	24	ψ*NF1*-18	TATTTCT(10nt)*T*GA—T**G**TTTC**C**(10nt) *T*GA
Exon 7	910C>T*†	24	ψ*NF1*-21	*T*GA—*T*G**G**
Exon 10b	1466A>G	25	ψ*NF1*-2	ACAAGAAGCT*G*T—AC**C**AG**G**AGCT*G*T
Exon 10b	1466A>G	25	ψ*NF1*-14A/B	AGAAGCT*G*T—**C**GAAGCT*G*T
			ψ*NF1*-14D/E	GAC(15nt)T*G*T—G**G**C(15nt)T*G*T
Exon 10b	1466A>G	25	ψ*NF1*-22	GACCTG(12nt)T*G*T—G**G**C**T**TG(12nt)T*G*T
Exon 10b	1513A>G	26	ψ*NF1*-14A/B/D/E, ψ*NF1*-22	ATA(24nt)*G*AG—AT**G**(24nt)*G*AG
Exon 13	2033-2034insC*	27	ψ*NF1*-15	GGAACCCCCCC*C*G—G**C**AA(ins14nt)CC**TT**CCC*C*G
Exon 13	2033-2034insC*	27	ψ*NF1*-15	GGAACCCCCCC*C*G—G**C**AA(ins13nt)CCC**T**CCC*C*G
Exon 13	2041C>T*†	25	ψ*NF1*-14A/B/D/E/F, ψ*NF1*-22	ATTTGC*T*GA—A**C**TTGC*T*GA
Exon 14	2288T>G	Fahsold *et al*, unpublished	ψ*NF1*-15	GC*G*G(6nt)ATTGA—GC*G*G(6nt)A**C**T**T**A
Exon 16	2842C>T	25	ψ*NF1*-14B/D/E	AATACC(21nt)*T*AA—AA**G**A**C**CC(21nt)*T*AA
			ψ*NF1*-14F	AATACC(21nt)*T*AA—AA**G**AC**G**C(21nt)*T*AA
Exon 16	2842C>T	25	ψ*NF1*-22	AATACC(21nt)*T*AA—A**GACG**C(21nt)*T*AA
Exon 20	3467A>G†	25	ψ*NF1*-15	A*G*CGTA—A*G*C**A**TA
Exon 21	3526-3528delAGA	Fahsold *et al*, unpublished	ψ*NF1*-15	GTTACCA(13nt)ACA---G—G**G**TAC**T**A(13nt)ACA---G
Exon 22	3721C>T†	25	ψ*NF1*-15	CTAGCT*T*GA—CT**G**GCT*T*GA
Exon 22	3826C>T*†	27	ψ*NF1*-15	TTC*T*GA—**C**TC*T*GA
Intron 25	4368–1G>T	25	ψ*NF1*-15	TTTGAA*T*GTTT—TT**CT**AA*T*GTTT
Intron 25	4368–1G>T	25	ψ*NF1*-15	TTTGAA*T*GTTT—TTT**T**AA*T*GTTT
Exon 27a	4537C>T*†	8	ψ*NF1*-15	*T*GA(9nt)AAGATG—*T*GA(9nt)AA**-**ATG

*Mutations recurrently found in the *NF1* gene of NF1 patients.
†Mutations with a pseudogene equivalent as reported in reference 25.
‡Disease causing mutations identified in the *NF1* gene of NF1 patients and their pseudogene equivalents are indicated in italics; additional mutations in the pseudogenes compared with the functional *NF1* gene are indicated in bold.

are present in the chromosome 22 *NF1* pseudogene. The same exons are represented in the *NF1* pseudogenes on chromosomes 2 and 14. Chromosome 14 contains several *NF1* pseudogenes. Sequence analyses of all exons present in four chromosome 14 *NF1* pseudogene variants and in the one on chromosome 2 have been performed.[13] The BLAST search yielded two clones each containing an additional pseudogene variant on chromosome 14. In one of them, sequences corresponding to exons 10b, 12a-19a, and 27b are present, while in the other only exons 12b-19a and 27b are represented. The chromosome 2 *NF1* pseudogene was also found among the results from the BLAST search. In the *NF1* pseudogene present in this particular clone, exons 12b-19a, and 27b are represented.

The complete sequence of the chromosome 21 *NF1* pseudogene has been determined (Weiss *et al*, unpublished data).[7] In this pseudogene, exons 7-9 and 11 are represented. For chromosome 15, three different *NF1* pseudogenes have been reported.[6 11 12] A fourth locus may be present on chromosome 15, but this could not be substantiated.[11] The representation of the chromosome 15 *NF1* pseudogenes starts in intron 12b and ends in intron 27b. These pseudogenes are the only *NF1* pseudogenes known so far with a nearly complete representation of the GAP related domain, which is encoded by exons 20-27a. Three chromosome 15 clones were found as a result of the BLAST search. Only one of them contains sequences corresponding to exons 24-27b, whereas in both the other two clones exons 13-23-1 and 24-27b are represented. The latter two clones contain the same *NF1* pseudogene variant, but differ from the *NF1* pseudogene present in the former. The BLAST search also yielded two unmapped clones, in which exons 13-23-1 and 24-27b are represented. The *NF1* pseudogene present in one of these unmapped clones is, with the exception of two nucleotides, identical to the *NF1* pseudogene variant present in the two clones that have been mapped to chromosome 15. Considering this and the fact that in both the unmapped clones exons 20-23-1 and 24-27b are represented, we presume these *NF1* related sequences to originate from chromosome 15. A number of exons of the published chromosome 15 *NF1* pseudogene variants have been sequenced. None of the three pseudogene variants that were identified in the BLAST search is identical to the sequences available from the published chromosome 15 *NF1* pseudogene variants. The chromosome 12 *NF1* pseudogene maximally contains exons 12b-23-1,[12] of which only exon 16 has been partially sequenced.[8] One of the *NF1* pseudogenes that resulted from the BLAST search contains sequences corresponding to exons 16 and 17. The clone containing this pseudogene was derived from chromosome 6. However, alignment of exon 16 of this pseudogene to other *NF1* pseudogenes showed a difference of only one nucleotide with the exon 16 sequence of the chromosome 12 *NF1* pseudogene. Since no indications for a chromosome 6 *NF1* pseudogene exist so far, we assume this *NF1* related sequence to originate from chromosome 12 rather than from chromosome 6. The *NF1* pseudogene on chromosome 18 consists at the most of exons 7-13.[12] Sequences of exons 8 and 9 have been reported.[8] The BLAST search yielded an *NF1* pseudogene, mapped to chromosome 18p11.2, in which exons 7-9 and 11 are represented. An overview of the exons represented in the various *NF1* pseudogenes is given in fig 1 and all accessible *NF1* pseudogene sequences are listed in table 1. When compared to the functional *NF1* gene, substitutions, deletions, and insertions are present in all *NF1* related sequences.

We continued by collecting all point mutations and/or minor lesions in the *NF1* gene. In total, we found 225 different disease causing mutations in exons 7-9, 10b, 11-23-1, and 24-27b of the functional gene, the four regions known to be represented in the pseudogenes. These mutations included 30 novel disease causing mutations that were taken from our own data (Fahsold *et al*, unpublished data; Nürnberg *et al*, unpublished data). Only a very limited number (13 of 225, 5.8%) of these disease causing mutations appears to have a pseudogene equivalent (table 2). In every pseudogene involved, we detected within a short distance (ranging from 2 to 25 nucleotides) from the disease causing mutation at least one extra mutation compared with the functional *NF1* gene (table 2). If the 13 mutations had been generated by interchromosomal gene conversion, it is likely that these extra mutations would also have been transposed into the functional gene of the NF1 patients. However, none of them has been identified in the *NF1* gene of these NF1 patients. Of the 13 mutations found, six reside in CpG sites resulting in C to T transitions. About 32% of all single base pair substitutions causing human genetic disease occur in CpG dinucleotides.[21] As CpGs of the *NF1* coding region are subject to methylation,[22] these six C to T transitions are probably the result of spontaneous deamination of 5-methylcytosine rather than of interchromosomal gene conversion. This susceptibility for C to T transitions is substantiated by the fact that the six mutations found in both the functional gene and pseudogenes include four recurrent mutations of the *NF1* gene (indicated in table 2). Taken together, these results imply that the contribution of interchromosomal gene conversion to the high mutation rate in NF1 is, at best, limited.

1 Huson SM, Hughes RAC. *The neurofibromatoses: a pathogenetic and clinical overview*. London: Chapman & Hall Medical, 1994.
2 Li Y, O'Connell P, Breidenbach HH, Cawthon R, Stevens J, Xu G, Neil S, Robertson M, White R, Viskochil D. Genomic organization of the neurofibromatosis 1 gene (*NF1*). *Genomics* 1995;**25**:9-18.
3 Martin GA, Viskochil D, Bollag G, McCabe PC, Crosier WJ, Haubruck H, Conroy L, Clark R, O'Connell P, Cawthon RM, Innis MA, McCormick F. The GAP-related domain of the neurofibromatosis type 1 gene product interacts with ras p21. *Cell* 1990;**63**:843-9.
4 Marchuk DA, Saulino AM, Tavakkol R, Swaroop M, Wallace, MR, Andersen LB, Mitchell AL, Gutmann DH, Boguski M, Collins FS. cDNA cloning of the type 1 neurofibromatosis gene: complete sequence of the *NF1* gene product. *Genomics* 1991;**11**:931-40.
5 Marchuk DA, Tavakkol R, Wallace MR, Brownstein BH, Taillon-Miller P, Fong CT, Legius E, Andersen LB, Glover TW, Collins FS. A yeast artificial chromosome contig encompassing the type 1 neurofibromatosis gene. *Genomics* 1992;**13**:672-80.
6 Legius E, Marchuk DA, Hall BK, Andersen LB, Wallace MR, Collins FS, Glover TW. *NF1*-related locus on chromosome 15. *Genomics* 1992;**13**:1316-18.
7 Suzuki H, Ozawa N, Taga C, Kano T, Hattori M, Sakaki Y. Genomic analysis of a *NF1*-related pseudogene on human chromosome 21. *Gene* 1994;**147**:277-80.
8 Purandare SM, Huntsman Breidenbach H, Li Y, Zhu XL, Sawada S, Neil SM, Brothman A, White R, Cawthon R, Viskochil D. Identification of neurofibromatosis 1 (*NF1*) homologous loci by direct sequencing, fluorescence *in situ* hybridization, and PCR amplification of somatic cell hybrids. *Genomics* 1995;**30**:476-85.
9 Cummings LM, Trent JM, Marchuk DA. Identification and mapping of type 1 neurofibromatosis (*NF1*) homologous loci. *Cytogenet Cell Genet* 1996;**73**:334-40.
10 Hulsebos TJ, Bijleveld EH, Riegman PH, Smink LJ, Dunham I. Identification and characterization of *NF1*-related loci on human chromosomes 22, 14 and 2. *Hum Genet* 1996;**98**:7-11.
11 Kehrer-Sawatzki H, Schwickardt T, Assum G, Rocchi M, Krone W. A third neurofibromatosis type 1 (*NF1*) pseudogene at chromosome 15q11.2. *Hum Genet* 1997;**100**:595-600.
12 Régnier V, Meddeb M, Lecointre G, Richard F, Duverger A, Nguyen VC, Dutrillaux B, Bernheim A, Danglot G. Emergence and scattering of multiple neurofibromatosis (*NF1*)-related sequences during hominoid evolution suggest a process of pericentromeric interchromosomal transposition. *Hum Mol Genet* 1997;**6**:9-16.
13 Luijten M, Wang Y, Smith BT, Westerveld A, Smink LJ, Dunham I, Roe BA, Hulsebos TJ. Mechanism of spreading of the highly related neurofibromatosis type 1 (*NF1*) pseudogenes on chromosomes 2, 14 and 22. *Eur J Hum Genet* 2000;**8**:209-14.
14 Baldini A, Ried T, Shridhar V, Ogura K, D'Aiuto L, Rocchi M, Ward DC. An alphoid DNA sequence conserved in all human and great ape chromosomes: evidence for ancient centromeric sequences at human chromosomal regions 2q21 and 9q13. *Hum Genet* 1993;**90**:577-83.
15 Harada F, Kimura A, Iwanaga T, Shimozawa K, Yata J, Sasazuki T. Gene conversion-like events cause steroid 21-hydroxylase deficiency in congenital adrenal hyperplasia. *Proc Natl Acad Sci USA* 1987;**84**:8091-4.
16 Watnick TJ, Gandolph MA, Weber H, Neumann HP, Germino GG. Gene conversion is a likely cause of mutation in PKD1. *Hum Mol Genet* 1998;**7**:1239-43.
17 Stone DL, Tayebi N, Orvisky E, Stubblefield B, Madike V, Sidransky E. Glucocerebrosidase gene mutations in patients with type 2 Gaucher disease. *Hum Mutat* 2000;**15**:181-8.
18 Eikenboom JC, Vink T, Briët E, Sixma JJ, Reitsma PH. Multiple substitutions in the von Willebrand factor gene that mimic the pseudogene sequence. *Proc Natl Acad Sci USA* 1994;**91**:2221-4.
19 Janevski J, Park PC, De Boni U. Organization of centromeric domains in hepatocyte nuclei: rearrangement associated with *de novo* activation of the vitellogenin gene family in *Xenopus laevis*. *Exp Cell Res* 1995;**217**:227-39.
20 Nagele R, Freeman T, McMorrow L, Lee HY. Precise spatial positioning of chromosomes during prometaphase: evidence for chromosomal order. *Science* 1995;**270**:1831-5.
21 Cooper DN, Krawczak M. The mutational spectrum of single base-pair substitutions causing human genetic disease: patterns and predictions. *Hum Genet* 1990;**85**:55-74.
22 Andrews JD, Mancini DN, Singh SM, Rodenhiser DI. Site and sequence specific DNA methylation in the neurofibromatosis (*NF1*) gene includes C5839T: the site of the recurrent substitution mutation in exon 31. *Hum Mol Genet* 1996;**5**:503-7.
23 The Sanger Centre, The Washington University Genome Sequencing Center. Toward a complete human genome sequence. *Genome Res* 1998;**8**:1097-108.
24 Hoffmeyer S, Nürnberg P, Ritter H, Fahsold R, Leistner W, Kaufmann D, Krone W. Nearby stop codons in exons of the neurofibromatosis type 1 gene are disparate splice effectors. *Am J Hum Genet* 1998;**62**:269-77.
25 Fahsold R, Hoffmeyer S, Mischung C, Gille C, Ehlers C, Kücükceylan N, Abdel-Nour M, Gewies A, Peters H, Kaufmann D, Buske A, Tinschert S, Nürnberg P. Minor lesion mutational spectrum of the entire *NF1* gene does not explain its high mutability but points to a functional domain upstream of the GAP-related domain. *Am J Hum Genet* 2000;**66**:790-818.
26 Park VM, Pivnick EK. Neurofibromatosis type 1 (NF1): a protein truncation assay yielding identification of mutations in 73% of patients. *J Med Genet* 1998;**35**:813-20.
27 Heim RA, Kam-Morgan LN, Binnie CG, Corns DD, Cayouette MC, Farber RA, Aylsworth AS, Silverman LM, Luce MC. Distribution of 13 truncating mutations in the neurofibromatosis 1 gene. *Hum Mol Genet* 1995;**4**:975-81.

A clinical study of patients with multiple isolated neurofibromas

Patricia Blakley, David N Louis, M Priscilla Short, Mia MacCollin

J Med Genet 2001;**38**:485–488

Genetics and Teratology Unit, Massachusetts General Hospital, Boston, MA, USA
P Blakley*

Departments of Pathology and Neurosurgery, Massachusetts General Hospital, Boston, MA, USA
D N Louis

Department of Neurology, Massachusetts General Hospital, Boston, MA, USA
M P Short†
M MacCollin

Correspondence to: Dr MacCollin, Neuroscience Center, MGH-East Building 149, 13th Street, Charlestown, MA 02129, USA, maccollin@helix.mgh.harvard.edu

*Present address: Department of Pediatrics, University of Saskatchewan and Kinsmen Children's Centre, Saskatoon, Saskatchewan, Canada

†Present address: Department of Pediatric Neurosurgery, University of Chicago, Chicago, Illinois USA

EDITOR—Neurofibromas are benign nerve sheath tumours of a heterogeneous nature consisting of Schwann cells, fibroblastic elements, and embedded axons. Neurofibromas may occur singly in genetically normal people at any point along the peripheral nervous system. Multiple neurofibromas are nearly pathognomonic for neurofibromatosis 1 (NF1). In patients with NF1, neurofibromas may be congenital and plexiform or, more commonly, may be smaller masses that begin to accumulate around the time of puberty. Cutaneous and subcutaneous neurofibromas may cause considerable cosmetic disfigurement, but rarely result in neurological dysfunction. Conversely, deep seated neurofibromas on peripheral nerves and spinal roots frequently lead to neurological disability. Inevitably, adult patients with NF1 have other stigmata of the disorder with the most common being café au lait spots, skin fold freckling, and Lisch nodules.[1 2] NF1 is an autosomal dominant disorder with full penetrance and a defined genetic aetiology that shows no evidence of locus heterogeneity.[3] Neurofibromatosis 2 patients are rarely found to have one or more neurofibromas.[4 5]

Recently, we have become aware of a small number of patients with multiple pathologically proven neurofibromas, who have no other stigmata of NF1. Here we report the clinical characteristics and pathological findings of these patients, and propose the terminology "multiple isolated neurofibromas" to describe this rare condition.

Material and methods

The criteria for inclusion in the study were multiple, pathologically proven neurofibromas without other defining features of NF1. Careful family histories were obtained in order to document other family members potentially affected, extending to all second degree relatives. Each participant underwent a clinical examination by one or more of the authors (PB, MM, MPS), which included a detailed neurological evaluation and inspection of the skin with a Wood's lamp. For patients who gave a positive family history, medical records from the potentially affected family member and tumour specimens were reviewed to confirm the diagnosis. Blood samples were collected and immortalised cell lines created for future studies.

All available histological and immunohistochemical materials from each patient were requested from treating institutions and reviewed centrally by a single neuropathologist (DNL). In all but two patients, two or more distinct tumours from separate procedures were obtained; in patient BNF9 only a single specimen was available and in patient BNF12 two specimens from the same procedure were reviewed. Specimens were also reviewed from the mother of patient BNF2 and the brother of patient BNF10.

Molecular genetic analysis of the *NF2* gene was limited to specimens from patient BNF11 and his affected son and was performed as previously described.[6] No molecular analysis was performed of the *NF1* locus.

This study was approved by the institutional review board of Massachusetts General Hospital and informed consent was obtained from all subjects donating tissue.

Results

A total of 10 adult probands were identified who met our criteria of multiple neurofibromas without other stigmata of NF1 (table 1). Age of onset ranged from 6 to 53 years (mean 27.8 years). An

Table 1 Clinical characteristics of patients with multiple neurofibromas. Tumour distribution includes both surgically removed tumours and those still in place

Patient	Age (y)	Sex	Age of onset (y)	First symptom	Distribution of tumours	Findings associated with NF1	Tumour pathology (No of tumours)	Family history
BNF1	44	F	35	Painless mass	Brachial plexus and chest (bilateral)	Single CAL, migraine	Neurofibroma and plexiform neurofibroma (2)	Brother, osteosarcoma
BNF2	36	F	18	Abdominal pain	Scalp, spine and pelvis	Learning disability, migraine, single CAL	Neurofibroma (2)	Daughter, four subcutaneous masses Mother, multiple NF without CAL Maternal aunt and brother, multiple NF (not confirmed)
BNF3	39	F	6	Painless mass	Head and neck, spine, extremities, torso	Leg length discrepancy	Neurofibroma and plexiform neurofibroma (5)	None
BNF4	44	F	16	Facial palsy	Skull base, brachial plexus, spine, chest, pelvis, extremities	None	Neurofibroma (2)	None
BNF9	49	F	48	Chest pain	Brachial plexus (bilateral)	Migraine	Neurofibroma (1)	None
BNF10	47	M	33	Spastic gait	Spine	Skin tags	Neurofibroma (2)	Brother, multiple NF
BNF11	65	M	53	Painless mass	Shoulder, chest, arm (all cutaneous)	Three CAL	Neurofibroma (7)	Son, NF2
BNF12	62	F	20	Painless mass	Face, extremities (all cutaneous)	Three CAL	Neurofibroma (2)	Multiple relatives with "tumours", none confirmed
BNF14	48	F	18	Facial pain	Head and neck (R greater then L)	Single GTC, hypertension	Neurofibroma (4)	None
BNF15	39	F	31	Hip pain	R hip and buttock	None	Neurofibroma with marked collagen deposition (2)	None

F = female, M = male, R = right, L = left, CAL = café au lait macules, GTC = generalised tonic clonic seizure, NF = neurofibromas.

Figure 1 *Multiple masses in the right supraclavicular area in patient BNF1. A surgical scar from a debulking procedure is present.*

initial diagnosis of neurofibromatosis was made in only two patients. All patients reported an increase in the size and number of tumours since diagnosis. Seven patients reported increased pain in association with the increase in tumour size. In five cases, the pain had been unresponsive to medical management and had necessitated a reduction or discontinuation of employment. Decreasing neurological function was reported by three patients. A total of 41 surgical procedures had been performed on these patients for pain, increasing tumour size, or cosmetic disfigurement. A single patient received radiation therapy because of aggressive growth of her tumours associated with bony erosion.

Four patients gave a history of relatives potentially affected by NF. In one case (patient BNF12), none of the potentially affected relatives nor their records were available for study. In a second case (patient BNF11), the proband's son had typical neurofibromatosis 2. Molecular genetic analysis of the son's tumour showed a typical truncating mutation of the *NF2* gene and loss of the paternal allele. Examination of genomic DNA extracted from peripheral blood lymphocytes from patient BNF11 showed that the *NF2* gene mutation seen in the son's tumour was not present. Two patients had first degree affected relatives with pathologically proven neurofibromas (BNF2 and 10). These 10 patients had a total of 15 children ranging in age from 9 to 40 years. Three of 15 were affected by the proband's report and one (child of BNF2) had been examined and found to have four subcutaneous tumours and no café au lait macules at age 9.5 years. The mean age at referral to our clinic was 42.7 years.

Figure 2 *Right arm and hand of patient BNF3 showing nearly contiguous involvement of the forearm by tumour masses and abnormal nail beds.*

Figure 3 *Coronal MRI of the cervical spine in patient BNF10 shows multiple poorly enhancing tumours (*) with significant mass effect on the cord. Contrast enhanced T1 weighted image.*

Examination of these patients showed that four had readily visible, firm, subcutaneous tumours and two had typical cutaneous tumours indistinguishable from those seen in NF1 (fig 1). Detailed skin inspection using a Wood's lamp showed that no patient had six or more café au lait macules (CAL) and no patient had skin fold freckling. Neurological examination was abnormal in four with weakness, sensory change, or Horner's syndrome that could be attributed to the tumours or to postoperative change. Slit lamp examination was performed in all patients and failed to show Lisch nodules, cataract, or retinal changes. A single patient had abnormalities of the fingernails (fig 2); no other dysmorphic features were seen.

MR imaging studies of the tumours showed T2 bright and T1 isointense masses which were often poorly or irregularly enhancing (fig 3). Radiographic progression of tumours was documented in seven patients. Cranial MRI scan was performed in seven patients and thin cuts through the skull base were performed in four patients. A single patient (BNF4) had enhancement along cranial nerves consistent with tumour formation (fig 4).

Pathological review was conducted on archival material from 23 of the 41 surgical procedures, including two specimens from potentially affected relatives. All specimens were neurofibromas (table 1). Two patients (BNF1 and BNF3) had neurofibromas that were classically plexiform (fig 5A), in addition to having typical non-plexiform neurofibromas. Two patients (BNF4, BNF15) and two affected relatives (the mother of BNF2 and the brother of BNF10) had diffusely infiltrative neurofibromas that were suggestive, but not diagnostic, of plexiform neurofibroma. All tumours were characterised by elongated, wavy nuclei, often in a prominent myxoid background (fig 5B). Both tumours from one patient (BNF15) had marked collagen

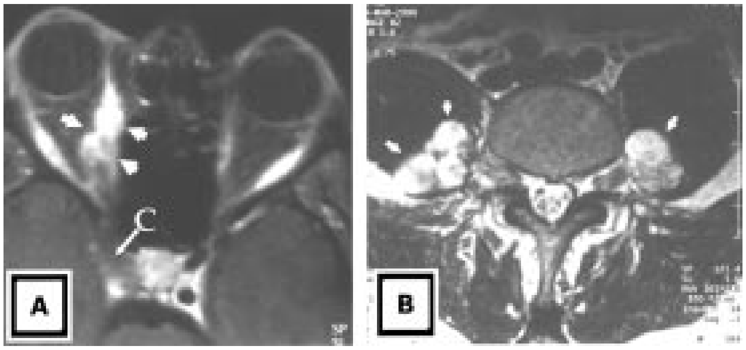

Figure 4 Imaging studies of patient BNF4. (A) Irregularly enhancing mass filling the right cavernous sinus (C) and extending forward into the orbit (arrowheads) causing proptosis. The right carotid artery is occluded at the level of the sinus. There is less prominent, irregular enhancement in the left cavernous sinus. T1 weighted, contrast enhanced image. (B) Multiple paraspinal masses at the level of L4 (arrowheads). T2 weighted image.

deposition. None of the tumours had defined capsules and many diffusely involved the affected nerves. Mitotic activity or necrosis was not noted in any specimen. None of the tumours had cytological or architectural features suggestive of schwannoma, such as Antoni A and B areas or Verocay bodies.

Discussion

In this report, we describe the clinical characteristics of 10 subjects with multiple, pathologically proven neurofibromas who do not have other diagnostic features of NF1 or NF2. These patients presented with a combination of pain and neurological disability that required frequent intervention and often prevented them from working. There was clear heterogeneity in tumour distribution, with five patients having anatomically localised tumours, and two patients having only cutaneous tumours. Detailed physical examination and imaging studies confirmed the lack of other features of the commonly recognised forms of NF. Pathological examination failed to show any distinguishing characteristics of their tumours; both plexiform and non-plexiform neurofibromas were seen. By the patients' reports, affected relatives were rare, and we were able to confirm a similarly affected relative in only two cases.

Careful classification of the neurofibromatoses has been essential to both natural history studies and the successful cloning and characterisation of the disease causing genes. Because of the pathology of their tumours, these patients were closely evaluated for the possibility of NF1. They met neither the original NIH diagnostic criteria[7] nor the proposed revision.[8] Especially remarkable is the lack of CAL spots (seen or reported in nearly 100% of adults with NF1), skin fold freckling (seen in 90%), and Lisch nodules (seen in 96%).[9] Neurofibromas are only rarely associated with NF2, and none of our patients had features suggestive of NF2, such as vestibular schwannoma, meningioma, or cataract. A single patient had an NF2 affected child, but we were able to exclude the diagnosis of NF2 in the patient using molecular methods.

In addition to NF1 and NF2, a number of variant forms of neurofibromatosis have been identified. Patients with marked anatomical and often dermatomal limitation of their tumours may represent segmental inactivation of the *NF1* tumour suppressor.[10] Although we did not observe any patient with strict dermatomal limitation, our patients BNF1, BNF9, BNF14, and BNF15 did show a localisation that suggests mosaicism. Several reports have been made of persons with anatomically limited tumours, which are all cutaneous and appear late in life.[11 12] Interestingly, two of our patients had only cutaneous tumours (BNF11 and BNF12), though neither had obvious anatomical limitation. The remainder of our patients had no cutaneous tumours, suggesting that cutaneous tumour formation may represent a distinct pathophysiological pathway. Finally, sporadic plexiform neurofibroma (in presumed genetically normal subjects) may adopt a complex anatomy which mimics multiple tumour masses. Without molecular analysis, we cannot completely exclude a single tumour in patients BNF1, BNF9, BNF14, and BNF15. However, we feel this is unlikely based on the radiographic appearance of the tumour burden.

There have been a number of recent studies suggesting that spinal neurofibromatosis is a separate entity. Closer evaluation of the families, however, suggests that many meet the diagnostic criteria for NF1. Pulst *et al*[13] reported two families with multiple spinal neurofibromas in the absence of cutaneous tumours, vestibular schwannomas, and Lisch nodules. In one of the families, however, all of the affected members had more than six CAL macules in association with their spinal neurofibromas. A similar family with spinal neurofibromas and CAL macules was reported by Poyhonen *et al*.[14] The three generation family reported by Ars *et al*[15] also meets the criteria for a diagnosis of NF1 and indeed was found to have a typical truncating mutation of the *NF1* gene. All affected family members had spinal neurofibromas, CAL macules, and either Lisch nodules or cutaneous neurofibromas. Spinal neurofibroma may, in fact, not be unusual in NF1 patients with or without symptoms.[16]

Careful pathological review is especially important in the classification of the neurofibromatoses. This is perhaps best illustrated by the observation that NF1 patients rarely, if ever, develop benign schwannomas and NF2 patients rarely develop neurofibromas.[4 5 17] In our review of the pathology of these patients and their affected family members, we found no patient with a schwannoma and no patient with malignant elements in their tumours. In clinical practice, pathological review of tumours in these patients was essential because their presentation was similar to those of patients with schwannomatosis (tumours often in an anatomically limited distribution and pain greater than neurological disability[18]). Interpretation of published reports of unusual NF phenotypes should be made with caution if detailed pathological descriptions are not given.

In summary, we present the clinical findings of 10 patients whose unifying feature is the presence of multiple neurofibromas without other stigmata of NF1. Those patients most severely affected have a unique, generalised

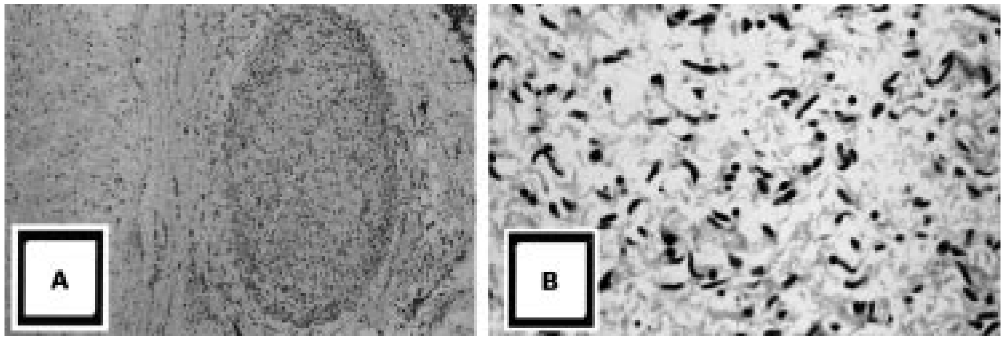

Figure 5 (A) Low power photomicrograph of plexiform neurofibroma from patient BNF3. The left half of the figure shows one ill defined nodule of neurofibroma, with a second, well defined fascicle in the right side of the figure. (B) High power photomicrograph of neurofibroma from patient BNF2. Note the wavy nuclei and myxoid background.

phenotype that at times was familial. Other patients may represent a mosaic form of NF1 with either localised manifestations or a generalised but attenuated form of the disease. Our current work is focused on identifying additional patients, clarifying the natural history of this phenotype, and studying patients' blood and tumour specimens in an effort to determine its molecular genetic aetiology.

We thank the patients and families for their participation in this work, and Dr Kevin Ruggles for his help with the evaluation of patient BNF4. This work was supported by National Institutes of Health grants R01 NS35878-02 (MM) and R01 NS24279 (DNL) and was presented in part at the 49th Annual Meeting of the American Society of Human Genetics, San Francisco, California, October 1999.

1 Huson SM, Harper PS, Compston DAS. Von Recklinghausen neurofibromatosis. *Brain* 1988;**111**:1355-81.
2 Creange A, Zeller J, Rostaing-Rigattieri S, Brugieres P, Degos JD, Revuz J, Wolkenstein P. Neurological complications of neurofibromatosis type 1 in adulthood. *Brain* 1999;**122**(pt 3):473-81.
3 Goldgar DE, Green P, Parry DM, Mulvihill JJ. Multipoint linkage analysis in neurofibromatosis type I: an international collaboration. *Am J Hum Genet* 1989;**44**:6-1.
4 Halliday AL, Sobel RA, Martuza RL. Benign spinal nerve sheath tumors: their occurrence sporadically and in neurofibromatosis types 1 and 2. *J Neurosurg* 1991;**74**:248-53.
5 Mautner VF, Lindenau M, Baser M, Kluwe L, Gottschalk J. Skin abnormalities in neurofibromatosis 2. *Arch Dermatol* 1997;**133**:1539-43.
6 Kluwe L, Mautner V, Parry D, Jacoby L, Baser M, Gusella J, Davis K, Stavrou D, MacCollin M. The parental origin of new mutations in neurofibromatosis 2. *Neurogenetics* 2000; **3**:17-24.
7 Mulvihill JJ, Parry DM, Sherman JL, Pikus A, Kaiser-Kupfer MI, Eldridge R. Neurofibromatosis 1 (Recklinghausen disease) and neurofibromatosis 2 (bilateral acoustic neurofibromatosis). An update. *Ann Intern Med* 1990;**113**: 39-52.
8 Gutmann DH, Aylsworth A, Carey JC, Korf B, Marks J, Pyeritz RE, Rubenstein A, Viskochil D. The diagnostic evaluation and multidisciplinary management of neurofibromatosis 1 and neurofibromatosis 2. *JAMA* 1997;**278**: 51-7.
9 Huson SM, Harper PS, Compston DA. Von Recklinghausen neurofibromatosis. A clinical and population study in south-east Wales. *Brain* 1988;**111**(pt 6):1355-81.
10 Tinschert S, Naumann I, Stegmann E, Buske A, Kaufmann D, Thiel G, Jenne DE. Segmental neurofibromatosis is caused by somatic mutation of the neurofibromatosis type 1 (*NF1*) gene. *Eur J Hum Genet* 2000;**8**:455-9.
11 Betti R, Cerri A, Gualandri L, Moneghini L, Crosti C. Regional eruptive neurofibromas. *J Dermatol* 1997;**24**:198-201.
12 Hager CM, Cohen PR, Tschen JA. Segmental neurofibromatosis: case reports and review. *J Am Acad Dermatol* 1997;**37**:864-9.
13 Pulst SM, Riccardi VM, Fain P, Korenberg JR. Familial spinal neurofibromatosis: clinical and DNA linkage analysis. *Neurology* 1991;**41**:1923-7.
14 Poyhonen M, Leisti EL, Kytola S, Leisti J. Hereditary spinal neurofibromatosis: a rare form of NF1? *J Med Genet* 1997; **34**:184-7.
15 Ars E, Kruyer H, Gaona A, Casquero P, Rosell J, Volpini V, Serra E, Lazaro C, Estivill X. A clinical variant of neurofibromatosis type 1: familial spinal neurofibromatosis with a frameshift mutation in the *NF1* gene. *Am J Hum Genet* 1998;**62**:834-41.
16 Thakkar SD, Feigen U, Mautner VF. Spinal tumours in neurofibromatosis type 1: an MRI study of frequency, multiplicity and variety. *Neurordiology* 1999;**41**:625-9.
17 Woodruff JM. Pathology of tumors of the peripheral nerve sheath in type 1 neurofibromatosis. *Am J Med Genet* 1999; **89**:23-30.
18 MacCollin M, Woodfin W, Kronn D, Short MP. Schwannomatosis: a clinical and pathologic study. *Neurology* 1996;**46**:1072-9.

B cell immunodeficiency, distal limb abnormalities, and urogenital malformations in a three generation family: a novel autosomal dominant syndrome?

Patrick Edery, Françoise Le Deist, Marie-Louise Briard, Marianne Debré, Arnold Munnich, Claude Griscelli, Alain Fischer, Stanislas Lyonnet

J Med Genet 2001;**38**:488–492

We report on a three generation family with four affected members presenting with a combination of B cell immunodeficiency, distal limbs abnormalities, genitourinary malformations, and mild dysmorphic features. All affected patients had normal intelligence and growth. No chromosomal abnormalities were observed using both standard and high resolution banding methods on the patients' lymphocytes. The observation of affected subjects of both sexes along with the occurrence of one male to male transmission suggests autosomal dominant inheritance of the trait with marked intrafamilial variable expression of the disease. While several multiple congenital anomalies (MCA) syndromes include both skeletal dysplasia and immune deficiency, the striking combination of congenital anomalies presented here, for which we propose the acronym BILU (B cell Immunodeficiency, Limb anomalies,

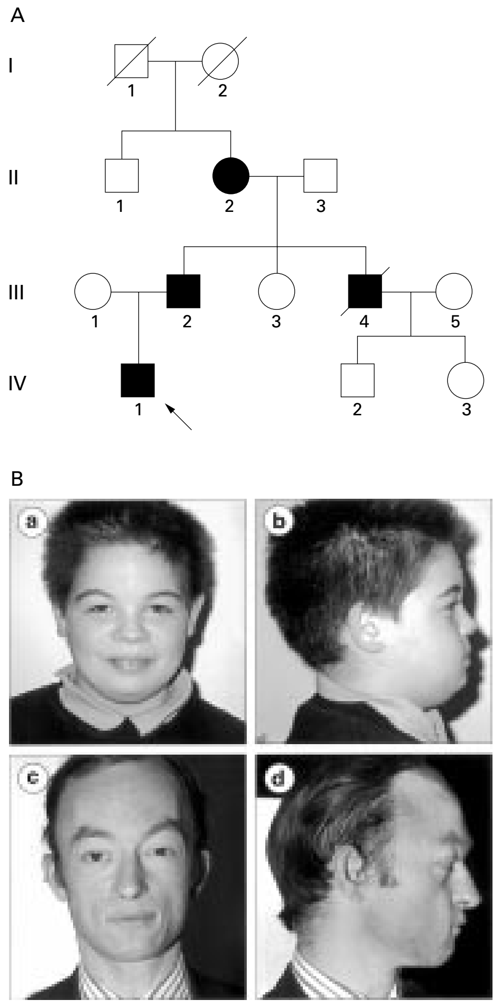

Figure 1 (A) Three generation pedigree including four affected members. The arrow indicates the proband. (B) (a, b) Face of the proband (IV.1). (c, d) Face of proband's father (III.2).

Service de Génétique Médicale, Hôpital Necker Enfants-Malades, 149 rue de Sèvres, 75743 Paris Cedex 15, France
P Edery
M-L Briard
A Munnich
S Lyonnet

Service de Génétique, Hospices Civils de Lyon, Hôpital Hôtel-Dieu, 1 place de l'Hôpital, 69288 Lyon Cedex 02, France
P Edery

Unité d'Immunologie et d'Hématologie, and INSERM U429 Hôpital Necker Enfants-Malades, 149 rue de Sèvres, 75743 Paris Cedex 15, France
F Le Deist
M Debré
C Griscelli
A Fischer

Correspondence to:
Dr Lyonnet,
lyonnet@necker.fr

and Urogenital malformations), is likely to represent a novel MCA syndrome.

Case reports

The proband (case 1, IV.1, fig 1) is an only child, born to unrelated parents. He was born at term by caesarian section with normal measurements (weight 3620 g, length 50 cm, and OFC 37 cm). Genital anomalies noted at birth included micropenis, scrotal hypospadias, and bilateral cryptorchidism, which required multiple surgical corrections. Despite testosterone substitution therapy, the size of the testes and penis only increased during puberty. Endocrine investigations including basal state testosterone, dihydrotestosterone, adrenal hormones, gonadotrophin plasma levels, gonadotrophin response to LHRH, and testosterone response to HCG were normal. Ultrasonography of the urinary system showed bilateral hydronephrosis.

Urography (IV) showed right hydronephrosis with atresia of the upper segment of the right ureter, right vesicoureteral reflux, and absence of secretion in the left kidney (fig 2). A left ureteronephrectomy was performed at 2½ months. Histological examination of the left urinary apparatus showed a dysplastic kidney

Figure 2 Urography of the proband (case 1). Note the absence of secretion of the left kidney and right hydronephrosis, ureteral stenosis, and vesicoureteral reflux.

with segmental cortical agenesis and localised ureteral atresia with a very thin underlying ureter. Atresia of the right ureter also required surgical correction.

As shown in fig 3, the proband also had bilateral distal limb abnormalities including short digits, thenar hypoplasia, bilateral palmar creases, brachymesophalangism of both fifth fingers, congenital flexion contractures of the interphalangeal joints of both thumbs and both big toes, skin syndactyly of toes 3-4, and clinodactyly of the fourth toes. *X* rays showed bilateral brachymesophalangism of toes 3-5 and short articular distances between phalanges P1 and P2 of the fourth toes. Mild dysmorphic features were noted including mild hypertelorism and fullness of the periorbital regions (fig 1).

A history of respiratory infections led us to investigate the haematological and immunological status of the proband. He had marked hypogammaglobulinaemia involving at least IgG and IgA (table 1). Anti-polio virus antibodies I, II, and III and anti-B allohaemagglutinins were undetectable in the plasma. No CD19 and no surface IgM could be detected in blood, indicating the absence of B cells. In contrast, other blood cell counts were repeatedly normal, as were T cell numbers when expressed as absolute values or ratios (CD3=85%, CD4=45%, CD8=35% (proband aged 13 months)) and T cell functions (PHA, candidin, and tetanus toxoid proliferation assays, mixed leucocyte reaction, natural killer (NK) activity, and cell mediated cytotoxicity). There has been no significant immunological change in the course of the proband's life. He still has marked hypogammaglobulinaemia involving IgG, IgA, IgM, and IgG 1-3

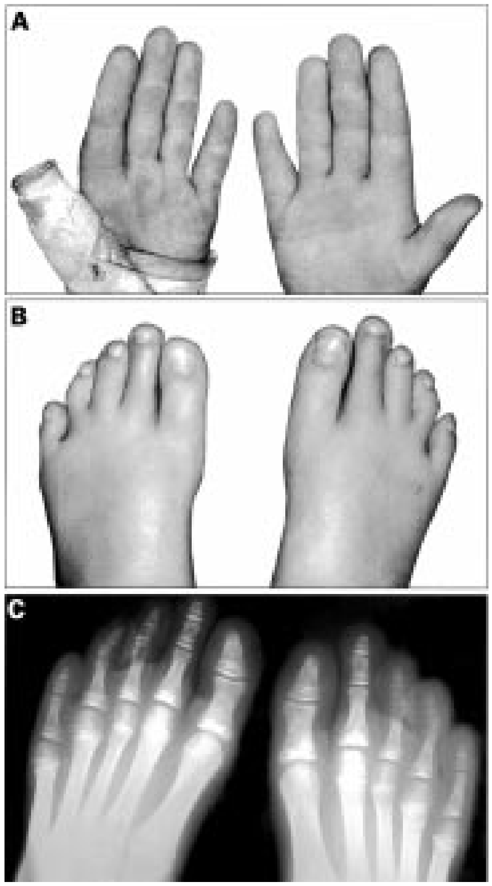

Figure 3 Proband (case 1). (A) Note short fingers, thenar hypoplasia, absence of flexion crease of the right thumb (left thumb not seen), and brachymesophalangism of the fifth fingers. (B) Note skin syndactyly of toes 3-4. (C) Brachymesophalangism of toes 3-5.

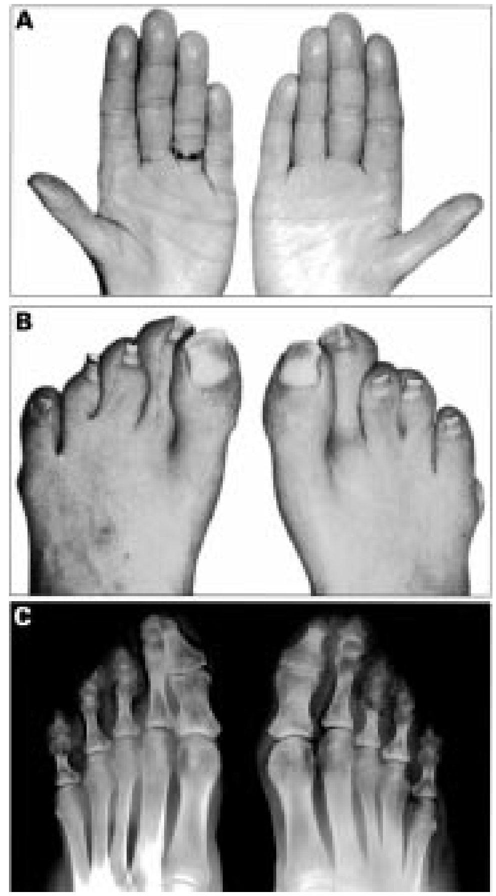

Figure 4 Father of the proband (case 2). (A) Hypoplasia of the thumbs and absence of flexion creases of the thumbs. (B) Overlapping first and second toes and skin syndactyly of toes 3-4. (C) Brachymesophalangism of toes 2-5 and absence of the third phalanx of the fifth toes.

subclasses (data not shown). Immunoglobulin perfusions were required every three weeks with a very good effect on respiratory infections. Unfortunately, we have not been able to perform a bone marrow biopsy as the proband has refused it so far, thus preventing the study of B lymphocyte precursors.

The proband had normal intelligence and growth until the age of 6 years when increased weight gain led to obesity (weight 113 kg, height 166 cm aged 15 years) and triggered or worsened psychological problems. Standard and high resolution banding karyotypes showed normal lymphocyte chromosomes.

Table 1 Results of significant haematological and immunological investigations in affected subjects

	Affected subjects				Control ranges in adults
	IV.1 (Proband aged 6 months)	III.2 (father)	III.4 (uncle)	II.2 (grandmother)	
Immunoglobulin values (mg/dl)					
IgG (total)	150 (control ranges: 280–680)	252	245	588	1410 ± 250
IgG1	ND	75	77	350	940 ± 190
IgG2	ND	15	13	287	320 ± 130
IgG3	ND	162	155	40	100 ± 45
IgG4	ND	0	0	11	62 ± 48
IgM	36 (control ranges: 40–84)	5.6	2.2	ND	53 ± 20
IgA	8 (control ranges: 10–58)	38	38	ND	194 ± 58
IgD	<2 (low)	2.2	1.8	ND	>3
CD19 (B cells) %	0	1 (low)	0	0	
Surface IgM (%)	0	<1	0	0	

ND: not determined.

The proband's father (case 2, III.2, fig 1) had recurrent episodes of respiratory infections, and had *Streptoccocus pneumoniae* meningitis at the age of 22, which led to investigation of his immune status (table 1). He had dissociated hypogammaglobulinaemia involving mainly IgG, IgA, and IgM with IgG1, IgG2, and IgG4 deficiency. Very few B cell lymphocytes could be detected using a CD19 specific antibody. He had normal T cell lymphocyte counts and functions. IV immunoglobulin substitution was initiated.

Fig 4 shows distal limb abnormalities including bilateral flexion contractures of the interphalangeal joints of the thumbs, hypoplasia of the thumbs, overlapping first and second toes, and skin syndactyly of toes 3-4. *X* rays showed brachymesophalangism of toes 2-5 with only two phalanges on the fifth toes and short metacarpophalangeal and interphalangeal articular distances of fingers (not shown). He had epispadias and his son (case 1) was born using artificial insemination.

Dysmorphic features consisted of mild hypertelorism (interpupillary distance of 6.5 cm), deep periorbital ridges, fullness of periorbital regions, mandibular hypoplasia, and a thin chin (fig 1). He had severe, non-progressive, bilateral, sensorineural deafness considered to be a consequence of his meningitis. Intelligence, height, and weight were

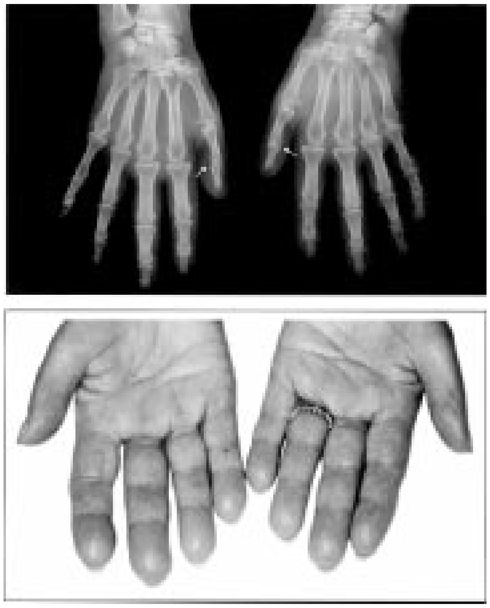

Figure 5 Paternal grandmother of the proband (case 4). (Top) Symphalangism of both thumbs is indicated by arrows. (Bottom) Absence of flexion crease of thumbs.

normal. Standard chromosome studies on blood lymphocytes showed no anomalies.

The proband's paternal uncle (case 3, III.4, fig 1) had a similar disease history to his brother (case 2) with recurrent respiratory infections and a *Streptoccocus pneumoniae* meningitis. He had dissociated hypogammaglobulinaemia with marked deficiency of IgG, IgA, and IgM and IgG1, IgG2, and IgG4 subclasses. No B cell lymphocytes could be detected (table 1). Bilateral symphalangism of the thumbs, epispadias which required surgical correction, and hypertelorism were noted. He had bilateral deafness considered to result from his meningitis, but which was not further investigated. He died from post-hepatitis cirrhosis. His blood karyotype performed using standard methods showed normal chromosomes.

The paternal grandmother of the proband (case 4, II.2, fig 1) had a humoral immune deficiency with slight IgG, IgG1, and IgG4 deficiencies but no detectable B cell lymphocytes (table 1) and normal T cell lymphocyte numbers and functions (lymphocyte proliferation after exposure to PHA). She had bilateral contractures of the interphalangeal joints of the thumbs and symphalangism of the thumbs as shown by *x* rays (fig 5), but no urogenital anomalies. Her parents were known to be healthy and her father was 38 years old at the time of her conception.

Discussion

Here, we report on a striking combination of congenital anomalies, including B cell immunodeficiency, distal limb malformations, urogenital anomalies, and mild dysmorphic features in four members of a single three generation family. We propose the acronym BILU (B cell Immunodeficiency, Limb anomalies, and Urogenital malformations) as a means to make this association of signs easier to remember. Two of the four affected subjects (cases 2 and 3) also had deafness and one was obese (the proband, case 1). However, deafness started after a *Streptococcus pneumoniae* meningitis in both cases and the type of deafness was sensorineural and non-progressive in case 2 (not studied in case 3), suggesting that this feature may not be part of the BILU syndrome. Also, obesity in case 1 was associated with a unfavourable psychosocial status and, in our opinion, should not be considered as a specific sign. The occurrence of one male to male transmission together with the intrafamilial variability in phenotypic expression of the disease suggests autosomal dominant inheritance of the trait. Alternatively, an infracytogenetic chromosomal rearrangement might be responsible for the disease phenotype. However, the latter hypothesis is unlikely since neither mental retardation nor growth delay was observed in the affected subjects. This combination of congenital anomalies including B cell immunodeficiency appears unique and thus may represent an as yet undescribed autosomal dominant MCA syndrome.

Several short limbed dwarfisms/skeletal dysplasias (SLSD) have been found to be associated with immunodeficiency.[1] Ammann *et al*[2] proposed a classification based on the immune defect. Type 1 includes early lethal SLSD with combined humoral (B cell) and cell mediated (T cell) immunodeficiency. Patients with type 1 SLSD appear to form a heterogeneous group.[3] Some have adenosine deaminase (ADA) deficiency.[3 4] Several reports have described type 1 SLSD cases associated with features of Ommen syndrome, namely eosinophilia, reticuloendotheliosis, alopecia, and ichthyosiform skin lesions.[3 5–7] Type 2, less common than type 1, includes SLSD and T cell immunodeficiency, an association reminiscent of the cartilage-hair hypoplasia syndrome (CHH, MIM 250250), a metaphyseal dysplasia with short stature, fine and sparse blond hair, chronic neutropenia, and abnormal cellular immunity.[8 9] This autosomal recessive condition has been mapped to chromosome 9p13.[10] Type 3 (two sibs reported by Ammann *et al*[2]) comprises SLSD with antibody mediated (B cell) immunodeficiency. It should be noted that skeletal phenotypes overlap considerably between these categories, apart from CHH which appears to be a genetically homogeneous condition. It is questionable whether this classification is relevant with regard to the underlying molecular pathology.

In the family presented here, the diagnosis of SLSD can easily be excluded since the patients do not have short stature. Moreover, urogenital anomalies are not commonly observed in SLSD. The pattern of congenital anomalies reported here shows some overlap with that of a 6 year old boy born to first cousin parents of Turkish origin described by Braegger *et al*.[11] This patient had panhypogammaglobulinaemia, hypospadias, bilateral cryptorchidism, and distal limb anomalies comprising short hands and digits, short middle phalanges of the fifth fingers, and mild skin syndactyly of the toes. However, we believe that we are dealing with a different condition since this boy also displayed mental retardation, ischiadic hypoplasia, renal dysfunction without any obstructive uropathy, and marked facial dysmorphism. He had neither symphalangism nor limitation of flexion of the thumbs.

We will briefly describe other immuno-osseous syndromes with short stature. Each of these conditions also appears to be different from the BILU syndrome. Schimke immuno-osseous dysplasia (MIM 242900) includes short trunk skeletal dysplasia, glomerulonephritis with immune complex formation, and a defect of T cell maturation.[12 13] Ainsworth *et al*[14] reported a syndrome of selective IgG2 deficiency with severe growth retardation of prenatal onset, developmental delay, distal limb hypotrophy, dental anomalies, and eczematous skin.[14] The Say-Barber-Miller syndrome includes B cell deficiency, short stature, hypoplastic patellae, multiple joint anomalies, microcephaly, mental retardation, hypogonadism, and unusual facies.[15 16] Two female sibs with hypogammaglobulinaemia, multiple epiphyseal dysplasia, prenatal growth deficiency, microcephaly, mental retardation, cataracts, enamel hypoplasia, and downward slanting palpebral fissures were reported by Toriello *et al*.[17] Unique combinations of immunodeficiency and skeletal dysplasia, such as those reported by Lichtenstein *et al*,[18] Castriota-Scanderbeg *et al*,[19] and Kultursay *et al*,[20] should also be mentioned. Rare disorders such as Shokeir syndrome (MIM 274190) combine B cell deficiency and/or immunoglobulin abnormalities and a radial ray defect.[21 22] Brewer *et al*[23] reported a male infant with low immunoglobulin values and bilateral radial aplasia, but this child also had anomalies absent in our patients, namely severe prenatal and postnatal growth retardation and markedly increased spontaneous chromosome breaks in leucocytes. This latter case may be related to the group of autosomal recessive chromosome breakage disorders including Fanconi anaemia. Finally, associations of B cell deficiency with alopecia, but without osseous anomalies, have also been reported by Ipp *et al*.[24]

Careful examination of the skeletal and urogenital systems in patients with B cell immunodeficiency may hopefully lead to the identification of other cases similar to those observed in the family described here. The diagnostic importance of two rare signs observed in the family presented here, namely epispadias (cases 2 and 3) and symphalangism (cases 3 and 4), is worth noting. Each of these two signs may suggest the diagnosis of BILU syndrome when associated with B cell immunodeficiency. Finally, this observation raises the question of which gene(s) might be involved in three different developmental fields, such as the immune, skeletal, and urogenital systems.

We thank Mrs A Reumert-Kazès for her help with writing this manuscript.

1 Ming JE, Stiehm ER, Graham JM Jr. Immunodeficiency as a component of recognizable syndromes. *Am J Med Genet* 1996;**66**:378-98.
2 Ammann AJ, Sutliff W, Millinchick E. Antibody-mediated immunodeficiency in short-limbed dwarfism. *J Pediatr* 1974;**84**:200-3.
3 MacDermot KD, Winter RM, Wigglesworth JS, Strobel S. Short stature/short limb skeletal dysplasia with severe combined immunodeficiency and bowing of the femora: report of two patients and review. *J Med Genet* 1991;**28**:10-17.
4 Cederbaum SD, Kaitila I, Rimoin DL, Stiehm ER. The chondro-osseous dysplasia of adenosine deaminase deficiency with severe combined immunodeficiency. *J Pediatr* 1976;**89**:737-42.
5 Schofer O, Blaha I, Mannhardt W, Zepp F, Stallmach T, Spranger J. Ommen phenotype with short-limbed dwarfism. *J Pediatr* 1991;**118**:86-9.
6 Gatti RA, Platt N, Pomerance HH, Hong R, Langer LO, Kay HE, Good RA. Hereditary lymphopenic agammaglobulinemia associated with a distinctive form of short-limbed dwarfism and ectodermal dysplasia. *J Pediatr* 1969;**75**:675-84.
7 Gotoff SP, Esterly NB, Gottbrath E, Liebner EJ, Lajvardi SR. Granulomatous reaction in an infant with combined immunodeficiency disease and short-limbed dwarfism. *J Pediatr* 1972;**80**:1010-7.
8 Lux SE, Johnston RB Jr, August CS, Say B, Penchaszadeh VB, Rosen FS, McKusick VA. Chronic neutropenia and abnormal cellular immunity in cartilage-hair hypoplasia. *N Engl J Med* 1970;**282**:231-6.
9 McKusick VA, Eldridge R, Hostetler JA, Egeland JA, Ruangwit U. Dwarfism in the Amish. II. Cartilage-hair hypoplasia. *Bull Johns Hopkins Hosp* 1965;**116**:285-326.
10 Sulisalo T, Klockars J, Makitie O, Francomano CA, de la Chapelle A, Kaitila I, Sistonen P. High-resolution linkage-disequilibrium mapping of the cartilage-hair hypoplasia gene. *Am J Hum Genet* 1994;**55**:937-45.
11 Braegger C, Bottani A, Hallé F, Giedion A, Leumann E, Seger R, Willi U, Schinzel A. Unknown syndrome: ischiadic hypoplasia, renal dysfunction, immunodeficiency, and a pattern of minor congenital anomalies. *J Med Genet* 1991;**28**:56-9.
12 Schimke RN, Horton WA, King CR, Martin NL. Chondroitin-6-sulfate mucopoly-saccharidosis in conjunction with lymphopenia, defective cellular immunity and the nephrotic syndrome. *Birth Defects* 1974;**10**:258-66.
13 Spranger J, Hinkel GK, Stoss H, Thoenes W, Wargowski D, Zepp F. Schimke immuno-osseous dysplasia: a newly recognized multisystem disease. *J Pediatr* 1991;**119**: 64-72.
14 Ainsworth SB, Baraitser M, Mueller RF, Massey RF. Selective IgG2 subclass deficiency - a marker for the syndrome of pre/postnatal growth retardation, developmental delay, hypotrophy of distal extremities, dental anomalies and eczema. *Clin Dysmorphol* 1997;**6**:139-6.
15 Say BA, Barber N, Miller GC, Grogg SE. Microcephaly, short stature, and developmental delay associated with a chemotactic defect and transient hypogammaglobulinaemia in two brothers. *J Med Genet* 1986;**23**:355-9.
16 Perandones C, Cerretini RI, Vargas Vera RM, Aranda EI, Alba LG, Pivetta OH. Microcephaly, characteristic facies, joint abnormalities, and deficient leucocyte chemotaxis: a further case of the syndrome of Say *et al*. *J Med Genet* 1996;**33**:227-9.
17 Toriello HV, Horton WA, Oostendorp A, Waterman DF, Higgins JV. An apparently new syndrome of microcephalic primordial dwarfism and cataracts. *Am J Med Genet* 1986; **25**:1-8.
18 Lichtenstein JR. A "new" syndrome with neutropenia, immune deficiency, and multiple congenital anomalies (spondylolysis, open posterior cervical arches, ulnar deviation of fingers, carp mouth). *Birth Defects* 1972;**8**:178-90.
19 Castriota-Scanderbeg A, Mingarelli R, Caramia G, Osimani P, Lachman RS, Rimoin DL, Wilcox WR, Dallapiccola B. Spondylo-mesomelic-acrodysplasia with joint dislocations and severe combined immunodeficiency: a newly recognised immuno-osseous dysplasia. *J Med Genet* 1997;**34**: 854-6.
20 Kultursay N, Taneli B, Cavusoglu A. Pseudoachondroplasia with immune deficiency. *Pediatr Radiol* 1988;**18**:505-8.
21 Shokeir MHK. Short stature, absent thumbs, flat facies, anosmia and combined immune deficiency (CID). *Birth Defects* 1978;**14**:103-16.
22 Semmekrot BA, Haraldsson A, Weemaes CMR, Smeets DFCM, Geven WB, Brunner HG. Absent thumb, immune disorder, and congenital anemia presenting with hydrops fetalis. *Am J Med Genet* 1992;**42**:736-40.
23 Brewer CM, Grace E, Stark, GD, Gregory DW, Howell RT, Fitzpatrick DR. Genomic instability associated with limb defects: case report and review of the literature. *Clin Dysmorphol* 1997;**6**:99-109.
24 Ipp MM, Gelfand EW. Antibody deficiency and alopecia. *J Pediatr* 1976;**89**:728-31.

Chromosome 2 interstitial deletion (del(2)(q14.1q21)) associated with connective tissue laxity and an attention deficit disorder

K L Baker, M I Rees, P W Thompson, R T Howell, T R Cole, H E Hughes, M Upadhyaya, D Ravine

J Med Genet 2001;**38**:493–496

Medical Genetics Service for Wales, University Hospital of Wales, Heath Park, Cardiff CF4 4XW, UK
K L Baker
P W Thompson
H E Hughes
M Upadhyaya
D Ravine

Department of Psychological Medicine and Medical Genetics, University of Wales College of Medicine, Cardiff, UK
M I Rees

Department of Molecular Medicine, University of Auckland, Private Bag 92019, Auckland, New Zealand
M I Rees

Regional Cytogenetics Centre, Southmead Hospital, Bristol, UK
R T Howell

West Midlands Regional Clinical Genetics Service, Birmingham, UK
T R Cole

Correspondence to: Dr Ravine
ravine@cardiff.ac.uk

EDITOR—Reports of interstitial deletions involving the long arm of chromosome 2 are uncommon.[1–10] Among these, there are only four which involve the region q14q21. We report a further case with a paternally derived de novo interstitial deletion of chromosome 2q14.1q21.

Case report

The proband was a male born by spontaneous vaginal delivery at term following an uneventful pregnancy. The parents are healthy, unrelated, and white. Birth weight was 4140 g (97th centile). Early childhood was complicated by hypotonia and recurrent sleep apnoea which resolved following adenoidectomy at 2 years of age. Otherwise, his medical history showed the normal range of intercurrent childhood viral illnesses. While childhood linear growth was rapid, during the second year there was considerable concern about poor weight gain. At 6 years of age he was noted to have a high, bossed forehead with a large head circumference (90-97th centile). A thoracolumbar kyphoscoliosis and a mild sternal depression was noted. He attended normal school although moderate learning difficulties were experienced. An attention deficit defect was identified and managed with the aid of methylphenidate hydrochloride. At 15 years of age, he was tall and thin (height 176 cm, 80th centile; weight 43.3 kg, 5th centile) with an associated moderate thoracolumbar kyphoscoliosis and pectus carinatum deformity. While the upper segment:lower segment ratio was 0.804, it was apparent that spinal height was somewhat reduced by the curvature of the scoliosis. The span measurement was 175 cm and head circumference was 56.0 cm (60th centile). He was a generally thinly muscled adolescent with little subcutaneous tissue. Some mild proximal upper limb weakness was detected and winging of the scapulae was evident, particularly on the right side. Examination of the musculature around the scapulae showed that the trapezius muscles were absent or possibly extremely hypoplastic. Ophthalmic examination showed normal fundi with no evidence of corneal or anterior chamber abnormalities, lens opacities, or dislocation. Other than findings of brisk lower limb reflexes, no other neuromuscular signs were present. No striae were evident. The forehead was high and the mandible was prominent owing to obtuse angulation. The ears were low set and dysplastic with some overfolding of the pinnae. The palate was high arched. Puberty had started, with stage 4 pubic hair development and a testicular volume of 25 ml. Cardiac echocardiography showed a mild degree of aortic root dilatation (aortic diameter 2.9 cm, calculated body surface area of 1.5 m^2) but otherwise normal cardiac anatomy. Cytogenetic studies showed a small proximal interstitial deletion on the long arm of chromosome 2 (46,XY,del(2)(q14.1-21)). Before this result, no syndromic diagnosis was immediately apparent, although the occurrence of a high birth weight, a markedly prominent forehead in early childhood (fig 1A, B), and later development of mandibular prominence, hypotonia, and disproportionately long limbs had raised the question of Sotos syndrome.[11] No bone age assessments were performed earlier in childhood and it was concluded that there were insufficient features present to confirm this diagnosis. Later photographs taken in mid childhood (fig 1C-F) were not supportive of the diagnosis.

In view of the phenotype observed in this child and the rarity of interstitial deletions within this region of chromosome 2, it was decided to delineate the breakpoints of the deletion further by both fluorescence in situ hybridisation and microsatellite analysis. FISH analysis with three YACS identified a region of deletion defined by YAC694-d-4. The deleted YAC contains marker D2S110 which provided an anchor point for the microsatellite work. Microsatellite markers (Genethon map) were selected and loss of heterozygosity analysis further defined the deletion within a genetic distance of approximately 10-12 cM and involves markers ranging from 2q14.1 to 2q21.1 (fig 2). The loss of alleles was paternal for all markers and the patient displayed only the maternal alleles for the deleted region.

Discussion

Common clinical features among the few reports of proximal interstitial deletions of chromosome 2 involving the region q14.1q21 include developmental delay, microcephaly, defects of the corpus callosum, prominence of the forehead, low set and malformed ears, cardiac anomalies, and a tendency to recurrent, severe infections (table 1). Our case has some of the characteristics reported in these earlier cases, including a prominent forehead and low set and malformed ears. Like the case reported by Frydman et *al*,[6] the birth weight of our case was unusually high. The older age of our patient, compared with those in earlier reports, provided an opportunity to document a more extensive medical history than has been recorded previously.

Weight gain was disproportionately poor from early childhood onwards, despite linear growth remaining above the 50th centile. In contrast to the earlier reports of marked microcephaly,[1 6] head growth in the case reported here was proportionate to linear growth. Similarly, the occurrence of moderate learning difficulties is in contrast to the severe developmental delay reported in the case of Frydman *et al*.[6]

The presence of kyphoscoliosis with pectus carinatum deformity and mild aortic root dilatation suggests an abnormality involving connective tissue. Although these features occur commonly in Marfan syndrome, there

Figure 1 The facial features of the proband at (A) 18 months; (B) 3 years; (C) 6 years; (D) 9 years; (E) 15 years, trunk and upper limbs; (F) 15 years, front facial view; (G) 15 years, lateral facial view; (H) 17 years, front facial view.

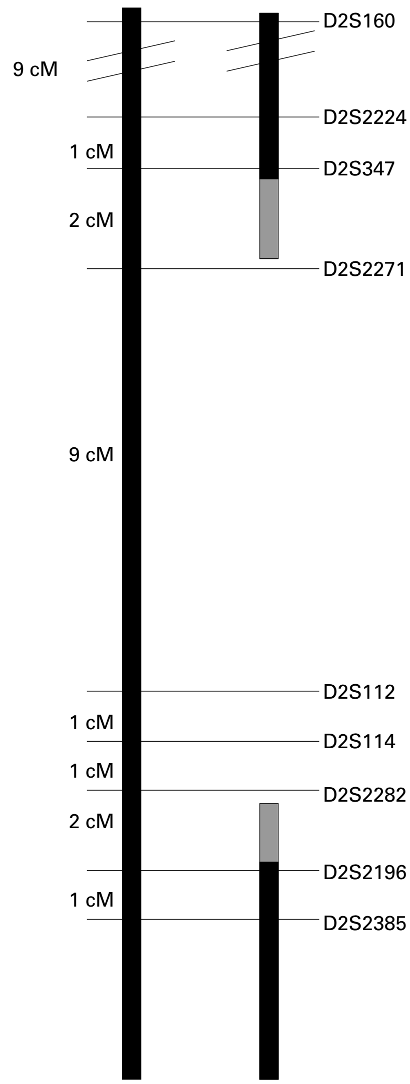

Figure 2 Deleted region at 2q14.1-q21. Markers proximal to D2S2224 and distal to D2S2385 were consistently biallelic. Grey portions of the del(2) chromosome represents the areas on which the deletion breakpoints can be localised.

were insufficient other physical features present to support this diagnosis. Nevertheless, there are some similarities, which raise the interesting possibility of another potential FBN gene within the chromosome 2 deleted region. Similarly, the associated occurrence of a moderate learning disability, together with an attention deficit defect, suggests that genes involved with higher level cerebral function are located within the deleted region. Occurrence of callosal defects among the other cases with interstitial deletions of this chromosomal region points to an abnormality of neuronal migration. Unfortunately, it was not possible to arrange neuroimaging in our own case. Nevertheless, the more moderate neurodeficit in our case contrasted with the earlier case reports of proximal 2q deletions and indicates that a variable CNS phenotype is associated with interstitial deletions in this region.

Haploinsufficiency involving one or more genes is a likely explanation for the observed phenotype. There are a number of genes within or close to the deleted region that are determinants for growth and development. Genes that could contribute to the phenotypes observed among those with interstitial deletions in this region include *GLI2* and the interleukin 1 genes and their receptors (*IL1A, IL1B, IL1RN*, and *IL1R2*). Gli2, a zinc finger transcription factor whose human homologue *GLI2* is positioned at 2q14, has been shown to have overlapping functions with Gli3 in Shh signalling.[12] It is of interest that the most proximal 2q interstitial deletion (q12-q14) has lower limb postaxial hexadactyly[4] in keeping with the polydactyly observed with *GLI3* mutations in Greig cephalopolysyndactyly syndrome, Pallister-Hall syndrome, and postaxial polydactyly type A syndrome.[13] The occurrence of severe childhood infections, and unexplained febrile episodes as well as leukaemoid reactions among many of these cases with interstitial deletions in this proximal region of 2q is of interest. In this context, it is notable that our case did not have such a history. Candidate genes for these features include the interleukin-1 (IL-1) gene cluster and the IL-1 receptor gene cluster which map in the region of chromosome 2q12 to 2q13.[14 15]

Other genetic explanations for the observed phenotype include the unmasking of autosomal recessive disease owing to hemizygosity, or a parent of origin, or imprinting, effect contributing in part or in whole to the observed differences. While microsatellite analysis showed that the deletion in this case was of paternal origin, the parental origins of the previously reported deletions were not determined. Interestingly, the father of the case with an interstitial deletion of the region q13q21, reported by Davis et *al*,[8] had a balanced translocation involving chromosome 2 as well as a pericentric inversion of chromosome 9 (46,XY,inv(9),t(2,7)(q32.2;p11). Other than this unusual report of co-occurrence of two chromosomal rearrangements involving the long arm of chromosome 2 in parent and child, there is insufficient evidence arising from earlier reports to determine whether a parent of origin effect occurs in this chromosomal region. Should such an effect occur, the paternal origin of the deletion reported here makes it possible to predict that maternal imprinting is involved. While reports of maternal disomy of chromosome 2 associated with phenotypic abnormalities is supportive of this concept,[16] a report of maternal isodisomy 2 owing to the de novo inheritance of two isochromosomes for chromosome 2 in a normal healthy female, karyotyped because of recurrent spontaneous abortions,[17] is strong evidence against.

To conclude, this case provides some additional insights into the effects of haploinsufficiency arising from a deletion of paternal origin in the proximal region of the long arm of chromosome 2.

Table 1 Reports of proximal deletions of chromosome 2

	Antich et al[4]	*German et al*[1]*	*Davis et al*[8]*	*Present case*	*Lucas et al*[5]*	*Frydman et al*[6]*	*Fryns et al*[2]	*McConnell et al*[3]
Deletion	q12-q14	q13-q21	q13-q21	q14.1-q21	q14-q21	q14-q21	q21-q24	q22-q31
Parental origin of deletion	Unknown	Unknown	Paternal karyotype 46,XY, inv (9), t(2,7)(q32.2;p11)	Paternal	Unknown	Unknown	Unknown	Unknown
Sex	M	M	F	M	F	F	F	F
Age	8 mth†	30 mth	29 mth†	17 y	11 mth	2 y	2 mth†	Newborn†
Birth weight (g)	2400		2790	4140 (97th centile)	3060	4900	2500	1500
Growth	Failure to thrive		Failure to thrive	Poor weight gain (5th centile) Linear growth normal (80th centile)		Weight 40th centile; Length 10th centile	Failure to thrive	Not applicable
Developmental delay/ learning difficulties	+ (Severe)		+ (Severe)	Mod learning difficulties Attention deficit disorder		Severe dev delay	+ (Severe)	Not applicable
OFC	Microcephaly Head circumference at birth 32 cm	Microcephaly	Macrocephaly Head circumference at birth: 36 cm (>95th centile)	Macrocephaly Head circumference 90–97th centile		Microcephaly	Microcephaly Head circumference at birth 32.5 cm (<3rd centile)	Hydrocephalus
Callosal defect	+		+	Unknown		+		+
Sutural irregularities	+			No	+	No		+
Prominent forehead	+			+	+	+	+	
Ocular anomalies				Normal ophthalmic examination		Corneal opacity Peter's anomaly	Cataract Microphthalmia	
Low set ears	+			+	+	+	+	+
Malformed ears	+		+	+		+		
Mandible	Micrognathia			Prominent, obtuse angulation		Micrognathia	Micrognathia	Micrognathia
Cleft lip/palate	+			No		No	+	+
Cardiac malformation	Ventriculoseptal defect		Atrial septal defect	Aortic root dilatation	No	Patent ductus arteriosus	Patent ductus arteriosus	Truncus arteriosus
Recurrent infections/ unusual immune responses	+		+ (Recurrent unexplained febrile episodes)	No	+	+ Leukaemoid reactions	+	
Other anomalies	Hydronephrosis Postaxial hexadactyly of toes Imperforate anus	Abnormal gait Hemizygosity at the MN locus	Loose skin Generalised hyperextensibility Dandy-Walker malformation Hydrocephalus Partial agenesis of the cerebellar vermis Ovarian dysgenesis Clinodactyly	Hypotonia in infancy Pectus carinatum Kyphoscoliosis Proximal upper limb weakness Winging of scapulae	Hypotonia in infancy	Cortical blindness Seizures Renal malrotation and ectopia Anteriorly placed anus	Polycystic ovaries	Encephalocele

*Cases with deleted regions which overlap that of the present case.
†Dead.

The contribution of Dr T Hutchison, who was central to the patient's coordinated paediatric management, is gratefully acknowledged. We thank Dr N Rahman for helpful criticism and suggestions.

1 German J, Walker ME, Stiefel FH, Allen FH Jr. MN blood-group locus: data concerning the possible chromosomal location. *Science* 1968;**162**:1014-15.
2 Fryns JP, Van Bosstraeten B, Malbrain H, Van den Berghe H. Interstitial deletion of the long arm of chromosome 2 in a poly-malformed newborn-karyotype: 46,XX,del(2)(q21;q24). *Hum Genet* 1977;**39**:233-8.
3 McConnell TS, Kornfeld M, McClellan G, Aase J. Partial deletion of chromosome 2 mimicking a phenotype of trisomy 18: case report with autopsy. *J Hum Pathol* 1980;**11**:202-5.
4 Antich J, Carbonell X, Mas J, Clusellas N. De novo interstitial deletion of the long arm of chromosome 2 in a malformed newborn with a karyotype: 46,XY,del(2)(q12q14). *Acta Paediatr Scand* 1983;**72**:631-3.
5 Lucas J, Faivre J, Le Mee F, Hubert S, Pluquailec K, Picard F. De novo interstitial deletion of the long arm of chromosome 2: 46,XX,del(2)(q14q21), associated with premature craniosynostosis. *Ann Genet* 1987;**30**:33-8.
6 Frydman M, Steinberger J, Shabtai F, Katznelson MB, Varsano I. Interstitial deletion 2q14q21. *Am J Med Genet* 1989;**34**:476-9.
7 Ramer JC, Ladda RL, Frankel CA, Beckford A. A review of phenotype-karyotype correlations in individuals with interstitial deletions of the long arm of chromosome 2. *Am J Med Genet* 1989;**32**:359-63.
8 Davis E, Grafe M, Cunniff C, Jones KL, Bogart M. Interstitial deletion of chromosome 2q associated with ovarian dysgenesis. *Clin Genet* 1991;**39**:386-90.
9 Nixon J, Oldridge M, Wilkie AO, Smith K. Interstitial deletion of 2q associated with craniosynostosis, ocular coloboma, and limb abnormalities: cytogenetic and molecular investigation. *Am J Med Genet* 1997;**70**:324-7.
10 McMilin KD, Reiss JA, Brown MG, Black MH, Buckmaster DA, Durum CT, Gunter KA, Lawce HJ, Berry TL, Lamb OA, Olson CL, Weeks FF, Yoshitomi MJ, Jacky PB, Olson SB, Magenis RE. Clinical outcomes of four patients with microdeletion in the long arm of chromosome 2. *Am J Med Genet* 1998;**78**:36-43.
11 Cole TR, Hughes HE. Sotos syndrome: a study of the diagnostic criteria and natural history. *J Med Genet* 1994;**31**:20-32.
12 Motoyama J, Liu J, Mo R, Ding Q, Post M, Hui CC. Essential function of Gli2 and Gli3 in the formation of lung, trachea and oesophagus. Nat *Genet* 1998;**20**:54-7.
13 Biesecker LG. Strike three for GLI3. *Nat Genet* 1997;**17**:259-60.
14 Nothwang HG, Strahm B, Denich D, Kubler M, Schwabe J, Gingrich JC, Jauch A, Cox A, Nicklin MJ, Kurnit DM, Hildebrandt F. Molecular cloning of the interleukin-1 gene cluster: construction of an integrated YAC/PAC contig and a partial transcriptional map in the region of chromosome 2q13. *Genomics* 1997;**41**:370-8.
15 Dale M, Nicklin MJ. Interleukin-1 receptor cluster: gene organization of IL1R2, IL1R1, IL1RL2 (IL-1Rrp2), IL1RL1 (T1/ST2), and IL18R1 (IL-1Rrp) on human chromosome 2q. *Genomics* 1999;**57**:177-9.
16 Shaffer LG, McCaskill C, Egli CA, Baker JC, Johnston KM. Is there an abnormal phenotype associated with maternal isodisomy for chromosome 2 in the presence of two isochromosomes? *Am J Hum Genet* 1997;**61**:461-2.
17 Bernasconi F, Karaguzel A, Celep F, Keser I, Luleci G, Dutly F, Schinzel AA. Normal phenotype with maternal isodisomy in a female with two isochromosomes: i(2p) and i(2q). *Am J Hum Genet* 1996;**59**:1114-18.